

USING SNOTEL DATA TO RUN THE SNOWPACK MODEL:
AN ANALYSIS OF MODEL PERFORMANCE AND WATER TRANSPORT METHODS

by
Hayden Clark Libby

A thesis submitted in partial fulfillment
of the requirements for the degree

of

Master of Science

in

Civil Engineering

MONTANA STATE UNIVERSITY
Bozeman, Montana

December 2025

©COPYRIGHT

By

Hayden Clark Libby

2025

All Rights Reserved

ACKNOWLEDGEMENTS

I want to take time here to thank my advisor, Siwei He, for taking me on as his first student. Siwei has been a great advisor and has helped me grow a lot as a researcher. I also want to thank Kevin Hammonds. Kevin is one of the reasons I came to MSU and helped to peak my interest in snow. Erich Pietzsch was also instrumental in my thesis. His knowledge of water in snow and help in edits to my writing is what got my work over the finish line. I also want to thank everyone I have worked with at the Snow Survey. Eric Larson, with Kevin, was why I decided to move to Bozeman. Eric, along with the rest of my coworkers (but more importantly, friends) made this thesis possible. Lastly, thank you to all my family and friends who bring so much joy into my life.

TABLE OF CONTENTS

1. INTRODUCTION	1
2. BACKGROUND	5
SNOWPACK Model	5
Overview	5
Inputs	6
Outputs	9
Physical processes	10
SNOWPACK validation in the United States	11
Water Transport in Snow	12
Overview	12
Water transport schemes in SNOWPACK	13
Bucket	14
NIED	14
Richards	17
Darcy's Law and Richard's Equation	19
Comparison of water transport equations	19
NRCS Snow Survey	20
Brief history	20
Mission and data	21
Standard setup	22
Supersites	23
Description of sensors	25
Snow Regimes in the US and Switzerland	27
3. METHODOLOGY	29
Overview	29
Site Selection	29
Running of SNOWPACK - R Workflow	31
Data download and quality control	32
Building input and parameter files	34
Running the model and converting outputs	36
Metrics for Analysis	37
Field Work	38
4. RESULTS AND DISCUSSION	39
SNOWPACK Simulations	39
Model case studies	39
Model validation	46
Field Observations	59

TABLE OF CONTENTS CONTINUED

Water Transport Methods.....	65
Melt season length	65
Liquid water content	70
Parameter, Empirical Formula, and Uncertainty Discussion	83
Wind sensitivity study.....	83
New snow density	86
Liquid water content thresholds.....	87
Increases in error with deeper snowpacks	90
Sources of uncertainty with my workflow and model setup.....	93
5. SUMMARY AND CONCLUSIONS.....	96
Running of SNOWPACK with SNOTEL Data	96
Water Transport Equations.....	99
Considerations for the Future.....	100
REFERENCES CITED.....	103
APPENDICES	108
SITE SPECIFIC MODEL OUTPUTS	109
NASH-SUTCLIFFE EFFICIENCY RESULTS	118
SAMPLE MODEL PARAMETER AND INPUT FILES	121
CODE SCRIPT SAMPLES	132

LIST OF TABLES

Table	Page
1. Table 1: Nash-Sutcliffe Efficiency values for all six model run types for the whole snow season, accumulation period, and for the melt period. NSE is determined based on the fit of hourly data at each of the 14 sites.....	47
2. Table 2: Full season mean error in SWE for different model run types	49
3. Table 3: Table of the accumulation period with mean error in SWE for different model run types	52
4. Table 4: The mean error in SWE during the melt period.....	54
5. Table 5: Days off of peak SWE for each site and different model run types.....	56
6. Table 6: Days off of melt out date for each site with different model run types	58
7. Table 7: Results from a wind sensitivity study during the accumulation period, results show error in SWE from model to observed (cm), the first three model results were forced with snow depth and the second three were forced with precipitation.....	84
8. Table 8: Results from a wind sensitivity study during the melt period	85
9. Table 9: Full season Nash-Sutcliffe Efficiency table.....	119
10. Table 10: Accumulation period Nash-Sutcliffe Efficiency table	119
11. Table 11: Melt period Nash-Sutcliffe Efficiency table	120

LIST OF FIGURES

Figure	Page
1. Figure 1: Important meteorological information for modeling snow with internal processes to model (Bartelt & Lehning, 2002).....	7
2. Figure 2: NIVIZ (niviz.org) visualization of SNOWPACK outputs, snow height and grain type for a snow season is on the left and an example pit profile is on the right. Each color represents a snow grain type: light green is new snow, dark green is decomposing fragmented snow, pink is round grains, light blue is faceted crystals, dark blue is depth hoar, purple is surface hoar, red is melt forms, red and black represent a melt freeze crust, teal is ice formation, and grey is graupel. NIVIZ is sponsored by many organizations and can visualize pit profiles, meteorological variables, and SNOWPACK outputs as used by the Swiss Avalanche Warning Service.....	10
3. Figure 3: Brackett Creek SNOTEL Supersite (with wind) June 2025. Each site used in this study is similar. (Photo Joe Kral)	24
4. Figure 4: Locations of SNOTEL standardized Supersites	25
5. Figure 5: Locations of enhanced SNOTEL sites used in this study.....	30
6. Figure 6: Flow chart showing the R-Studio workflow created to run SNOWPACK	32
7. Figure 7: Brackett Creek results for a model forced with snow depth and run with the Richards Equation for the water transport model. The top chart in the figure compares model SWE and observed SWE. Below these model outputs are weather inputs for snowfall, solar radiation, and air temperature to aid in determining snow and melt events throughout the winter (note that the new snow daily chart shows the amount of SWE added to the snowpack from one midnight value to the next). Below this are the density and liquid water content model outputs. The liquid water content is shown for the top, middle, and bottom of the snowpack. The middle is determined by the median calculation layer. The bottom chart is the changes in SWE.	40
8. Figure 8: Brackett Creek results for the model being forced with precipitation and run with the Richards equation for the water transport model.....	42
9. Figure 9: Turnagain Pass results for the model being forced with snow depth and being run with the Richards method for water transport.....	43

LIST OF FIGURES CONTINUED

Figure	Page
10. Figure 10: Turnagain Pass results for the model being forced with precipitation and being run with the Richards method for water transport	44
11. Figure 11: Boxplot of Snow Season error in SWE for different model run types, precipitation (prec) model runs are in green and snow depth (snwd) model runs are in light blue. The data in this plot is the average hourly error for each site (n = 16).	48
12. Figure 12: The date and value (cm) of peak SWE at each SNOTEL site.....	50
13. Figure 13: Boxplot of Accumulation period with error in SWE for different model run types.....	51
14. Figure 14: Boxplot of ablation period for different model run types	53
15. Figure 15: Boxplot of days modelled peak SWE is from observed peak SWE	55
16. Figure 16: Days off of melt out for different model types.....	57
17. Figure 17: Bracket Creek SNOTEL site on April 16th 2025.....	60
18. Figure 18: Density profile measurements (left) and liquid water content measurements (right)	60
19. Figure 19: Brackett Creek site visit notes	61
20. Figure 20: Brackett Creek site visit notes continued	61
21. Figure 21: Liquid water content (dots) and density (red bars) profiles at the Brackett Creek SNOTEL site. Density is in kg/m^3 and liquid water content is in relative percent.	62
22. Figure 22: NIVIZ visualized profile of measured liquid water content (line) and hand hardness (blocks) at Brackett Creek	63
23. Figure 23: NIVIZ outputs showing liquid water content and hardness profiles for snow depth model runs using each water transport equation: Bucket (left), NIED (middle), and Richards (right).....	64

LIST OF FIGURES CONTINUED

Figure	Page
24. Figure 24: Melt season lengths for observed SNOTELs (Tower, Elwood Pass, Castle Peak, Berthoud Summit) and three water transport equations at high elevation sites (above 10,500 ft) with a continental snowpack, numbers at the end of lines represent the total days of melt season, and for each site the observed length is followed by model results with Bucket, NIED, then Richards method	65
25. Figure 25: Melt season lengths for observed sites (Upper Rio Grande, Long Draw Resv, Lizard Head Pass, Joe Wright, and Hourglass Lake) and three water transport equations at low elevation sites (below 10,500 ft) with a continental snowpack.....	66
26. Figure 26: Melt season lengths for observed sites (Mores Creek Summit, Midway Valley, and Brackett Creek) and three water transport equations at sites with a intermountain snowpack	68
27. Figure 27: Melt season lengths for observed sites (Turnagain Pass and Heavenly Valley) and three water transport equations at sites with a maritime snowpack	69
28. Figure 28: Liquid water content outputs at Brackett Creek SNOTEL site for three different water transport equations at the start of the melt season. The top chart shows observed precipitation, air temperature, solar radiation, and snow depth as recorded from the SNOTEL site to help identify what may be affecting water transport at any given time (along with the type of melt occurring). Next, each transport equation has two charts. The first shows liquid water content outputs at the top of the snow, at the middle between the top and middle of the snowpack, the middle of the snowpack, at the middle between the middle and the bottom of the snowpack, and at the bottom layer. The second plot shows observed and modeled daily SWE loss in centimeters per day. The plot also has two-hour SWE loss from the model to show the timing of melt for each transport method. The data are shown in two-hour increments because decreases in SWE occur only at two-hour intervals in our model outputs.....	71
29. Figure 29: Liquid water content outputs at Brackett Creek SNOTEL site for three different water transport equations from April 5th to April 20th.....	73
30. Figure 30: Liquid water content outputs at Brackett Creek SNOTEL site for three different water transport equations from May 1st to May 15th.....	75

LIST OF FIGURES CONTINUED

Figure	Page
31. Figure 31: Liquid water content outputs at Brackett Creek SNOTEL site for three different water transport equations from May 6th to May 10th.....	76
32. Figure 32: Liquid water content outputs at Brackett Creek SNOTEL site for three different water transport equations at the end of the snow year	78
33. Figure 33: NIVIZ outputs for three water transport equations (Bucket – top, NIED – middle, Richards – bottom) with snow grain type (left) and liquid water content (right) from April 1st 2025 to April 30th 2025 at the Brackett Creek SNOTEL site. Red on the snow grain chart represents melt forms and darker blue on the liquid water content charts represent higher liquid water content (ranging from 0 to 4 %)......	80
34. Figure 34: NIVIZ outputs for three water transport equations (Bucket – top, NIED – middle, Richards – bottom) with snow grain type (left) and liquid water content (right) from May 6th 2025 to May 10th 2025 at the Brackett Creek SNOTEL site.	82
35. Figure 36: Scatterplot of the average mean error in SWE for three water transport equation model outputs at each SNOTEL site versus the peak SWE at that site for the accumulation period. The points are also broken up into Continental (diamonds), Intermountain (squares), and Maritime (triangles)	91
36. Figure 37: Scatterplot of the average mean error in SWE for three water transport equation model outputs at each SNOTEL site versus the peak SWE at that site for the melt period. The points are also broken up into Continental (diamonds), Intermountain (squares), and Maritime (triangles)	92
37. Figure 38: SNOWPACK results at Brackett Creek for a model forced with precipitation data and run with the Bucket water transport method	110
38. Figure 39: SNOWPACK results at Brackett Creek for a model forced with snow depth data and run with the Bucket water transport method	111
39. Figure 40: SNOWPACK results at Brackett Creek for a model forced with precipitation data and run with the NIED water transport method	112
40. Figure 41: SNOWPACK results at Brackett Creek for a model forced with snow depth data and run with the NIED water transport method.....	113

LIST OF FIGURES CONTINUED

Figure	Page
41. Figure 42: SNOWPACK results at Turnagain Pass for a model forced with precipitation data and run with the Bucket water transport method	114
42. Figure 43: SNOWPACK results at Turnagain Pass for a model forced with snow depth data and run with the Bucket water transport method.....	115
43. Figure 44: SNOWPACK results at Turnagain Pass for a model forced with precipitation data and run with the NIED water transport method.....	116
44. Figure 45: SNOWPACK results at Turnagain Pass for a model forced with snow depth data and run with the NIED water transport method.....	117

ABSTRACT

Snow modelling is useful for both avalanche forecasting and water supply prediction. With increasing numbers of winter recreationalists, a growing population, and more variable weather patterns due to climate change, there is a need for improved snow modelling in the United States. One example of a snow model is the SNOWPACK model. SNOWPACK was originally developed in Switzerland as an avalanche forecasting aid and was created in conjunction with a dense array of mountain weather stations. Today SNOWPACK is used, or being tested for use, as an avalanche forecasting tool in North America, Europe, and Japan. In the United States, there is also an array of winter weather stations, although these are generally used for water supply prediction. The weather stations are called SNOW TELEmetry (SNOTEL) sites and are run by the Natural Resource Conservation Service's Snow Survey program. Until recently, these stations lacked the necessary inputs to run the SNOWPACK model. With the necessary data now available, we look to answer the questions: Can the SNOWPACK model be effectively run with freely available SNOTEL data, what are the differences between three water transport methods (Bucket, NIED, and Richards), and when should each be used? We develop a novel workflow to run the SNOWPACK model with SNOTEL data for 14 sites across the western United States, addressing our research questions. We find that using SNOTEL data to run the SNOWPACK model produces good agreement with observations. A mean absolute average hourly snow water equivalent error of 2.79 cm during the accumulation phase of the snow season and 6.08 cm of error during the melt season is found. We find that Richard's transport method is most appropriate when internal snow properties are required; otherwise, the Bucket method performs well. Lastly, we find an increase in model error when deeper snowpacks are modelled. In this work, we explore the effects of model parameters and input types (e.g., wind and precipitation data) on model performance. Our work provides a framework for running the SNOWPACK model with SNOTEL data given different applications.

CHAPTER ONE

INTRODUCTION

With a rise in backcountry winter recreationists, rapid population growth in the water-scarce American West, and increasing variability and non-stationarity due to climate change, there is a need for more accurate snow modelling. Snow modelling supports avalanche forecasting, water-supply prediction, and natural-disaster preparedness. One snow model is SNOWPACK, which has seen increased use in North America by avalanche centers, hydrologists, and natural-disaster predictors. The SNOWPACK model was created at the Institute for Snow and Avalanche Research (Das WSL-Institut für Schnee- und Lawinenforschung, more commonly known as the SLF) in Davos, Switzerland. The model performs 1D physical modelling on meteorological input data to produce snowpack profiles.

Since 2023, the United States Department of Agriculture Natural Resources Conservation Service's (NRCS) SNOW TELEmetry (SNOTEL) winter weather stations run by the Snow Survey program have been upgraded to collect a wider array of more accurate data. With the addition of new sensors, the data from these stations can now be used to force SNOWPACK. At a time when detailed snow information is needed, there is interest in using SNOWPACK, and we now have weather stations in the United States that can run the model, span a large spatial extent, and provide freely available data, a study into running SNOWPACK with SNOTEL data was needed.

In this work, we answer two questions: first, can the SNOWPACK model be run effectively using publicly available and free SNOTEL data? We investigate what model

parameters should be set based on location and model application. We chose to focus on water transport within the model, as it is a current topic of interest in the snow community and aligns with SNOWPACK's use as an aid for both avalanche forecasting and hydrologic modelling. There are three water transport equations available in SNOWPACK: the bucket method, the NIED (National Research Institute for Earth Science and Disaster Prevention) method, and Richard's equation. Hence, our second research question investigates the performance of each water transport equation, clarifies the causes of differences among the three methods, and identifies when each method should be used. We expect that SNOWPACK can run on only SNOTEL data, since a combination of SNOTEL and other weather stations data was used in the past. However, we do not know how the model will perform in different snow regimes and climates. We also expect Richard's method to perform the best of the three water transport methods.

To answer these questions, we first identified the model parameters and inputs required to run the model, as well as the SNOTEL sites with the required sensors. The inputs we use to run the SNOWPACK model are air temperature, wind speed, snow depth, precipitation, incoming shortwave radiation, incoming longwave radiation, and relative humidity. We also create a workflow for downloading SNOTEL data, performing quality control, creating input and parameter files for the model, running the model, and transforming the model outputs into a usable form.

Our work builds on previous research with the SNOWPACK model. Lundy et al. (2001) validated the SNOWPACK model using an in situ weather station in the Bridger Mountains, Montana, USA. They found that simulated snowpack temperatures and densities correlated well

to observed values, but that the model typically underestimated the settlement of snow. Lundy et al. (2001) used temperature, density, and grain size and type to evaluate model performance. We instead use snow water equivalent (SWE) for validation. Additional validation with snow temperature profiles will be possible in the future with data from SNOTEL sites. We use precipitation and longwave radiation as inputs to the model. However, we do not input the snow surface temperature as Lundy et al. (2001) do (the model uses longwave radiation as a proxy for snow surface temperature when it is not directly measured). Two major differences between Lundy et al. (2001) and our research are that we use multiple weather stations with freely available data and that we investigate liquid water content in snow.

Katz et al. (2023) provided insight into using SNOTEL data to run SNOWPACK. In this study, data from three standard SNOTEL sites were augmented with data from three closely located towers with additional sensors. Katz et al. (2023) investigated rain-on-snow effects on runoff under different snow conditions and used SWE for validation, though only before and after specific rain events. We build on this work by using solely SNOTEL data to force SNOWPACK and validate seasonal snowpacks using SWE.

We also draw upon two existing studies aimed at improving the water transport methods in SNOWPACK. Hiroshima et al. (2010) introduced a new water transport equation to the SNOWPACK model using Darcy's Law as the driving force. Following this, Wever et al. (2014) introduced the use of Richard's equation for water transport in snow. Wever et al. (2014) used two study sites with 14 and 17 years of data, respectively. Their work used lysimeter flow measurements and snow heights for validation.

We build on Wever et al. (2014) by examining the different water-transport methods across three snow climates in North America. Rather than using flow measurements and snow heights, we use SWE for validation. We have hourly SWE data from SNOTEL sites; SWE is an output of the SNOWPACK model, but is not required as an input. As such, SWE works as a better predictor of model accuracy than snow height. A decrease in spring SWE is interpreted as water leaving the snowpack. This metric is similar to that used by Wever et al. (2014) for validation, providing precedent for the use of SWE in model verification. We also investigate water transport methods across a large spatial area, rather than only at two sites, as Wever et al. (2014) do.

This thesis provides a workflow for researchers, avalanche professionals, and snow hydrologists to run the SNOWPACK model with SNOTEL data. Running SNOWPACK with SNOTEL data provides an easy entrance for model use by avalanche forecasters since these stations are already used when making forecasts. We also provide guidance on which parameters to use when running the model and why, and highlight potential sources of error in SNOWPACK and SNOTEL data. Using a snow model to determine snowpack characteristics enables users to understand conditions without physically visiting the site. We answer our questions and determine if our hypothesis is correct; can we run SNOWPACK with SNOTEL data and is Richards method the best water transport method in all cases?

CHAPTER TWO

BACKGROUND

SNOWPACK ModelOverview

SNOWPACK is a one-dimensional physical snow model that solves partial differential equations for conservation of mass, energy, and momentum (Bartelt & Lehning, 2002). The model was developed by the Swiss Federal Institute for Snow and Avalanche Research (SLF) in Davos, Switzerland, and was first used operationally in the winter of 1998 / 99 (Lehning et al., 1999). The model was first introduced to support a more robust avalanche warning system in Switzerland. A system of winter weather stations was built in the late 1990s to support the avalanche warning system. SNOWPACK supplements the data collected at the automatic weather stations to aid forecasters (Lehning et al., 1999). The model is still used in Switzerland, and has since been implemented in Italy, Austria, Canada, Japan, and the United States for aid in avalanche warning systems (Morin et al., 2020). Avalanche Canada has been working to introduce a forecast aid that is also public-facing (Horton et al., 2025). This tool runs SNOWPACK using the High-Resolution Deterministic Prediction System (HRDPS) 2.5km forecast to predict avalanche hazard for the day in a selected area, allowing users to view avalanche type, a pit profile, and meteorological variables. SNOWPACK is being tested as a tool with the Colorado Avalanche Information Center and in Canada (Horton et al., 2025).

While we use the SNOWPACK model in this work, many other snow models are available. Examples include Crocus, SNOWGRID, and seNorge. These were developed in

France, Austria, and Norway, respectively (Morin et al., 2020). The Viper and M4 models, developed by the NRCS Snow Survey, are statistical models used for water supply forecasting (Fleming & Goodbody, 2019). HEC-HMS is a hydrologic model that can incorporate snow, developed by the United States Hydrologic Engineering Center.

For more information on snow models and operational use of the SNOWPACK model, I suggest looking at both the Avacollabra group and the AWSOME model framework. Avacollabra helped to create the AWSOME framework and is a collaborative group of people from around the world aiming to ease the use of SNOWPACK and other snow models in operational avalanche forecasting, as well as combine efforts for model improvements. Soon, people in the group will publish xsnow, a post-processing tool, validation best practices, and more information on new wind transport methods within the model (Horton, 2025). The work we present will mesh well with xsnow for operational use of SNOWAPCK using SNOTEL data.

Inputs

SNOWPACK performs physical modelling using meteorological forcings and snow profiles as inputs. The meteorological inputs can come from weather stations, weather models, or a combination of the two. The required meteorological inputs are air temperature, relative humidity, wind speed, incoming shortwave radiation and/or reflected shortwave radiation, incoming long wave radiation and/or snow surface temperature, precipitation and/or snow height, and ground temperature (snowpack 3.7.0 doc release).

Figure 1 highlights the inputs and processes modeled. The model can be configured to perform various consistency checks and input bounds. The bounds are helpful as most model problems arise from poor data quality, data editing, or missing data (snowpack 3.7.0 doc release).

Validation data is also needed for the model. Snow temperature profiles, snow water equivalent, observed grain size, and measured snowpack outflow are good metrics for validation of model performance.

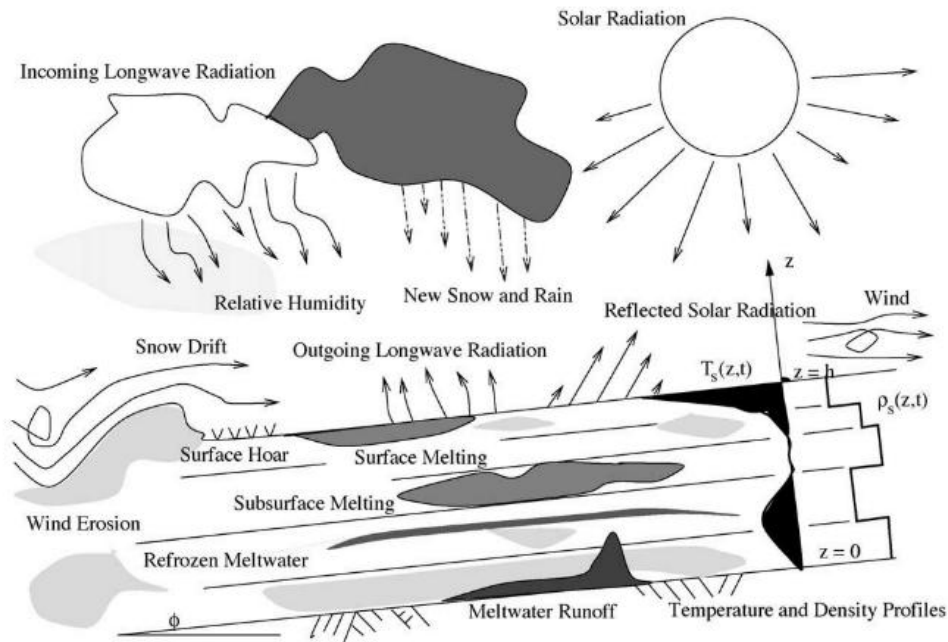


Figure 1: Important meteorological information for modeling snow with internal processes to model (Bartelt & Lehning, 2002)

To run the model, at least one snow profile input is required. It is best to start the model at the beginning of the snow season for most objectives; as such, the initial profile indicates that there is no snow on the ground. Snow pit profiles dug near the modelling site can be uploaded to the model throughout the winter; the model will use this data to apply corrections. The profiles used for the SNOWPACK model are more complex than most pit profiles done in the field. The required variables include snow depth, volume fractions of ice, water, and air, sphericity, and

grain size. For this study, only initial profiles with no snow on the ground were used to initialize the model.

As previously stated, SNOWPACK can be forced using weather station or weather model inputs. Weather stations provide the best data and, therefore, better model agreement. However, weather station data is not always available or representative of the larger area. For instance, in Western Canada, the average area covered per available weather station is 1345 km², while in Switzerland each weather station covers approximately 100km² (Bellaire et al., 2011). When avalanche forecasters have a large area to forecast over and low spatial variability in weather station data, forecasted weather data are useful. For example, some forecasting zones in Canada are over 50,000 km². Thus, Avalanche Canada has been working to use weather models rather than weather stations for SNOWPACK model inputs (Horton et al., 2025).

Bellaire et al. (2011) investigated the use of modelled meteorological inputs for the SNOWPACK model. At the Mt. Fidelity Study Plot in Canada during the 2009-10 winter, SNOWPACK was forced with the Global Environmental Multiscale model at 15km resolution and 58 atmospheric levels (GEM15), using both filtered and unfiltered data (Bellaire et al., 2011). Three different filtering methods were used to correct for the overestimation of precipitation in the forecasting data: either divided by a correction factor, subtracted from a correction factor, or divided by a constant. They found that SNOWPACK consistently overestimated snow depth when forcing it with unfiltered data. When using filtered precipitation data, they reported overestimations during October to November and underestimations from November through February. From February through May, some filtering methods showed good agreement, whereas one overestimated snow depth (Bellaire et al., 2011). The 24-hour new

snow amounts showed agreement within +/- 10cm for 75% of the 3-hour periods examined in the study, and model agreement was generally good.

Accuracy is important for SNOWPACK inputs and outputs for operational use. In the western US, many avalanche forecast areas are smaller and less remote than in western Canada. Given the growing number of SNOTEL sites with the data required to run SNOWPACK, following the methods used in Switzerland could be a viable option. This is especially true because, for SNOWPACK to be used as a tool for forecasters, there must be forecaster buy-in. Trust in outputs is higher when trusted data are used as inputs. Günther et al. (2019) compared multiple 1-dimensional snow models and analyzed the factors controlling model skill. They found that, when investigating model performance across an entire snow season, input data errors had the greatest effect on performance. Followed by model structure and then parameter choice (when investigating those three factors). Using weather station data for inputs, as is done in Switzerland, provides more accurate model outputs.

Outputs

The SNOWPACK model outputs a time series of snow profiles. This output, a .pro file, can be uploaded to niviz.org for easy visualization (Figure 2). Standard outputs include grain size and type, snow height, liquid water content, density, temperature profile, and a hardness profile. Additional outputs that give snow stability metrics include critical cut length, hardness difference, snow shear strength, grain size difference, hand hardness, natural stability index, and stability index snowpack (3.7.0 doc release). Each of these outputs can be manually pulled from the .pro file using code to produce individualized graphics of the results from each model run.

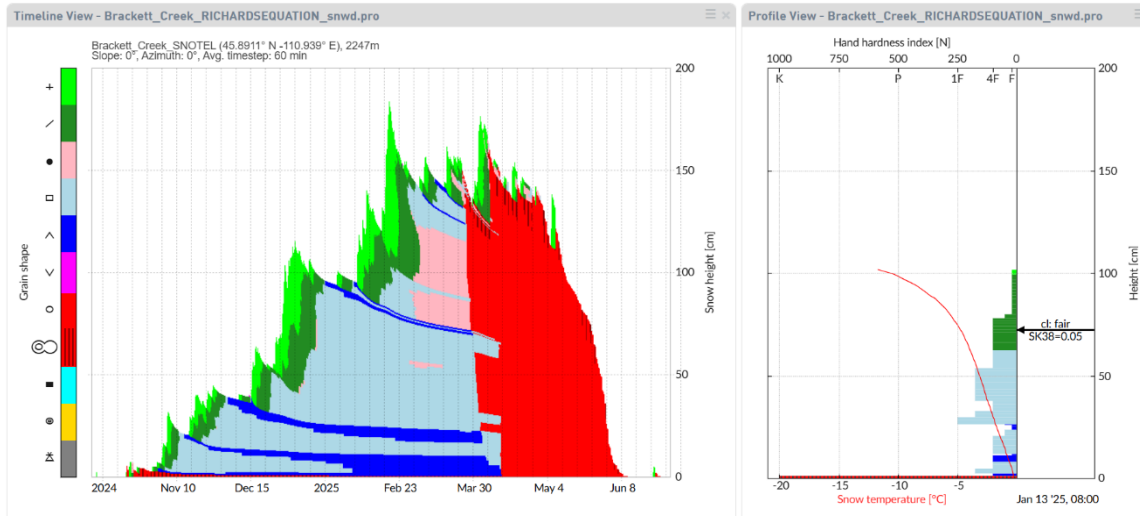


Figure 2: NIVIZ (niviz.org) visualization of SNOWPACK outputs, snow height and grain type for a snow season is on the left and an example pit profile is on the right. Each color represents a snow grain type: light green is new snow, dark green is decomposing fragmented snow, pink is round grains, light blue is faceted crystals, dark blue is depth hoar, purple is surface hoar, red is melt forms, red and black represent a melt freeze crust, teal is ice formation, and grey is graupel. NIVIZ is sponsored by many organizations and can visualize pit profiles, meteorological variables, and SNOWPACK outputs as used by the Swiss Avalanche Warning Service.

Physical processes

Each snow layer is described using three constituents: ice, water, and moist air (Bartelt & Lehning, 2002). The SNOWPACK model is governed by four differential equations based on the three constituents: bulk temperature (energy conservation), vapor diffusion (mass conservation of air phase), water transport (mass conservation of water phase), and settlement momentum (conservation of ice phase). It is assumed that the self-weight of the snowpack is held by the solid ice lattice, snow stress varies based on microstructural grain-bond stress, and that grain-bond strength is directly related to water content and bulk temperature (Lehning et al., 2002).

SNOWPACK models snow microstructure, grain type and size, and metamorphism.

These variables are important for avalanche forecasters because they help determine avalanche risk. SNOWPACK models these properties with the aforementioned general equations, as well as microstructure-based models of viscosity and thermal conductivity (Lehning et al., 2002). These equations provide a good representation of natural snow; however, the empirical formulas for the constants are calibrated from observations. The observational constants are needed to correctly model natural snow because the model's description of snow material properties is based on those of pure ice (not snow). Also, the model does not include the process of intergranular glide, and the effect of liquid water on viscosity is not included, but parameterized only (Lehning et al., 2002).

Density, grain metamorphism, and water content are important properties within the snowpack. In the model, the internal bulk density is calculated as the product of the volumetric contents of ice, water, and air and their respective material densities. These values are calculated based on strain (compaction), wind densification, and phase changes. Temperature gradients, vapor fluxes, and sintering determine grain metamorphism. Water content is calculated based on phase-change, water transport, and compaction of snow layers. (snowpack version 3.7.0 snowpack.cc)

SNOWPACK validation in the United States

The SNOWPACK model was validated in Montana, USA in 2000 with a combination of scientists from the SLF, Montana State University, and the Gallatin National Forest Avalanche Center (Lundy et al., 2001). For their study, a weather station was set up to collect the meteorological inputs near the Bridger Bowl Ski Area in the Bridger Mountain Range. Snow pits

were dug weekly near the weather station to compare snow temperature gradient, snow density, and grain type with model outputs. It was found that SNOWPACK predicted the snow temperature profile well - however model performance worsened with colder temperatures (Lundy et al., 2001). The modelling of a correct temperature profile is important because many snowpack internal processes are dependent on the temperature gradient. It was also found that snow density outputs were reasonable, though the model tended to underpredict density when the observed density exceeded 250 kg/m^3 (Lundy et al., 2001). Lastly, it was found that grain size was difficult to compare because of differences in observer's definitions of grain size and type and the model's definitions and parameters.

The study concluded that SNOWPACK has the potential to be a useful tool for forecasters who need to know the snow properties and structure but can't dig frequent snow pits at a given location. Lundy et al. (2001) emphasize that limitations of the model need to be known by the user for use of outputs. Their study used the first version of SNOWPACK, and many improvements have been made to the model since, which we discuss in the next sections.

Water Transport in Snow

Overview

Modelling liquid water transport in snow is difficult because snow is near its triple point and metamorphism happens rapidly when water is flowing through a snowpack, especially if the snowpack is dry. Water flow occurs horizontally and vertically in the snowpack. Horizontal flow occurs when there is a large density difference between layers, such as at an ice lens. We investigate vertical flow only in this study. Vertical water transport will only occur when the

percentage of liquid water content has reached the limit of that layer, and liquid water can only exist in the snowpack if the temperature of the snow is zero degrees Celsius, meaning the cold content is zero (HEC-HMS Technical Reference Manual, n.d.). Vertical water transport is primarily gravity-driven. Complexity arises from layers in the snow that impede water flow, such as ice layers and capillary barriers (E. Peitzsch et al., 2010). Ice layers can temporarily block water movement, while capillary barriers form when fine-grained snow overlies coarser snow. Because fine-grained snow has higher suction, water accumulates at the interface until capillary pressures equalize (E. H. Peitzsch, 2009). When snow is on a slope, water may travel downslope along ice layers or capillary barriers.

There are generally two types of flow that describe vertical water transport within a snowpack: matrix and preferential (Schneebeli, 1995, Donahue & Hammonds, 2022). Matrix flow is semi-uniform, similar to water transport in uniform soils. Here, a wetting front moves at roughly a constant rate through the snowpack. Preferential flow paths (or finger flow) are areas of concentrated flow within the snowpack. Preferential melt paths will form in different spatial areas for each melt event. A snowpack will trend towards having primarily matrix flow as the melt season progresses and the snowpack becomes homogeneous (Webb et al., 2018). Both matrix and preferential water transport in the snowpack can occur during rain-on-snow or solar-melt events.

Water transport schemes in SNOWPACK

Water transport in SNOWPACK is vertical flow only, and three schemes are available for this modeling: the Bucket method, National Research Institute for Earth Science and Disaster Prevention's method (NIED), and Richard's Equation.

Bucket The Bucket method is the original water transport equation used in SNOWPACK.

In the first of three papers describing the first iteration of SNOWPACK, Bartelt and Lehning (2002) state that Darcy's equation is not used because the volumetric water content is seldom higher than 0.15, water flow is not homogeneous, with preferential flow paths, and highly nonlinear flow is too computationally intensive. Therefore, the bucket method was created.

(1) The relationship between water content and residual water content for flow in the Bucket method:

$$\frac{\partial J_W}{\partial z} = \begin{cases} 0 & \text{for } \theta_w \leq \theta_r \\ \dot{\theta}_f & \text{for } \theta_w \geq \theta_r \end{cases}, \quad \dot{\theta}_f = \frac{\partial(\theta_w - \theta_r)}{\partial t}$$

In the Bucket method, the J_W term represents the rate of water flow per unit area, θ_w is the volumetric water content, and θ_r is the residual water content. Flow occurs only when the water content exceeds the residual water content. The water content remaining in the snow layer is set to the residual water content, a constant 0.04, in the Bucket method (watertransport.cc in source code). When the water content is less than the residual, free water remains fixed within the ice matrix (Bartelt & Lehning, 2002).

NIED The NIED method was developed for SNOWPACK to improve the simulation of the water content profile, as the Bucket method oversimplifies this simulation (Hirashima et al., 2010). Below is the NIED method with comments on how Hirashima et al. (2010) adjusted Darcy's Law and the van Genuchten water retention curve.

(2) Darcy's Law for vertical water flux:

$$q = K \left(\frac{dh}{dz} + 1 \right)$$

Here, q is the water transport amount in the calculation layer, K is the unsaturated hydraulic conductivity, h is the pressure head, and z is the vertical coordinate. The water transport calculated in one time step usually is q multiplied by the time step in Darcy's Law. However, this would require extremely small time steps to work and would cause SNOWPACK to take over 4 hours to run a single winter season (Hirashima et al., 2010). As such, Hirashima et al. (2010) developed a calculation technique to derive a new water-flux-per-timestep equation that uses one-minute time steps and allows SNOWPACK to run in approximately 6 minutes for a single winter season. Below, the components of Darcy's law are discussed.

(2.1) The unsaturated hydraulic conductivity (K) in equation 2 is shown here:

$$K(\Theta) = K_s \cdot K_r(\Theta)$$

(2.1.1) The saturated hydraulic conductivity (K_s) is calculated below from Shimizu (1970), where d is snow grain diameter (Hirashima et al., 2010):

$$K_s = 7.7 \times 10^{-4} d^2 \frac{g}{v} \exp(-7.8 \times 10^{-3} \rho_s)$$

(2.1.2) The relative unsaturated conductivity (K_r) from Maulem/van Genuchten is calculated here. See how m is calculated in 2.2.2 below.

$$K_r = \Theta^{1/2} \left[1 - \left(1 - \Theta^{1/m} \right)^m \right]^2$$

(2.2) The van Genuchten (1980) water retention curve using suction pressure head:

$$h = \frac{1}{\alpha} (\theta^{-\frac{1}{m}} - 1)^{\frac{1}{n}}$$

(2.2.1) The saturated water content (used to calculate theta – the volumetric liquid water content) in the van Genuchten water retention curve (eq. 2.2) is calculated using an empirical conversion to transform snow density to pore space. (snowpack 3.7.0 vangenuchten.cc)

$$\theta_s = \left(\frac{\left(1000 - \left(\frac{\rho_s}{0.917} \right) \right)}{10.0 * 0.9} \right) * \frac{1}{100}$$

(2.2.2) Standard relation for m in van Genuchten (1980):

$$m = 1 - 1/n$$

(2.2.3) Parameterization used for n where d is snow grain diameter (Hirashima et al., 2010):

$$n = 15.68 \exp(-0.46d) + 1$$

(2.2.4) Parameterization for alpha from Hirashima et al. (2010) experiments where d is snow grain diameter:

$$\alpha = 7.3 \times d + 1.9$$

The NIED method was found to increase water content during snowmelt periods, form capillary barriers at the boundaries between layers of different grain sizes, and have rapid grain growth at the water-saturated layer with water discharge (Hirashima et al., 2010). Compared to the bucket method, NIED was found to have slightly better agreement with the observed liquid

water content and grain size over the 2002-2003 winter at a site in Japan (Hirashima et al., 2010). The method also had better agreement with snow pits dug on two separate dates for the grain size, volumetric water content, and density profiles (Hirashima et al., 2010). Although these findings showed better agreement than when the Bucket method is used, this study examined only one site and season, and water transport in the SNOWPACK model could still be improved.

Richards The Richards equation describes water movement in variably saturated porous media and was adapted for water transport in snow by Wever et al. (2014) for the SNOWPACK model. Equation 3 is the form of the Richards equation used in SNOWPACK.

(3) The governing Richards equation (Richards, 1931)

$$\frac{\partial \theta}{\partial t} - \frac{\partial}{\partial z} \left(K(\theta) \left(\frac{\partial h}{\partial z} + \cos \gamma \right) \right) + s = 0$$

where θ is the volumetric liquid water content, K is the hydraulic conductivity, h is the pressure head, z is the vertical coordinate, γ is the slope angle, and s is the source or sink term.

(3.2) The van Genuchten (1980) retention curve is used for theta:

$$\theta = \theta_r + (\theta_s - \theta_r) \frac{(1 + (\alpha|h|)^n)^{-m}}{S_c}$$

Where θ_r is the residual water content, θ_s is the saturated water content, α is a fit coefficient related to the maximum pore size in the snow, m is a fit coefficient related to pore size distribution (same as in eq. 2.2.2), n is a fit coefficient related to pore size distribution (same as equation 2.2.3), and S_c is a correction factor.

(3.2.1-2) The parameter values are shown here; SNOWPACK offers options for both the Daanan and Yamaguchi parameters.

$$1a) \alpha = 30(2r_g) + 12 \text{ (Daanan and Nieber (2009))}$$

$$1b) \alpha = 7.3(2r_g) + 1.9, \text{ when } r \text{ is } < 5 \text{ mm (Yamaguchi et al. 2010)}$$

$$2a) n = 0.800(2r_g) + 3 \text{ (Daanan and Nieber (2009))}$$

$$2b) n = 15.68e^{(-0.46(2r_g))} + 1, \text{ when } r \text{ is } < 5 \text{ mm (Yamaguchi et al. 2010)}$$

(3.2.4) Saturated water content:

$$\theta_s = (1 - \theta_i) \frac{\rho_i}{\rho_w}$$

(3.2.5) Residual water content (Wever et al., 2014):

$$\theta_r^t = \min\langle 0.02, \max\langle \theta_r^{t-1}, f \cdot \theta_w \rangle \rangle$$

(3.3) Hydraulic conductivity:

$$K(\theta) = K_{sat} \Theta^{1/2} \left[1 - \left(1 - \Theta^{1/m} \right)^m \right]^2, \quad \Theta = \frac{\theta - \theta_r}{\theta_s - \theta_r}$$

(3.3.1) Saturated conductivity (Calonne et al. (2012) is the default in SNOWPACK, Shimizu (1970) is another option (eq. 2.1.1).

$$K_{sat} = \left(\frac{\rho_w g}{\mu} \right) \left[0.75 \left(\frac{r_{es}}{1000} \right)^2 \exp(-0.013 \theta_i \rho_i) \right]$$

Wever et al. (2015) found that using the Richards equation in SNOWPACK improved the simulation of water flow at both daily and sub-daily timescales compared to the Bucket and NIED methods, with sub-daily timescales showing the largest improvements. This comparison was done using lysimeters at two separate sites in Switzerland (Wever et al., 2014). Improvements stem from the ability to model ponding at capillary barriers and varied liquid water content using the Richards method (Wever et al., 2015).

Darcy's Law and Richard's Equation

Darcy's law and Richard's equation for snow use the same base equations as the two methods' original purposes, water transport in soil. The differences arise from the constants used to describe snow instead of soil. Darcy's law describes a linear relationship between pressure differences and flow rate in a saturated porous media (Mawlood et al., 2020). Richard's equation combines aspects of Darcy's law and the mass continuity law to describe flow under capillary conditions in both saturated and unsaturated porous media. Richards equation uses a nonlinear partial differential equation to describe this process (Mawlood et al., 2020); (Richards, 1931). Darcy's law is considered the governing equation for saturated soils, while Richards' equation is considered the governing equation for flow in unsaturated soil.

Comparison of water transport equations

Wever et al. (2014, 2015) investigate model results using the three different water transport methods in Switzerland. They found that on a sub-daily timescale, the Bucket and NIED lag correlation coefficients indicated that the model released meltwater too early in the day compared to the measured snowpack runoff (Wever et al., 2014). Also, on a seasonal scale, the Nash Sutcliffe Efficiency was found to be similar between the Richards and Bucket methods at a

lower elevation site. Bucket and NIED seem to retain meltwater in the snowpack too long, underestimating the arrival of meltwater at the base of the snowpack in the early stages of the melt season, particularly at a site with a higher average snowpack than other sites they examined (Wever et al., 2014). During midwinter melt events, Wever et al. (2014) found the bucket method had less snowpack runoff than observed.

Shallow snowpacks may result in smaller differences in outputs among the three transport equations. At the lower elevation site, the NIED and Bucket methods had better estimations of peak water outflow than the Richards equation (Wever et al., 2014). The biggest advantage of the Richards equation was found to be its modelling of snow properties (Wever et al., 2015). The difference in model error between Bucket and Richards in a given winter is less than the difference between the modeled and observed liquid water content (Wever et al., 2015), meaning that the skill of the model may have more of a factor than the skill between each transport equation.

NRCS Snow Survey

Brief history

The Natural Resource Conservation Service (NRCS) Snow Survey was established, then under the soil conservation service, in the 1930s following work by Dr. James Church of the University of Nevada-Reno (Fleming et al., 2023). Once established, snow surveys were conducted at manual snow courses that remain in use today, with some data records dating back more than 100 years. These snow courses are conducted by a surveyor who visits the same

location each month and measures snow height and snow water equivalent (SWE) using snow tubes. Data are now collected from a mix of snow courses and weather stations.

In the early 1960s SNOw TELEmetry (SNOTEL) stations were first installed. The weather stations were set up to remotely measure air temperature, snow height, and SWE at a finer temporal resolution than is possible with snow course measurements. The stations initially used a system of line-of-sight radios and repeaters to transmit data, then transitioned to Meteor Burst antennas (Zukiewicz, 2024). Today, cellular antennas and the National Oceanic and Atmospheric Administration's (NOAA) Geostationary Operational Environmental Satellites (GOES) are used to transmit data.

Snow Survey data are the primary source for in situ mountain snowpack measurements and associated meteorological information in the western United States and Alaska. These data provide direct observational metrics that are used for many different snow models and airborne surveys (Fleming et al., 2023). There are now over 900 SNOTEL sites across the western US and Alaska with hourly data records up to 61 years, and 825 manual snow courses with monthly data records up to 113 years.

Mission and data

The Snow Survey provides free, publicly available data. However, the mission of the Snow Survey is to provide reliable, accurate, long-term snow and climate data to be used for water supply forecasts (Fleming et al., 2023). In mountainous areas in the western United States, about 70% of runoff for water supply comes directly from the snowpack (Li et al., 2017). As such, the stream volume forecasts have immense health and economic impacts. As an example,

even modest improvements in the forecast can yield over \$100 million per year in benefits for a single river basin (Fleming & Goodbody, 2019).

The water supply forecasts are statistics-based and use a machine-learning model to predict volumetric water for approximately 580 forecast points. Official forecasts are written for each state within the program at least once per month from January to June. The forecasts provide critical information for water managers, ranchers, and water operations. Especially in the face of a growing population, water scarcity issues in the Western US, and the impacts of human-caused climate change (Fleming et al., 2023).

The Snow Survey data (available at <https://nwcc-apps.sc.egov.usda.gov/imap>) are quality-controlled by the various snow survey offices. The standard data of SWE, snow depth, and precipitation are edited almost daily, but only the midnight values are edited due to daily sensor fluctuations. Other additional sensors, also called extended sensors, such as wind and solar radiation, have data edited only monthly, again for midnight values. When using SNOTEL data for research purposes, users must perform their own quality control of the hourly data.

Standard setup

The sensor suite at all SNOTEL stations includes a precipitation can, a snow pillow, a snow depth sensor, and an air temperature sensor. These are “standard” sites. Pressure sensors are located in the shelters at each SNOTEL site and measure precipitation and SWE. Figure 3 shows a SNOTEL site with extended sensors. All SNOTEL sites are located in the subalpine zone, most often in forests. The sites are normally located in a small natural or cut meadow. This location setup provides the most consistent data for water-supply forecasting and reduces wind-induced variability in snowpack.

Supersites

The supersite initiative began within the Snow Survey program with upgrades to selected existing sites beginning in 2023 (Fleming et al., 2023). The selected sites contain an array of standardized extended sensors, including relative humidity, solar radiation, soil moisture and temperature, and a snow temperature profile. See Figure 4 for the locations of current supersites. The Snow Survey historically installed extended sensors before standardized supersites, both to aid in forecasts and provide additional data for researchers.

Figure 3 shows the Brackett Creek SNOTEL site in the Bridger Mountain Range just north of Bozeman, Montana. This site is an example of a supersite with a wind sensor added. All available extended sensors are shown in Figure 3. Some SNOTEL sites may have one or two extended sensors. The location of extended sensors (and supersites) is determined by water supply forecast needs, cooperator requests for specific data types, site-specific attributes, starting initial data records for research and development, or data gap filling. Currently, the goal is to have at least one standardized supersite per major watershed.

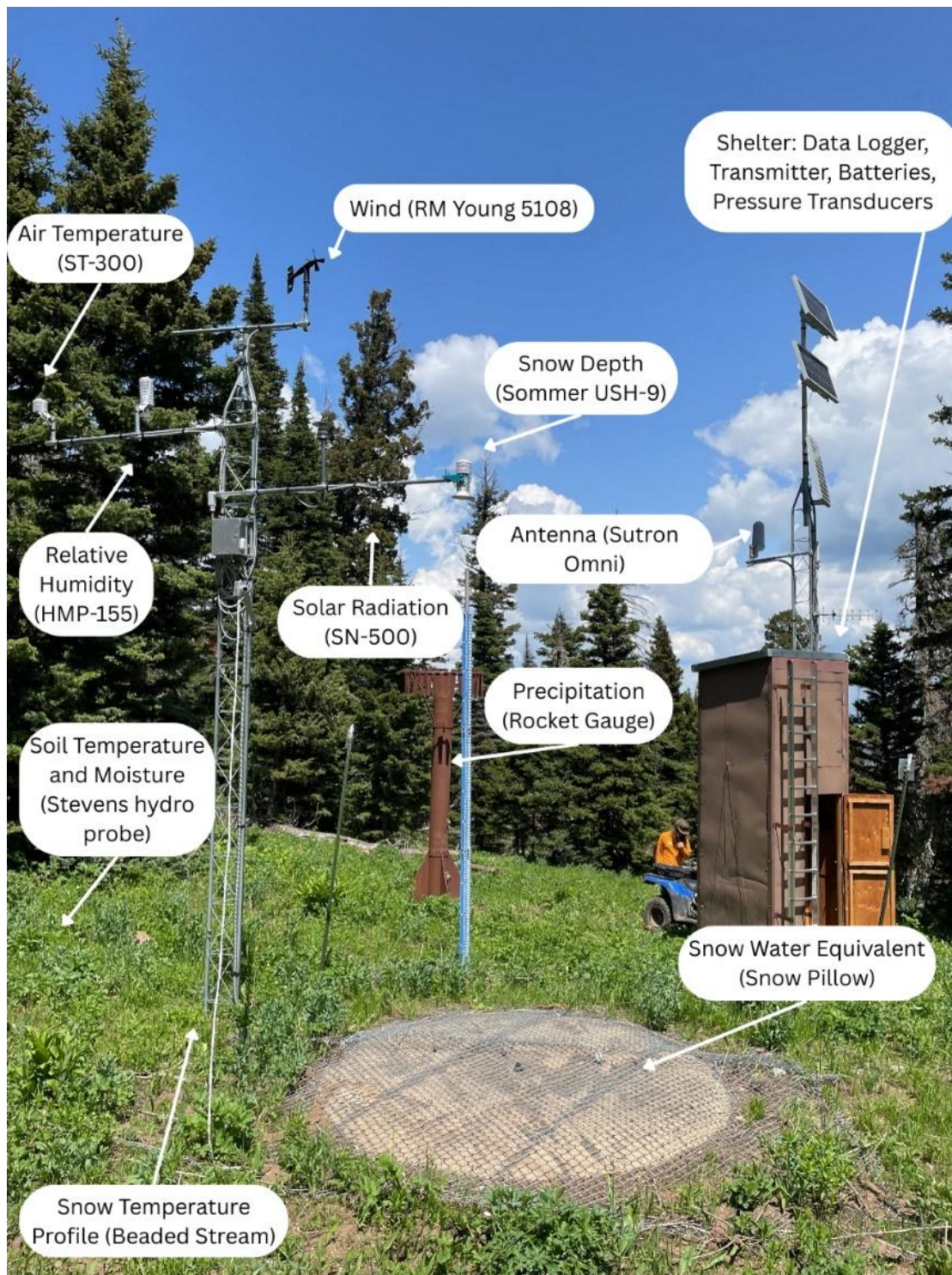


Figure 3: Brackett Creek SNOTEL Supersite (with wind) June 2025. Each site used in this study is similar. (Photo Joe Kral)

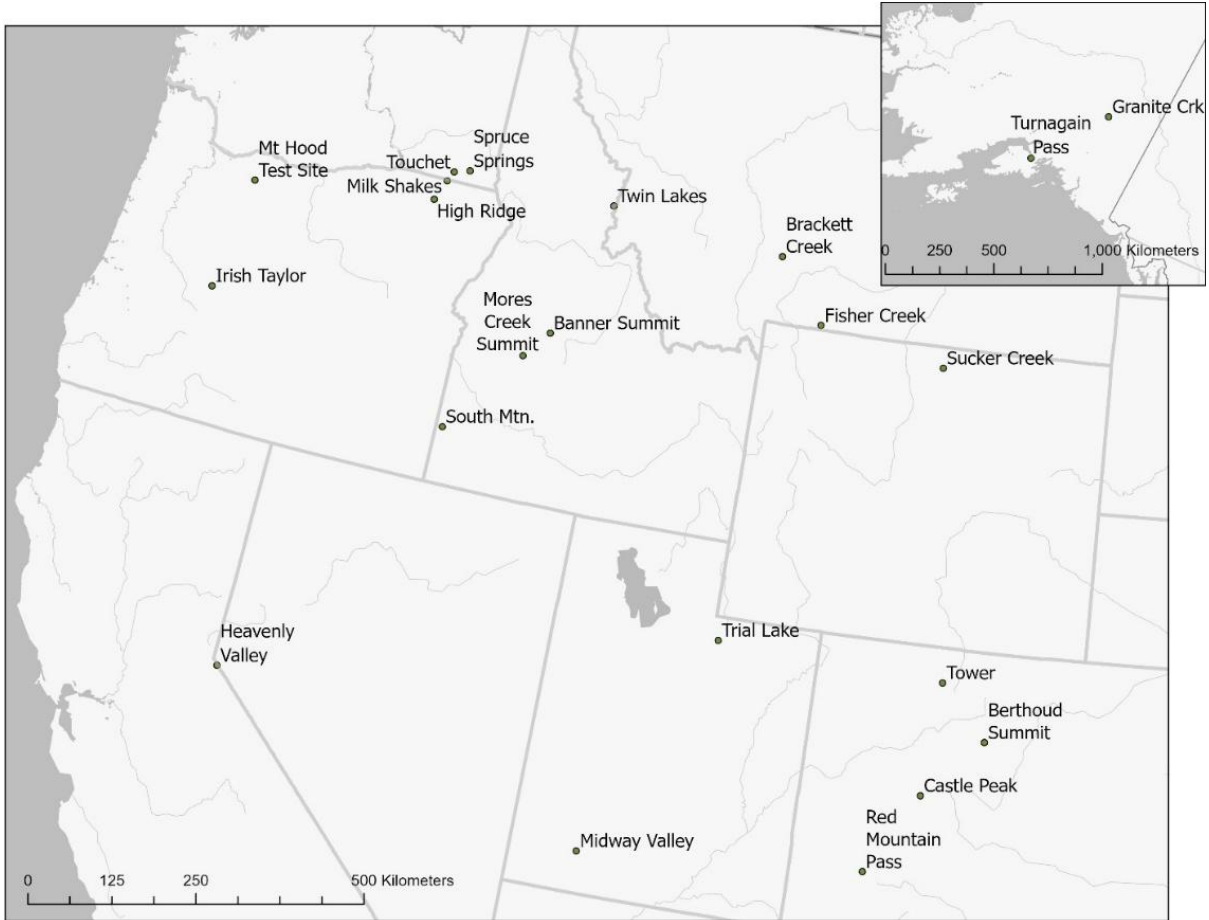


Figure 4: Locations of SNOTEL standardized Supersites

Description of sensors

The wind sensor at SNOTEL sites is either an RM Young 5108 or 5103 anemometer. The Montana Data Collection Office (a subset of the Snow Survey) sets sensors to scan every 5 seconds and average wind direction and speed over those 5 seconds. The hourly outputs are based on these five-second scans, meaning the hourly average wind speed is the average speed of all the five-second scans, the instantaneous value is the last five-second scan taken, and the maximum wind speed is the maximum speed of the five-second scans in that hour. Other Snow Survey offices have a similar setup.

Both wind sensors have a 2.2 mile per hour wind threshold for the turbine to spin, and for a value to be recorded (Young, 2014). During a study conducted by the Snow Survey research and development team at test sites, the 5103 sensor performed better for the lower wind speeds at SNOTEL sites, whereas the 5108 sensor performed better at higher wind speeds, such as ridgelines. The reason wind data at SNOTEL sites may appear low or misrepresentative is that the sites are in forested areas, with wind conditions different from those in the alpine zone.

The solar radiation sensors at SNOTEL sites are being upgraded from Apogee SP-510/610 to Apogee SN-500 sensors. The SP-510/610 sensors collect only net shortwave radiation. The SN-500 sensors collect incoming and outgoing shortwave and longwave radiation. The hourly radiation data is the average radiation over the last hour. Only sites with upgraded radiation sensors were used in this research, as longwave radiation is required as an input for SNOWPACK.

Other Snow Survey sensors measure snow depth, relative humidity, air temperature, SWE, and precipitation. The snow depth sensor used in this study is the Sommer USH-9. The USH-9 is an ultrasonic sensor; thus, it is an active sensor that sends out a noise and waits for the return signal. The snow depth is calculated from the time it takes the sensor to receive the return signal. This sensor is more frequently accurate than prior snow depth sensors at SNOTEL sites because it has a downward-facing cone shield to capture the signal, a wide noise distribution, and an internal process to backfill bad readings. The sensor performs well during snowstorms for these reasons. The Vaisala HMP-155 measures relative humidity. It is a capacitive humidity sensor that measures changes in moisture by finding changes in electrical capacitance as water vapor condenses on a film in the sensor. An Apogee ST-300 temperature sensor is replacing the

current YSI temperature sensors at most sites. The ST-300 sensor is a platinum resistance thermometer that measures electrical resistance. Lastly, both the SWE and precipitation measurements are obtained using pressure sensors. These sensors correlate measured pressure or weight with height. Note that SWE is the amount of water that would be present if the snow in a specific volume was liquid water in that same volume and is equal to the density of snow over the density of water multiplied by snow depth (HEC-HMS Technical Reference Manual, n.d.). For snow depth, relative humidity, air temperature, SWE, and precipitation, the instantaneous value at the top of the hour is used in this work.

Snow Regimes in the US and Switzerland

There are three climatic zones and snowpack regimes recognized in the Western US: maritime, intermountain, and continental (Mock & Birkeland, 2000). A maritime snowpack consists of higher snowfall, shorter accumulation periods, higher snow density, higher temperatures, and a more homogenous snowpack (Mock & Birkeland, 2000, Trujillo & Molotch, 2014). A continental snowpack generally has lower snowfall totals, longer accumulation periods, lower snow density, lower air temperatures, higher snowpack temperature gradients, and a generally more unstable snowpack resulting from more persistent weak layers (Mock & Birkeland, 2000, Trujillo & Molotch, 2014). An intermountain snow regime exhibits characteristics of both maritime and continental settings.

Generally, the term "intermountain" is used to describe the snowpack in Montana, Idaho, and Utah (Mock & Birkeland, 2000). Sometimes, Eastern Washington and Eastern Oregon are described as having an intermountain snowpack, whereas the Wasatch Range in Utah and the

Montana mountains east of the Continental Divide are not. It should also be noted that snow regimes generally follow an elevation gradient, increasing from maritime to continental (Schweizer et al., 2024). These general weather and climate processes of each regime drive snowpack stability and hydrologic properties within each region.

CHAPTER THREE

METHODOLOGY

Overview

Wever et al. (2014, 2015) and Katz et al. (2023) provide the foundation of the methods in this study to improve water transport simulations in the SNOWPACK model. Although in this study we analyze differences among three water transport schemes available in SNOWPACK across different North American snow regimes. We use snow water equivalent (SWE) as our validation metric. We investigate whether SNOTEL sites can be used to run SNOWPACK, as this has not been well documented before. This section discusses the selection of SNOTEL sites, the workflow created for running SNOWPACK, the methods used for analysis, and the procedure for collecting field data.

Site Selection

The Snow Survey program has a standardized supersite program to aid in water-supply forecasting and snow research. Current sites were first upgraded in the summer of 2023 and are dispersed across the American West. However, wind is not included as a standard sensor at supersites, yet wind is a required input in SNOWPACK. Our analysis for this study on using wind data from SNOTEL sites to run SNOWPACK will be discussed later in the results section. Ultimately, we run SNOWPACK with wind data to minimize the effect of changing variables on the outputs and isolate only the change in the water transport equations.

As such, we pivoted from using SNOTEL supersite data to what I will refer to as enhanced SNOTEL sites. These sites have all the required inputs for SNOWPACK, including

wind, but lack a snowpack temperature profile sensor, which is not necessary to initiate SNOWPACK. Snow surface temperature is required for initiation, but can be derived using longwave radiation. See Figure 5 for a map of the enhanced sites that we use in this work. The enhanced sites used in this analysis have short and longwave radiation, wind speed, and relative humidity sensors, in addition to the standard sensor suite for snow depth, SWE, and air temperature data. Refer to Figure 3 in the background section for an example of an enhanced site.

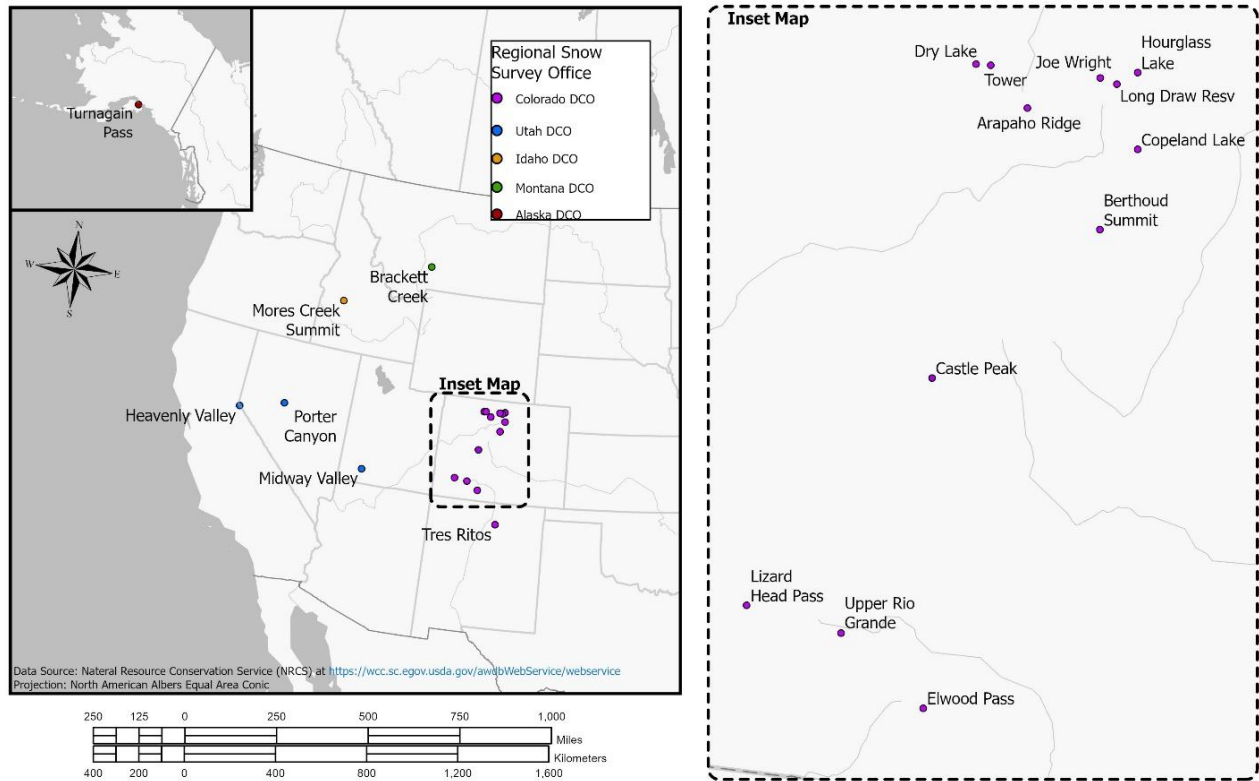


Figure 5: Locations of enhanced SNOTEL sites used in this study

A query of the Snow Survey database found 19 sites that fit our criteria, 12 of which are in Colorado. One site, Mores Creek Summit, has two winters of data while all other sites have

one winter of data. We selected sites that met all necessary criteria, including only those with the new SN-500 solar radiation sensor and those for which data for the entire winter 2024-2025 snow season or earlier were available. The decision to use only SN-500 sensors for solar radiation resulted in fewer sites and fewer winters of data than if we had also used data from sites with SP-510/610 sensors.

The SNOWPACK model needs wind as an input to run. Wind is an integral component of many empirical formulas used to determine new-snow density and energy balances in the model. However, not all SNOTEL sites have an anemometer, and this sensor is not part of a standard supersite. Additionally, the wind at a SNOTEL site is in the same “meadow” as the site and, as such, is in an area of relatively low wind. A brief analysis of the impact of using SNOTEL wind data on SNOWPACK results was conducted to assess the role of wind in our study. The results are shown in Table 7 and Table 8 in the Results section.

After the winter season, only 14 sites could be modeled and used for analysis. Unsuitable sites were either from too-low snow years or from a sensor being broken for an extended period during the winter of 2024-25. In the future, a snow temperature profile to validate SNOWPACK outputs should be evaluated further. We chose not to use the snow temperature profile from the beaded stream sensors since they are still being validated at SNOTEL sites and are not at all enhanced sites.

Running of SNOWPACK - R Workflow

The SNOWPACK model can be run using the user interface in INISHELL, by compiling the source code, or by running the SNOWPACK application from a computer’s command terminal. We developed a workflow in R (version 4.5.1) that encompasses all necessary steps to

produce SNOWPACK outputs and results (Figure 6). The workflow includes a primary script that allows the user to change site information, the dates and data to download, model parameters, and file names. The primary script then runs a series of separate scripts to download SNOTEL data, perform quality control on the data, create input files with the required meteorological data, create a parameter file for the individual model run, runs SNOWPACK calling the created files, transforms outputs into a more useable form, and graphs specific outputs from the model run as a visual check for the user. A separate script is used to upload all model run outputs from all sites for analysis.

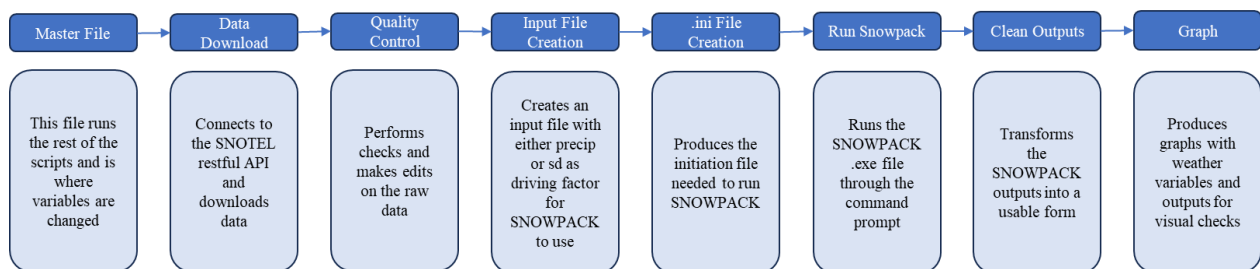


Figure 6: Flow chart showing the R-Studio workflow created to run SNOWPACK

Data download and quality control

Data is downloaded from the Snow Survey database using an Application Programming Interface (API). A URL for the API specifies the station and the desired data. The R script then iterates over downloading each element from the selected station and combines all data frames into a single raw data file for the site. For each site, snow water equivalent, snow depth, precipitation, observed temperature, observed relative humidity, average wind speed, incoming shortwave radiation, and incoming longwave radiation are downloaded. Observed values are used in all cases except for radiation values, which are an average over the last hour, and the

wind values, which are an average wind speed for the hour. There are options for instantaneous wind values and maximum wind speeds from SNOTEL; however, we decided to use the average wind speed to avoid missing any wind events within the hour. Instantaneous wind values are likely to underrepresent or miss wind events, and maximum wind speeds likely overrepresent wind for the hour. Katz. Et al (2023) also use the average wind speed to run SNOWPACK.

Performing quality control on data from each site is essential, since SNOTEL data are regularly quality-controlled only for snow depth, precipitation, and snow water equivalent at the daily timescale (midnight values). Thus, the hourly SNOTEL data require correction. In addition, the other elements are only quality-controlled once a month. If you are using this data in the winter, you need to perform quality control on every data point. The script we created performs this quality control semi-automatically, but significant data errors prevent its execution. In addition to filling in missing data and removing incorrect values during the quality control routine, SNOWPACK has its own quality control measures that use upper and lower limits for each element. These can be set within the parameter file to better align with conditions in the specific region. The limits will catch incorrect values while still allowing the SNOWPACK model to run. The model will also exclude data points that are not consistent with other parameters. For example, if precipitation is predicted based on the inputs but relative humidity is low (the air is dry), the precipitation will be rejected (Snowpack 3.7.0 documentation).

The first step in the quality control routine is to fill in the missing values. If the element had only missing values, an error would be shown. Likewise, if there were no missing values, this step is skipped. The missing values were grouped into two categories: five or more consecutive hours of missing data and fewer than five consecutive hours of missing data. Five

hours was used as the splitting metric because it is common at SNOTEL sites for a few hours of data to be missing, and five hours grouped most of this type of missing data. When the data has a gap of 5 hours or less, linear interpolation between the two known values is used to fill it. A larger gap typically indicates a sensor failure. When this happens, the Snow Survey office estimates the midnight value for the SNOTEL data using in-house estimation tools, like the degree-day method for estimating SWE. As such, gaps in missing data greater than 5 hours are filled with the nearest midnight value in our workflow. The midnight value is quality-controlled by the Snow Survey staff because of daily fluctuations in pressure-sensor readings due to temperature changes.

The last two steps in quality control are setting all negative incoming shortwave radiation values to 0 and ensuring that all precipitation values are always increasing or constant. The precipitation data is then converted from a water-year total to an hourly increment.

Building input and parameter files

Two input files are required for each model run. The first is a .smet text file with the meteorological data. This file contains a header that provides site information, including the number and types of elements, and the order of elements. The model reads the file line by line, with each line starting with a timestamp and followed by comma-separated data. The data are converted from imperial to metric units in this step. The .smet file is used to specify snow depth or precipitation to force the model.

The SNOWPACK model uses ground-surface temperature in its energy-balance equations. The ground surface temperature is included in the .smet file, even though we do not download this metric from the SNOTEL site. We initially assumed this value should be set to 0

degrees Celsius for the modeled period because the highest soil sensor at SNOTEL sites hovers near 0 degrees Celsius in winter. However, after discussions with other researchers, we changed this value to -0.2 Celsius. With the change, we found better model agreement during the first month of snow on the ground and similar agreement for the rest of the winter. We use -0.2 degrees Celsius for the ground surface temperature in this study.

The second input file is a .sno text file. This file provides a snow profile for model initialization. Since we start each model run with no snow, the data in this file is all set to zero except for temperature (since these are in Kelvin). The profile input header also contains site information, as well as environmental factors around the site, such as canopy height and soil albedo. The profile differs when using Richard's equation as the water-transport method, since we then need to include a soil profile.

When using Richard's method, four depths are included in the .sno file to match the soil sensor depths at SNOTEL sites: 4, 8, 20, and 40 inches (or 2, 4, 8, and 20 inches, depending on the site). Volume fractions of ice, water, and voids need to be included and were estimated based on soil moisture readings from the SNOTEL site and web soil survey. The vanGenuchten.cc source code file for the SNOWPACK model includes information for what soil properties to use for different soil types. If using Richard's method for running a specific site in the future, it is recommended to do more in-depth soil analysis for the model. See SNOWPACK documentation (<https://snowpack.slf.ch/doc-release/html/snowpackio.html>) for more specifics on model inputs.

The parameter file is a configuration text file (.ini file) that provides the SNOWPACK model with desired settings. This is also where SNOWPACK can be tuned to better represent real-world conditions of a specific area. We use the standard model parameters and keep all

parameters the same across site runs, only changing the water transport method and setting the model to use either snow depth or precipitation as model forcing. The parameter file also specifies the paths to the input files and where to store the outputs. This file sets the heights of sensors for different meteorological inputs. See Appendix B for the specific settings used. The creation of the .smet, .sno, and .ini files was all based on example SNOWPACK documentation, again see the documentation page for more on this.

Running the model and converting outputs

Once all input and parameter files are created, SNOWPACK can be run. We use SNOWPACK version 3.7.0 for this analysis. The R script that runs SNOWPACK creates a file path to the location where the inputs are stored and where outputs are saved, then runs SNOWPACK from the local command line. Here, the start and end dates for the model run are set, and the file path is specified.

For each site, six models were run, and each of the three water transport equations was run twice. Once with snow depth forcing the model and once with precipitation forcing the model. Each site was run for the winter of 2024-25, and Mores Creek Summit was additionally run for winter 2023-24. Each of these model runs has an associated graphical summary output to determine model run accuracy and if there were errors in inputs or model parameters.

After the model run, outputs are saved as a .pro file that can be uploaded to niviz.org for easy visualization. We transformed the .pro file into a more usable format for our specific analysis. The transformation converts the outputs from list form to tabular form. Graphs for each model run depicting SWE (modeled and observed), melt rates, density, liquid water content, and meteorological values are created from this tabular data for both the total snow season and the

melt season for that site. The snow season is from when snow is on the ground at a specific site until the site is snow-free, and the melt season is the peak SWE date to the melt-out date. We use the peak SWE date as the start of the melt season because peak SWE coincides with snowmelt runoff onset (Gagliano et al., 2023). These graphs are used for initial visual inspection of model output issues. If a problem is found, the model is run again after corrections are made. The data from each model run is then uploaded to a separate script to perform analysis.

Metrics for Analysis

The two main metrics for SNOWPACK's viability at SNOTEL sites are the observed-versus-modeled SWE error and Nash-Sutcliffe Efficiency (NSE) for model fit. We compare hourly SWE as our metric for model error in values, and days off-peak SWE and melt-out at the site as our metric for timing error. SWE is used for validation because it is not an input into the model, but can be found from model outputs. The total SWE at a given timestamp in model outputs is found by dividing each layer's density by the density of water, then multiplying by that layer's height. The SWE at each layer is then summed to get the total SWE for the timestep.

The performance of each water transport method is analyzed at daily and hourly time scales. For the daily time scale, differences in modeled and observed peak SWE, melt-out date, melt season length, and timestep differences in SWE are determined. For the hourly timescale, differences in the layer's liquid water content are determined. This is done only from model to model, since it is not data observed at SNOTEL sites.

We base our analysis methods on Katz et al. (2023) and Wever et al. (2014, 2015). In Katz et al. (2023), they use the root-mean-square-error (RMSE) of the difference between observed and simulated values of SWE at the start of a rain-on-snow event and the RMSE in the

sum of SWE losses over the melt event. Wever et al. (2014) validated SNOWPACK using an average difference in snow height between model outputs and observed values for the entire snow season, and Wever et al. (2015) used the RMSE for snow height, difference in, and RMSE for SWE, and NSE for runoff. For the SWE analysis, Wever et al. (2015) used only point data from snow pit measurements, and Katz et al. (2023) used SNOTEL outputs.

For our analysis, we calculate the hourly error at each site between model outputs and observed SNOTEL data, then compute the site's mean hourly error. We then calculate the mean absolute error for each of the six model run types across all sites. With this, the metric uses the error at all hourly timesteps across 14 sites. We also use NSE for SWE at each site (based on the hourly data) for a metric that accounts for sites that both over-estimate and underestimate SWE.

Field Work

I conducted fieldwork to better understand the data collected from SNOTEL sites and the outputs from SNOWPACK model runs. The data will not be used to draw any conclusions. The field work consisted of one day in April, visiting the Brackett Creek SNOTEL site in the Bridger Mountain range. A snow pit was dug to record grain types, a hardness profile, density, and liquid water content. We took measurements and conducted a full pit profile using Snow, Weather, and Avalanche Guidelines (American Avalanche Association, 2022). Density was taken every 5 cm with a density cutter. Liquid water content was also measured at 5 cm intervals using the SLF SNOWPRO-17 (fpga company SLF, 2024).

CHAPTER FOUR

RESULTS AND DISCUSSION

SNOWPACK Simulations

This first section of results (along with the daily analyses) addresses whether SNOTEL data can be used to run SNOWPACK and tests our novel R workflow described in the methods section. Figure 7, Figure 8, Figure 9, and Figure 10 are used as examples of outputs examined after each model run to provide an initial impression of effectiveness.

Model case studies

Figure 7, Figure 8, Figure 9, and Figure 10 show results from both precipitation and snow depth model runs when using the Richards equation for water transport at the Bracket Creek site in Montana and the Turnagain Pass site in Alaska. The output charts from all other modelled sites are similar, and the rest of the Bracket Creek and Turnagain Pass results are in Appendix A. Results from other sites can be obtained by email request. Here, I discuss these two individual model runs as a case study in our workflow. These sites are chosen because they are discussed (as examples) throughout the rest of the thesis.

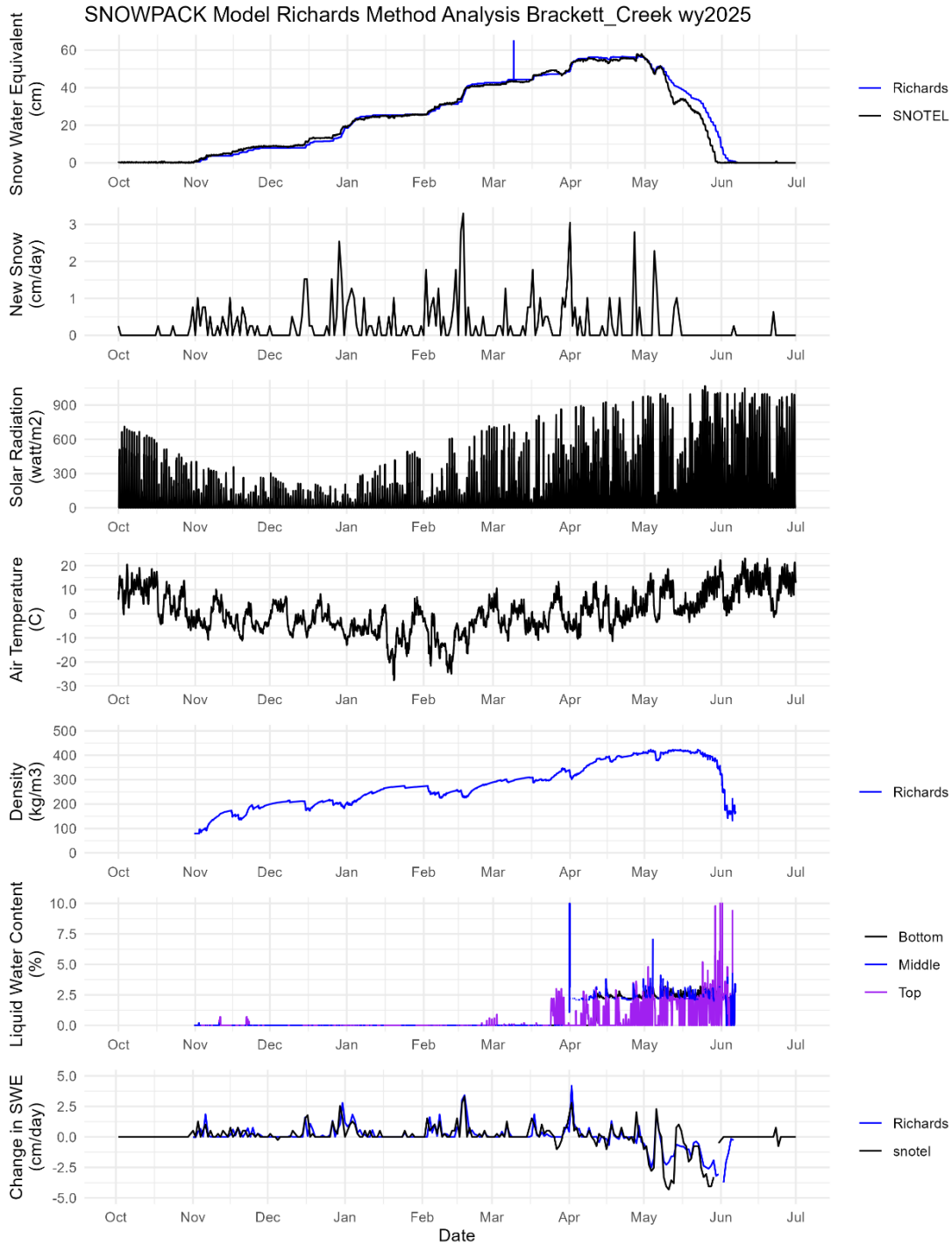


Figure 7: Brackett Creek results for a model forced with snow depth and run with the Richards Equation for the water transport model. The top chart in the figure compares model SWE and observed SWE. Below these model outputs are weather inputs for snowfall, solar radiation, and air temperature to aid in determining snow and melt events throughout the winter (note that the

new snow daily chart shows the amount of SWE added to the snowpack from one midnight value to the next). Below this are the density and liquid water content model outputs. The liquid water content is shown for the top, middle, and bottom of the snowpack. The middle is determined by the median calculation layer. The bottom chart is the changes in SWE.

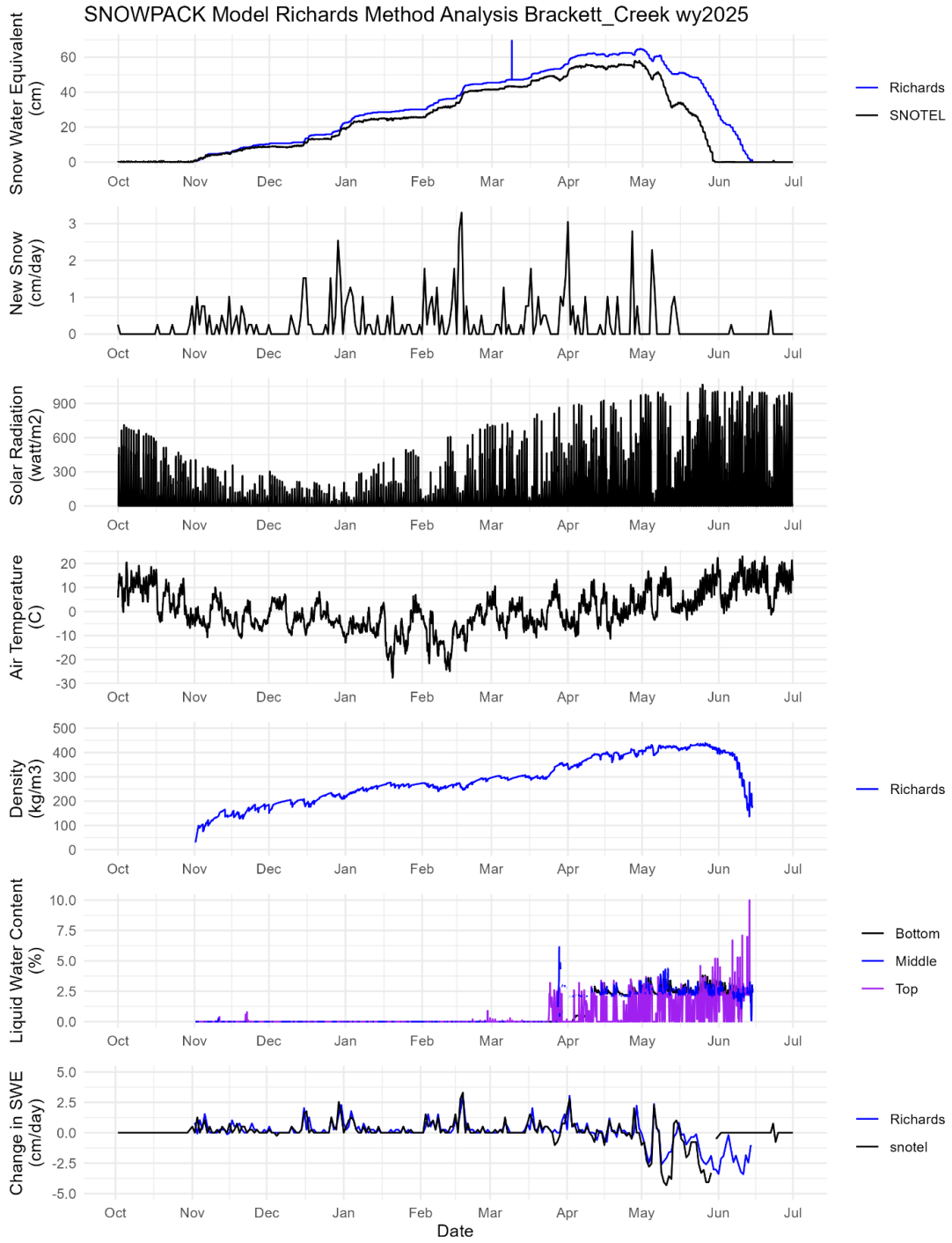


Figure 8: Brackett Creek results for the model being forced with precipitation and run with the Richards equation for the water transport model

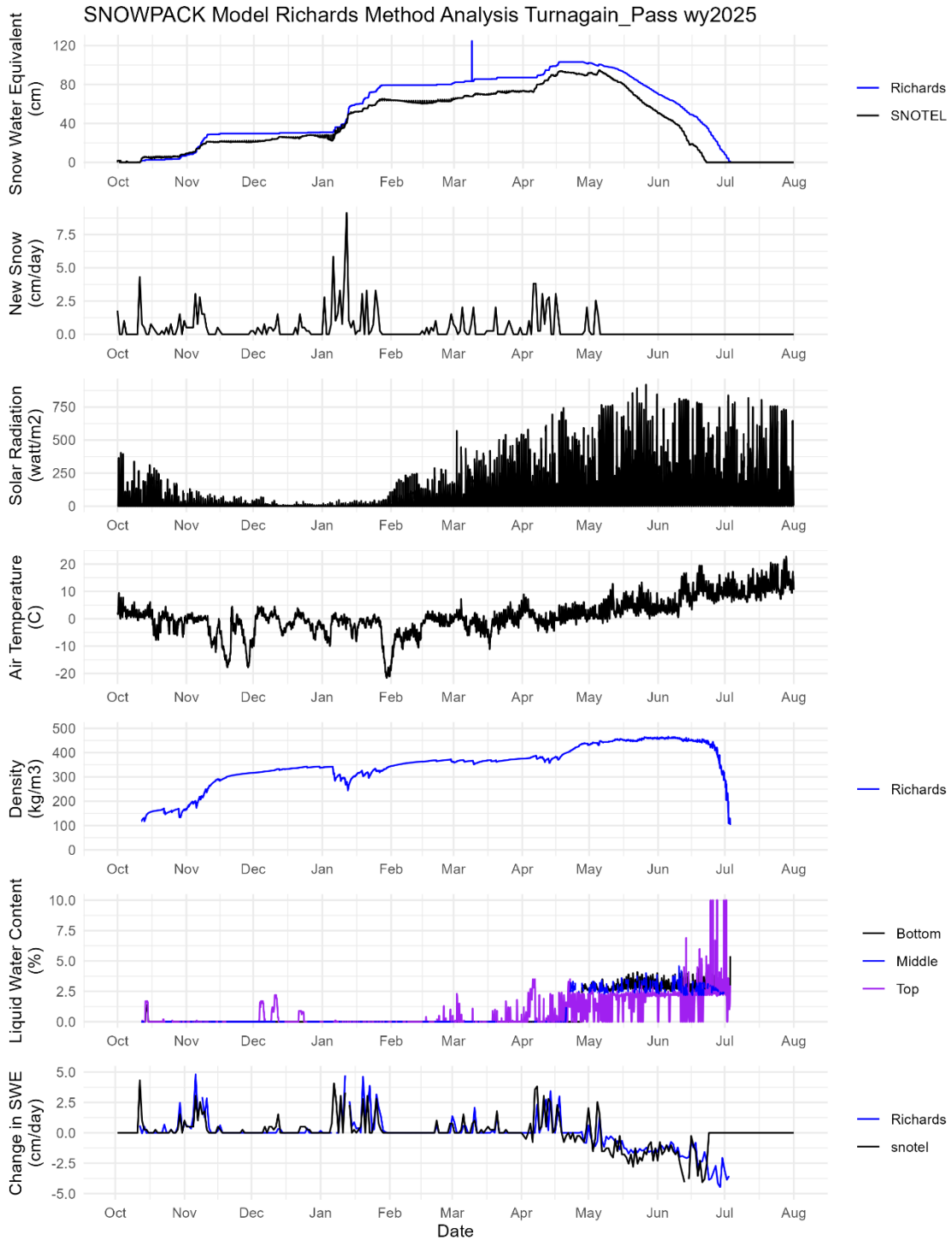


Figure 9: Turnagain Pass results for the model being forced with snow depth and being run with the Richards method for water transport

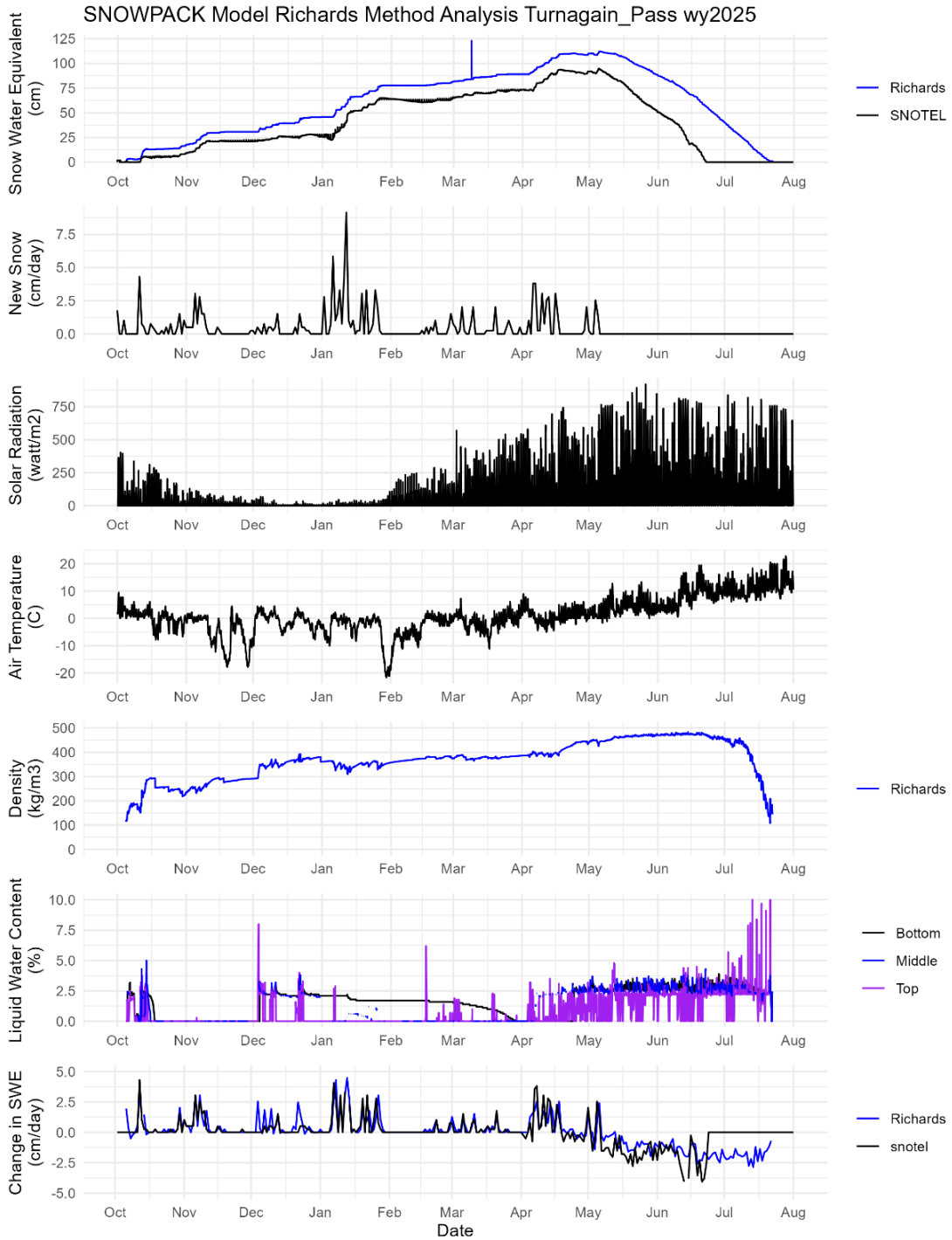


Figure 10: Turnagain Pass results for the model being forced with precipitation and being run with the Richards method for water transport

Our novel model workflow successfully ran SNOWPACK with SNOTEL data at all 14 sites. The workflow proved flexible enough to run the model with different parameters, perform sensitivity analyses, and run across many sites. In Figure 7, Figure 8, Figure 9, and Figure 10 we visualize the differences between modelled and observed SWE in the top plot. Both precipitation and snow depth model runs overestimate SWE during the melt period in these plots. The precipitation run slightly overestimates SWE during the accumulation period, while the snow depth run closely tracks the observed SWE at Brackett Creek. The vertical blue line in all output plots (Figure 7 for example) is an error in graphing that we had issues resolving. This point was removed for additional analysis.

At Turnagain Pass (Figure 9 and Figure 10), we see that SWE is overestimated from observed data more than at Brackett Creek. When comparing both sites' snow depth forcing models and new snow graphs, hints as to why are seen. At Brackett Creek, winter 2024-25 was characterized by many snowfall events, adding 0.5-2 cm of SWE, with 5 events totaling 2-3 cm of additional SWE to the snowpack. None of the larger snow events appears to change the error in SWE, and the modelled SWE aligns with the observed SWE during the accumulation period. At Turnagain Pass, there were three main spells of snowfall lasting about a month and a half each, with a few weeks' lull between each. Most storms added between 0.5 and 3 cm of SWE to the snowpack, with three adding between 3 and 8 cm. The first larger snow event came in October and did not affect the error much; the last November storm caused the first bump in error. The largest storm event of the winter in January added 8 cm of SWE in a day and caused the error in SWE to increase in overestimation to 20cm. This leads us to hypothesize two possible sources of error in the SNOWPACK model. Either the model struggles with large snow

events, when the initial density of the snow is high (as it is in the maritime snowpack compared to intermountain), or some combination of the two. This will be discussed further in the model error section.

Model validation

Here, we analyze overall model performance using Nash-Sutcliffe Efficiency (NSE) and present the mean absolute error in SWE values. The mean error in SWE values for all model runs is combined in Figure 11 and Table 2. Error in SWE is the difference between the modeled and observed SWE at each hourly time step. Once the output graphs for each site were examined, it was determined that this method was reasonable for error, as outputs tended to be consistent in over- or underestimating SWE for that specific model run. The season summary plot provides a big-picture view of the results; however, the SWE error differs greatly between accumulation and melt seasons. Because of this, we split our results into these two periods for further analysis.

In Table 1 we find the overall model performance using NSE. The closer the NSE value is to 1, the better the model's fit. If the number is negative, this means that taking the average data value would give a better fit than the model. Values from 0.75 to 1 indicate very good model performance, 0.65 to 0.75 indicate good fit, 0.50 to 0.065 indicate satisfactory fit, and an NSE below 0.5 means we have an unsatisfactory fit with the model (Nash & Sutcliffe, 1970)(Legates & McCabe, 1999).

Table 1: Nash-Sutcliffe Efficiency values for all six model run types for the whole snow season, accumulation period, and for the melt period. NSE is determined based on the fit of hourly data at each of the 14 sites.

Snow Season	Bucket SNWD	NIED SNWD	Richards SNWD	Bucket PREC	NIED PREC	Richards PREC
Full	0.868	0.887	0.835	0.345	0.418	0.436
Accumulation	0.928	0.929	0.882	0.604	0.619	0.507
Melt	0.759	0.803	0.735	-0.327	-0.127	0.177

We find that out of our 6 model run types, all snow depth model runs have good or better fit with the observed data, while models run with precipitation data have satisfactory or worse model fit, with the highest NSE being 0.619. When looking at the model over the entire snow season, all snow depth runs have a very good model fit, while all precipitation model runs have an unsatisfactory model fit. During the accumulation period, model performance improved across all six model types, with NIED snow depth runs achieving the highest NSE of 0.929. In the melt period, all model runs decrease in performance. Here, snow depth runs for the Bucket and NIED methods are on the lower end of “very good,” and the Richards method has a good model fit. For the precipitation model runs, the Bucket and NIED NSE values are below zero, and the Richard’s method fit is unsatisfactory. See Appendix B for NSE results at each individual site.

Wever et al. (2015) had similar findings between forcing SNOWPACK with snow depth versus precipitation. They conclude that one reason for the significant difference in model performance is that snow depth allows the model to compensate for deviations between measured and modelled snow height due to over- or underestimated snow settling, snowmelt, or wind-driven erosion and deposition. This compensation is not possible when precipitation data is used as an input instead. An effect of this is that overestimations in SWE from specific snow events will persist in the model throughout the snow season when precipitation data is used

instead of snow depth. This is what we saw in Figure 10: Turnagain Pass results for the model being forced with precipitation and being run with the Richards method for water transport.

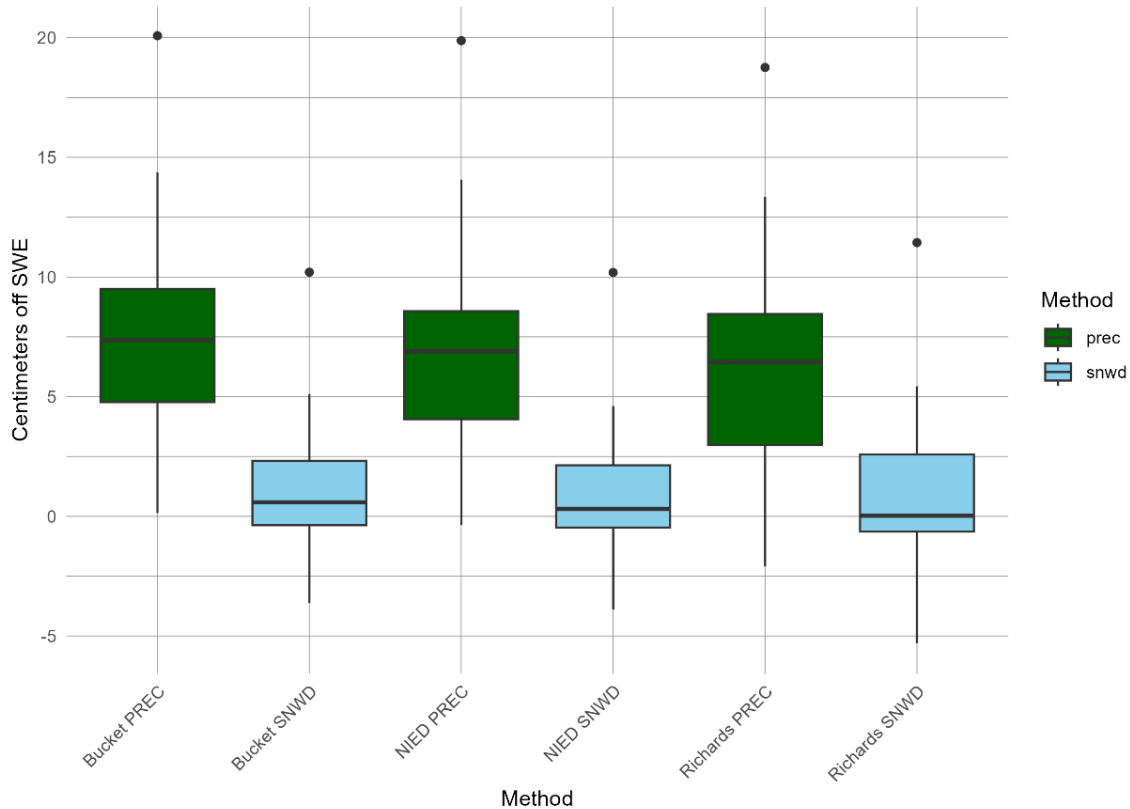


Figure 11: Boxplot of Snow Season error in SWE for different model run types, precipitation (prec) model runs are in green and snow depth (snwd) model runs are in light blue. The data in this plot is the average hourly error for each site ($n = 16$).

Figure 11 presents conclusions on the amount of SWE error for each model type. As found in Table 1, using precipitation to force the model results in greater error than forcing with snow depth. The snow depth performance ranges from -5 to 5 cm relative to observed values, although these numbers appear better than they are because snow depth slightly underestimates SWE during accumulation and slightly overestimates during the melt period. Precipitation as model forcing introduces more error than using snow depth; some of this error is due to greater

model tuning needed to determine when precipitation is solid, liquid, or a mix – especially given the many different snowpack regimes and site elevations used in this study.

Table 2: Full season mean error in SWE for different model run types

	Site	Bucket SNWD	NIED SNWD	Richards SNWD	Bucket PREC	NIED PREC	Richards PREC
1	Berthoud_Summit	1.214	0.525	0.881	14.099	14.088	13.338
2	Brackett_Creek	1.254	1.411	0.791	6.210	5.805	6.381
3	Castle_Peak	-0.367	-0.256	-0.493	8.123	7.597	7.464
4	Elwood_Pass	-0.084	-0.093	-1.067	0.138	-0.370	-2.083
5	Heavenly_Valley	0.386	0.096	-0.180	10.779	10.161	11.420
6	Hourglass_Lake	-1.978	-1.744	-2.877	2.104	1.808	1.512
7	Joe_Wright	-3.629	-3.887	-5.302	14.361	13.778	12.665
8	Lizard_Head_Pass	-0.381	-0.715	-0.152	6.187	4.074	2.585
9	Long_Draw_Resv	-2.153	-2.456	-3.538	8.205	8.040	6.521
10	Midway_Valley	2.624	2.551	2.876	0.818	0.985	0.055
11	Mores_Creek_Summit_24	2.732	2.193	2.676	9.072	7.961	6.678
12	Mores_Creek_Summit_25	5.111	4.606	5.431	6.947	6.471	5.592
13	Tower	0.783	0.560	0.207	4.533	4.003	3.109
14	Turnagain_Pass	10.201	10.188	11.436	20.080	19.875	18.754
15	Upper_Rio_Grande	-0.328	-0.385	-0.468	4.851	4.724	5.445
16	Absolute Average	2.215	2.111	2.557	7.767	7.315	6.907

From Table 2, we can see that for all transport equations forced with snow depth, the error is mostly between -3 and 3 cm, with Turnagain Pass in Alaska as the biggest standout from the others. Turnagain pass has about 10 cm of error for all three transport models. This site had the third-highest peak SWE of any other site run (94.0 cm), the first being Tower in Colorado (the only site to reach above 100cm of SWE), and the second being Mores Creek Summit in Idaho (97.8 cm peak SWE). The Turnagain Pass site is also the lowest-elevation site used, at 567 meters above sea level, and is the closest to the ocean.

The full-season error is similar to what Wever et al. (2014, 2015) found. They had snow height errors ranging from -23 to 42 cm across different model runs for entire snow seasons, with RMSEs of 4.16 and 4.11 cm for the Bucket and Richard's method model runs (respectively)

when snow depth was used in the input data. For SWE error when comparing snow depth forced model outputs to snow pit measurements, they found 3.93 cm of error with both the Bucket and Richards methods. We found 2.22 and 2.56 cm of error in these two cases, although again, we compare across the entire snow season at each hour. When running the model with precipitation as an input, Wever et al. (2015) found 8.50 cm of error for the Bucket method and 9.90 cm for the Richards method. For these model types, we found errors of 7.77 and 6.91 cm, respectively.

The results when breaking the outputs into accumulation and melt periods are presented next. Each site was broken into the two periods based on when the observed peak SWE was reached. Figure 12 shows the peak SWE date and value for each site, providing context for the results split on either side of this date.

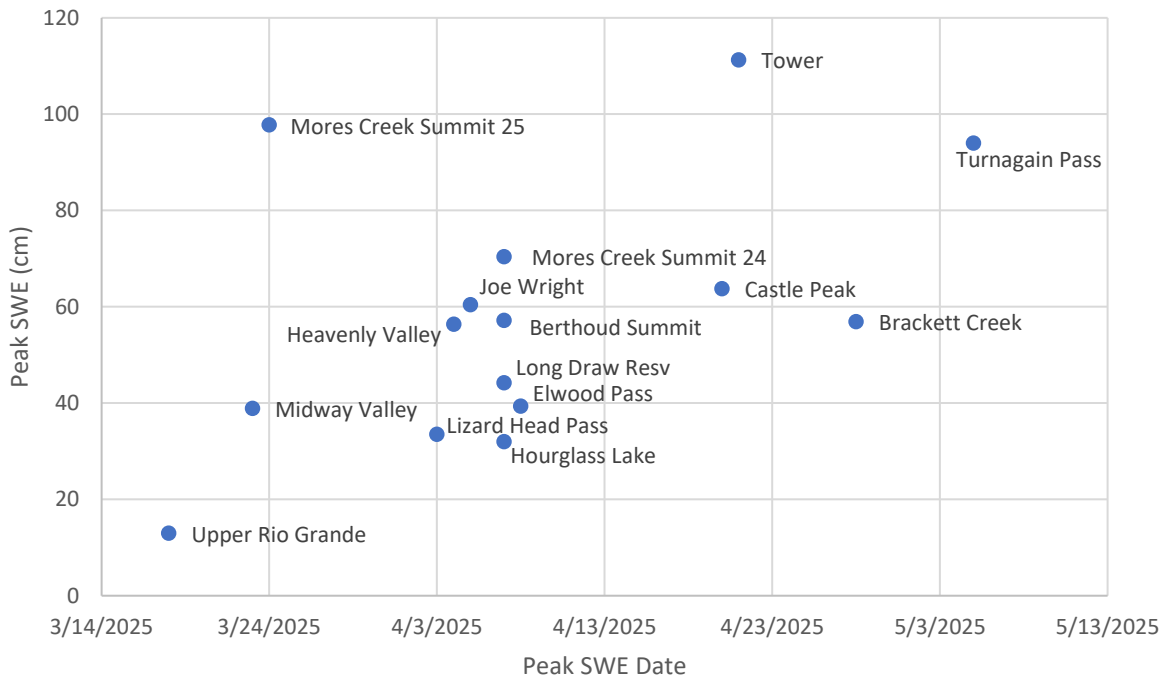


Figure 12: The date and value (cm) of peak SWE at each SNOTEL site

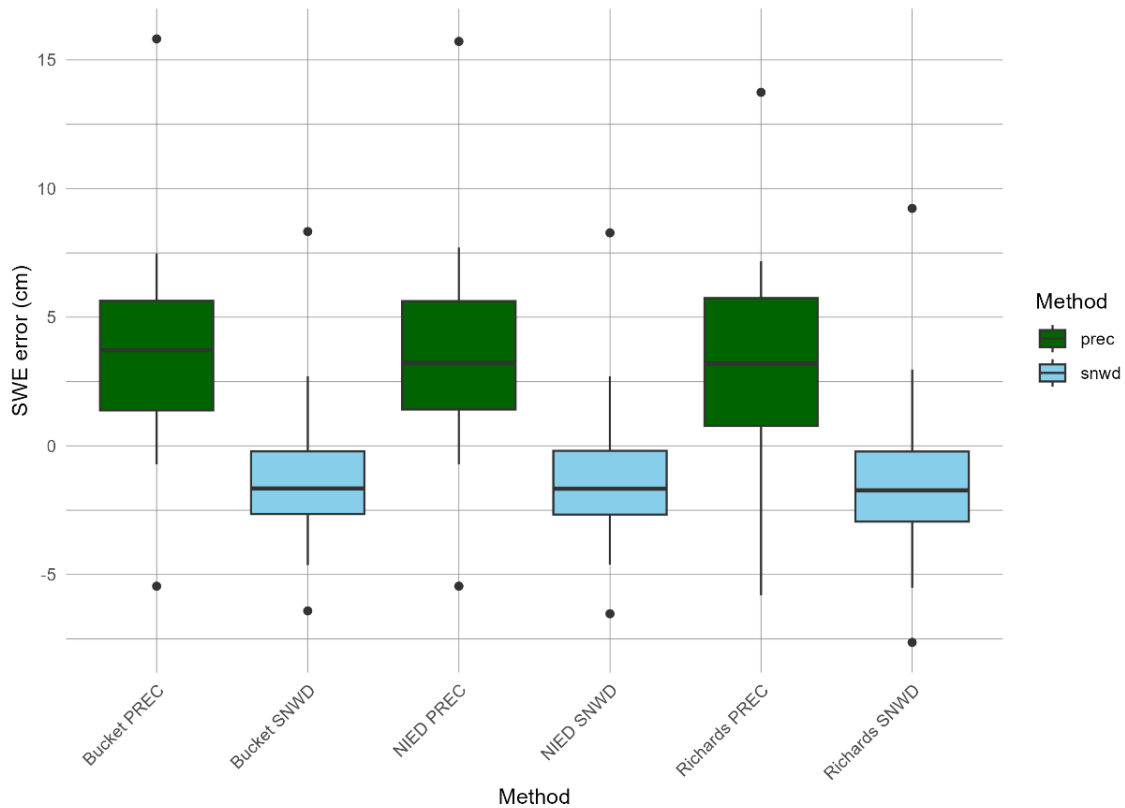


Figure 13: Boxplot of Accumulation period with error in SWE for different model run types

We first examine results for the accumulation period. In Figure 13 we see that in general model runs have lower error than the error for the entire snow season. The precipitation runs have a higher spread and generally overestimate SWE while the snow depth runs are more consistent in error between separate sites and underestimate SWE slightly in most cases. Each model run also has outliers both above and below the medians. With snow depth as an input the model outputs are on average underpredicting SWE, whereas for the entire snow season values were overestimated.

In the accumulation error Table 3 we can see that Turnagain Pass again had the most error. Overall, the differences between precipitation and snow depth model runs are slightly less during the accumulation period.

Table 3: Table of the accumulation period with mean error in SWE for different model run types

	Site	Bucket SNWD	NIED SNWD	Richards SNWD	Bucket PREC	NIED PREC	Richards PREC
1	Berthoud_Summit	-1.487	-1.499	-1.790	5.070	5.082	5.348
2	Brackett_Creek	0.185	0.266	-0.221	3.588	3.406	3.569
3	Castle_Peak	-1.922	-1.861	-2.000	5.573	5.578	5.955
4	Elwood_Pass	-3.262	-3.169	-3.082	-5.453	-5.452	-5.807
5	Heavenly_Valley	-2.446	-2.501	-2.899	6.024	6.031	7.030
6	Hourglass_Lake	-3.694	-3.501	-3.796	0.836	0.815	0.572
7	Joe_Wright	-6.411	-6.524	-7.637	7.473	7.710	7.186
8	Lizard_Head_Pass	-2.241	-2.199	-1.664	3.848	2.306	1.484
9	Long_Draw_Resv	-4.633	-4.616	-5.513	2.795	3.042	2.833
10	Midway_Valley	-0.344	-0.344	-0.206	-0.710	-0.710	-0.677
11	Mores_Creek_Summit_24	-1.271	-1.305	-1.436	2.350	2.119	0.841
12	Mores_Creek_Summit_25	1.897	1.824	2.433	1.559	1.612	0.841
13	Tower	-1.821	-1.832	-1.874	-0.289	-0.403	-1.076
14	Turnagain_Pass	8.331	8.279	9.230	15.819	15.719	13.741
15	Upper_Rio_Grande	-0.732	-0.726	-0.688	5.852	5.769	5.678
16	Absolute Average	2.712	2.696	2.964	4.483	4.384	4.176

Figure 14 illustrates the melt period error. All model run types have more error than they had during the accumulation period. The spread in the precipitation error increased more than the spread in error for the snow depth runs when compared to the accumulation period. Additionally, all model runs except one over estimated melt. On average the mean error was at least 5.4 cm above observed. The mean melt error for snow depth runs was 6.08 cm across the three transport methods and all sites compared to 2.79 cm during the accumulation period. Also, the mean melt error for the precipitation runs was 15.78 cm compared to 4.35 cm during the accumulation phase.

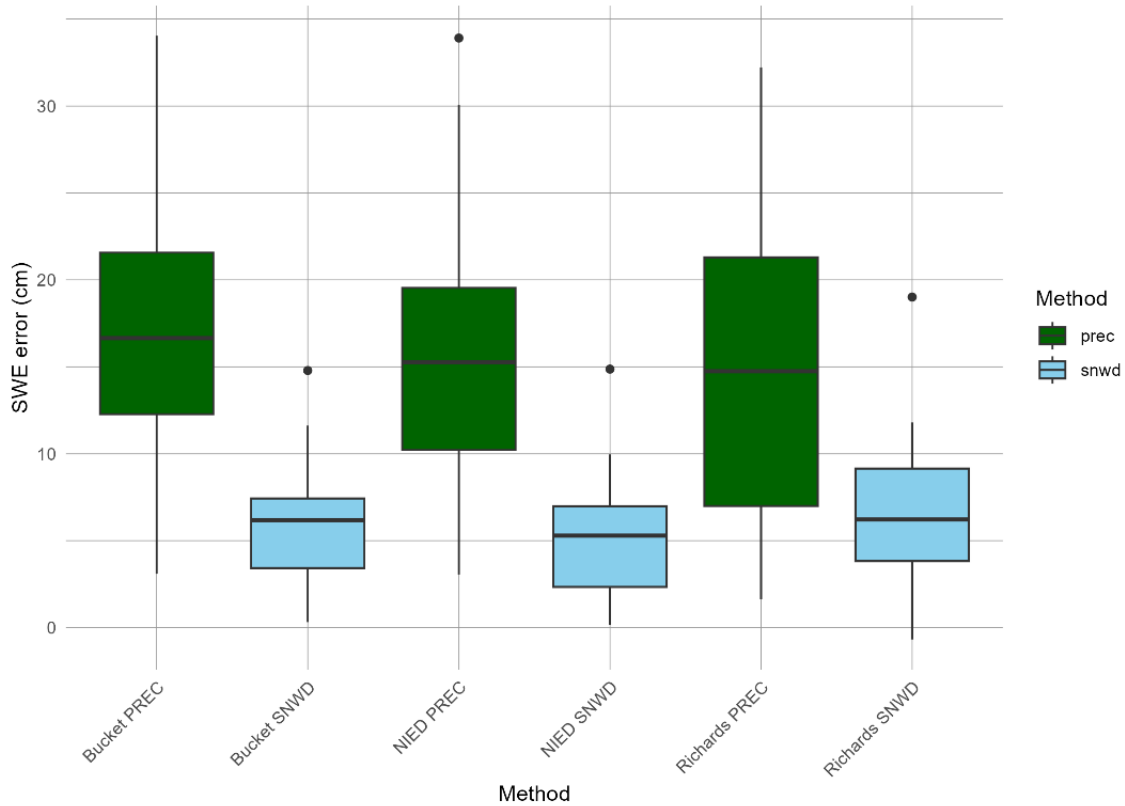


Figure 14: Boxplot of ablation period for different model run types

Table 4 highlights the difference between precipitation and snow depth model runs. Snow depth produces better results and requires less model tuning (precipitation can be tuned in parameter settings for when it will fall as rain versus snow). These outputs show that, for operational use of SNOWPACK by avalanche centers in the United States, when using SNOTEL sites as inputs, snow depth may be a good option. Of interest in Table 4 is that only one site had better model performance with precipitation forcing. This happened at Midway Valley, a site in southwestern Utah. The higher SWE error in the melt season compared to the accumulation period could result from inaccuracies in modeling melt, transpiration, and wind-driven energy fluxes.

Table 4: The mean error in SWE during the melt period

	Site	Bucket SNWD	NIED SNWD	Richards SNWD	Bucket PREC	NIED PREC	Richards PREC
1	Berthoud_Summit	7.177	4.997	6.883	34.038	33.912	29.091
2	Brackett_Creek	4.742	5.147	5.305	14.759	13.626	16.731
3	Castle_Peak	3.970	4.217	4.066	15.233	13.227	11.761
4	Elwood_Pass	7.055	6.818	6.189	12.698	11.047	7.467
5	Heavenly_Valley	6.331	5.548	8.872	20.758	18.829	22.744
6	Hourglass_Lake	0.801	1.101	3.109	4.155	3.414	4.668
7	Joe_Wright	0.749	0.262	-0.677	25.202	22.832	23.058
8	Lizard_Head_Pass	3.459	2.348	5.830	11.017	7.721	5.581
9	Long_Draw_Resv	3.325	2.315	1.619	20.154	19.078	14.678
10	Midway_Valley	7.039	6.856	9.971	3.091	3.505	1.640
11	Mores_Creek_Summit_24	11.621	9.960	11.592	23.996	20.931	20.814
12	Mores_Creek_Summit_25	10.751	9.487	11.805	16.402	14.995	14.821
13	Tower	8.181	7.358	6.250	18.233	16.522	14.166
14	Turnagain_Pass	14.788	14.870	19.013	30.523	30.063	32.221
15	Upper_Rio_Grande	0.318	0.159	0.758	3.252	3.055	4.605
16	Absolute Average	6.020	5.430	6.796	16.901	15.517	14.936

The next set of figures shows the days off of peak SWE and the melt-out date from the model compared to the observed date. Here, we are analyzing timing errors in SNOWPACK outputs rather than value errors. Figure 15 shows the days off of peak SWE. In contrast to the mean error analysis, all six model runs are relatively similar in the error of prediction of peak SWE. The Bucket and NIED precipitation model runs have the largest spread. The means for each model run range from 9 to 15 days off peak SWE. When we forced SNOWPACK with precipitation and excluded Berthoud Summit, Joe Wright, Long Draw Reservoir, and Elwood Pass, the absolute error for the bucket approach is 7.4 days and 6.6 days for the NIED scheme. The sample size for this analysis is 15. Consistency in error across model runs indicates that the water transport equations have less impact on model outputs and errors during the accumulation period than during the melt period. This makes sense as there is less melt during this time.

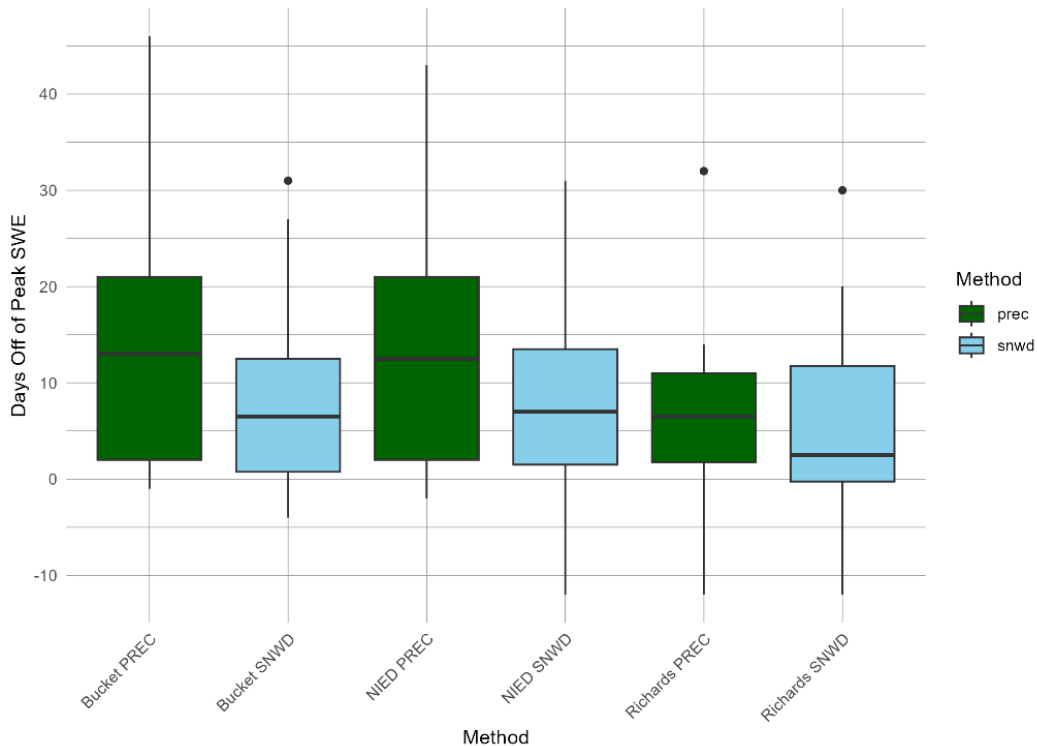


Figure 15: Boxplot of days modelled peak SWE is from observed peak SWE

Looking at Table 5 we see that it is mostly Colorado sites that were more than 10 days off peak SWE, with the exception of the Lizard Head Pass and Upper Rio Grande sites that are both only 1 to 4 days off peak SWE for all model runs. These sites are located in a similar area of southwest Colorado. The other site in that area, Elwood Pass, was also interesting. The bucket and NIED model runs for both snow depth and precipitation overestimated the timing of peak SWE by more than 10 days, whereas the two Richards equation model runs slightly underestimated it. That was the only occurrence of this situation. The NRCS Snow Survey database shows that Upper Rio Grande was at 56% of its median (observed value of 2.7 in SWE) at the end of March 2025, and Lizard Head Pass was at 86% of its median (observed value of 12.4 in SWE).

Also, of interest in Table 5 is that the error at Turnagain Pass was low for days off peak SWE, even though the modeled SWE error was high at the site. This happens because, while the SWE is consistently modeled higher than observed at the site, the general shape of the SWE time series is very similar across model runs compared to the observed SWE (Figure 10). This occurrence is what is causing the precipitation runs across all sites to have a more similar error to the snow depth models for peak SWE compared to the error in SWE analysis.

Table 5: Days off of peak SWE for each site and different model run types

	Site	Bucket PREC	Bucket SNWD	NIED PREC	NIED SNWD	Richards PREC	Richards SNWD
1	Berthoud_Summit	43	31	43	31	32	30
2	Brackett_Creek	2	0	2	0	2	0
3	Castle_Peak	18	16	18	19	11	11
4	Elwood_Pass	32	12	32	13	-1	-3
5	Heavenly_Valley	1	2	1	4	-2	-1
6	Hourglass_Lake	-1	-1	-2	-12	-12	-12
7	Joe_Wright	46	27	32	27	14	20
8	Lizard_Head_Pass	3	2	3	3	3	1
9	Long_Draw_Resv	30	12	30	12	12	4
10	Midway_Valley	15	14	15	15	11	14
11	Mores_Creek_Summit_24	11	5	2	6	3	7
12	Mores_Creek_Summit_25	17	8	16	8	9	17
13	Tower	11	0	11	0	11	0
14	Turnagain_Pass	0	-4	1	-3	1	-8
15	Upper_Rio_Grande	2	1	2	2	4	1
16	Absolute Average	15	9	14	10	9	9

With days off melt out error, seen in Figure 16, the precipitation model runs have more error than the snow depth runs. The snow depth model runs show similar errors in melt-out dates as they did for the days of peak SWE, though with a smaller spread. The average errors for the three transport models being 6 or 7 days off. The average error for the precipitation forced models was 15 days for the Richards method, 20 days for NIED, and 21 days for the bucket method. Turnagain Pass has the second most errors to Berthoud Summit. This will be discussed

more in Figure 36, whether this error is from the overestimation of SWE causing a longer melt out than observed, or issues with the model in a maritime climate.

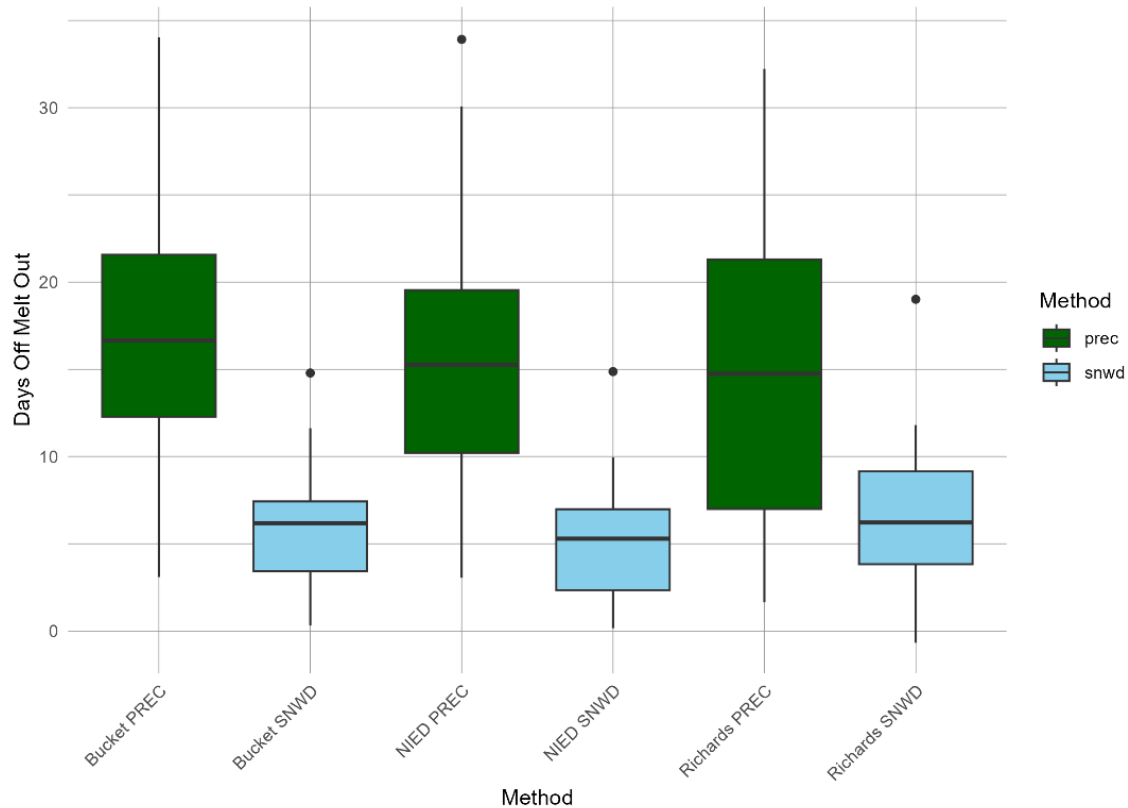


Figure 16: Days off of melt out for different model types

These tables show that 14 sites were analyzed (Mores Creek Summit has two winters of data, hence the 15 lines of results), even though 19 enhanced sites were found. Two of the sites, Tres Ritos in New Mexico and Porter Canyon in Nevada, had too low of snow years for the model to work. They both had multiple periods with no snow on the ground during the winter of 2024-25. The SNOWPACK model does not work well in these instances. Copeland Lake in Colorado was not used due to large daily fluctuations in precipitation data, and model SWE results consistently overestimating SWE by more than two times the observed. Dry Lake and

Arapaho Ridge also had sensor issues. At Dry Lake in Colorado, there was no shortwave radiation data for most of the winter, and many issues with the snow depth data. At Arapaho Ridge, the relative humidity sensor did not have data until an issue was fixed with a site visit in June. These were the reasons those five sites were left out of the study.

Table 6: Days off of melt out date for each site with different model run types

	Site	Bucket PREC	Bucket SNWD	NIED PREC	NIED SNWD	Richards PREC	Richards SNWD
1	Berthoud_Summit	35	8	34	7	29	6
2	Brackett_Creek	15	6	14	7	14	5
3	Castle_Peak	11	4	10	3	9	3
4	Elwood_Pass	21	5	20	5	9	2
5	Heavenly_Valley	27	8	26	8	23	7
6	Hourglass_Lake	20	-3	20	-3	8	4
7	Joe_Wright	28	10	26	9	20	8
8	Lizard_Head_Pass	34	7	30	5	14	4
9	Long_Draw_Resv	22	7	21	6	19	3
10	Midway_Valley	15	8	15	8	10	7
11	Mores_Creek_Summit_24	26	17	25	16	23	14
12	Mores_Creek_Summit_25	18	9	18	9	15	8
13	Tower	6	-1	5	-2	4	-2
14	Turnagain_Pass	29	12	29	12	29	10
15	Upper_Rio_Grande	13	0	13	-1	3	-2
16	Absolute Average	21	7	20	7	15	6

Overall, the SNOWPACK model performed well when comparing SWE outputs to observed SWE. It was found that precipitation-forced models tend to overpredict snowfall and, consequently, snow height, similar to findings in Canada when forcing models with forecasted data (Bellaire et al., 2011). This highlights the issue with using forecasted data. One, it is hard to forecast correct precipitation amounts over a large area, and two, even when using measured precipitation (as found here), the model does not perform as well as when snow depth is used as the input instead. We also see that more model tuning is needed when forcing with precipitation in each area to run the model accurately. It is easier and more accurate to run the model with

snow depth and standard parameters and still get reliable results when forcing the SNOWPACK model with weather station data.

Field Observations

The field work for this study consisted of one day at the Brackett Creek SNOTEL station in April of 2025 (see Figure 17). However, during my time working on this project, I also worked with the NRCS Montana Snow Survey. This work consisted of summer maintenance and upgrades of the existing SNOTEL network, and the installation of a new site in the Absaroka Mountains of Montana. The summer maintenance work allowed me to gain an intimate knowledge of site characteristics, the sensors used and how they operate, and where the data comes from. Winter work consisted of data quality control, writing water supply forecasts, and collecting data at snow courses. This work helped me learn how to work with SNOTEL data and better understand SWE measurements. Working for the Snow Survey is part of what made this project possible.

The results from a pit profile, density profile, and a liquid water content profile are presented here. These results are compared to SNOWPACK outputs from the same time as when the pit was analyzed. During this site visit, my coworker Javier and I also took measurements to validate SWE, snow height, and the snow temperature profile from site sensors. While we were at the site it was mostly sunny with a light breeze, and the air temperature hovered around 0 degrees Celsius.



Figure 17: Bracket Creek SNOTEL site on April 16th 2025

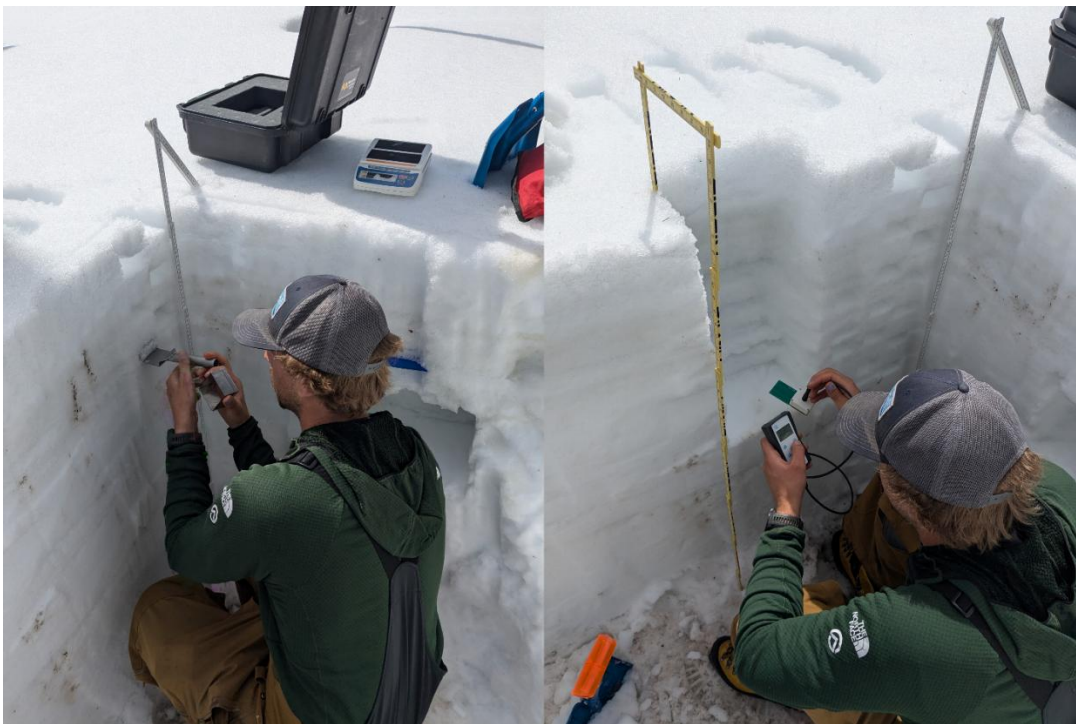


Figure 18: Density profile measurements (left) and liquid water content measurements (right)

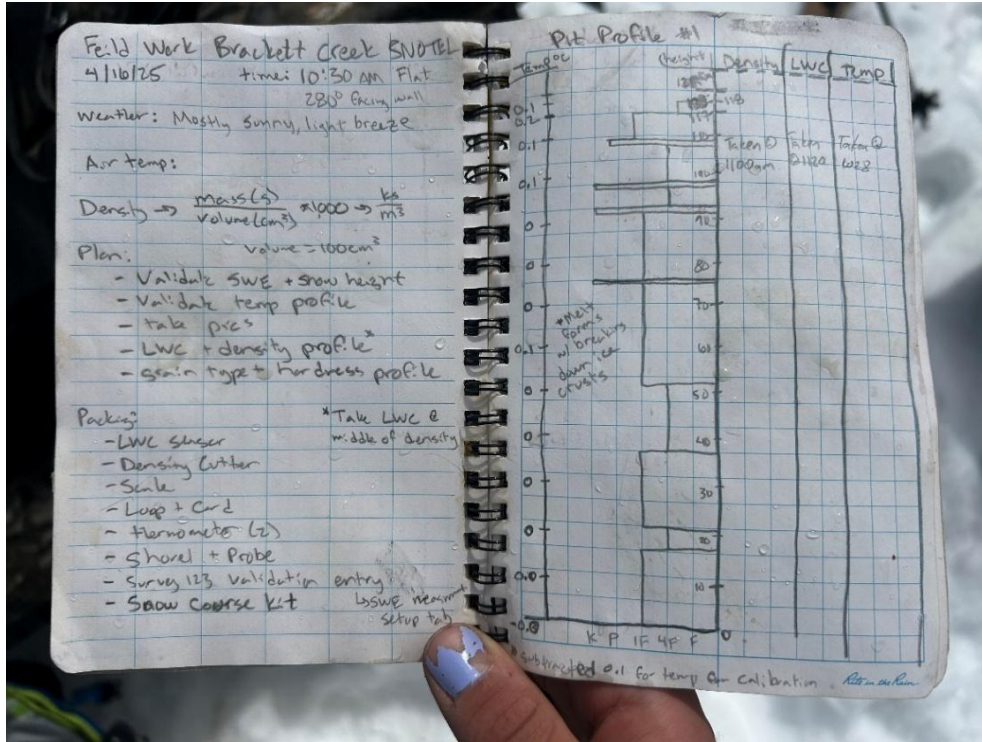


Figure 19: Brackett Creek site visit notes

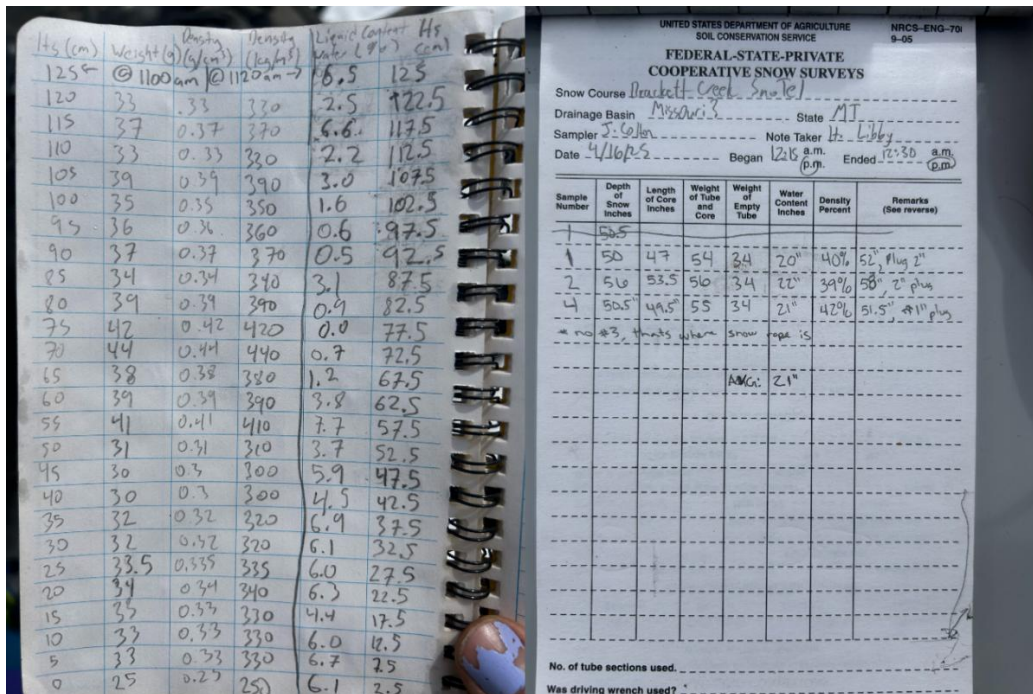


Figure 20: Brackett Creek site visit notes continued

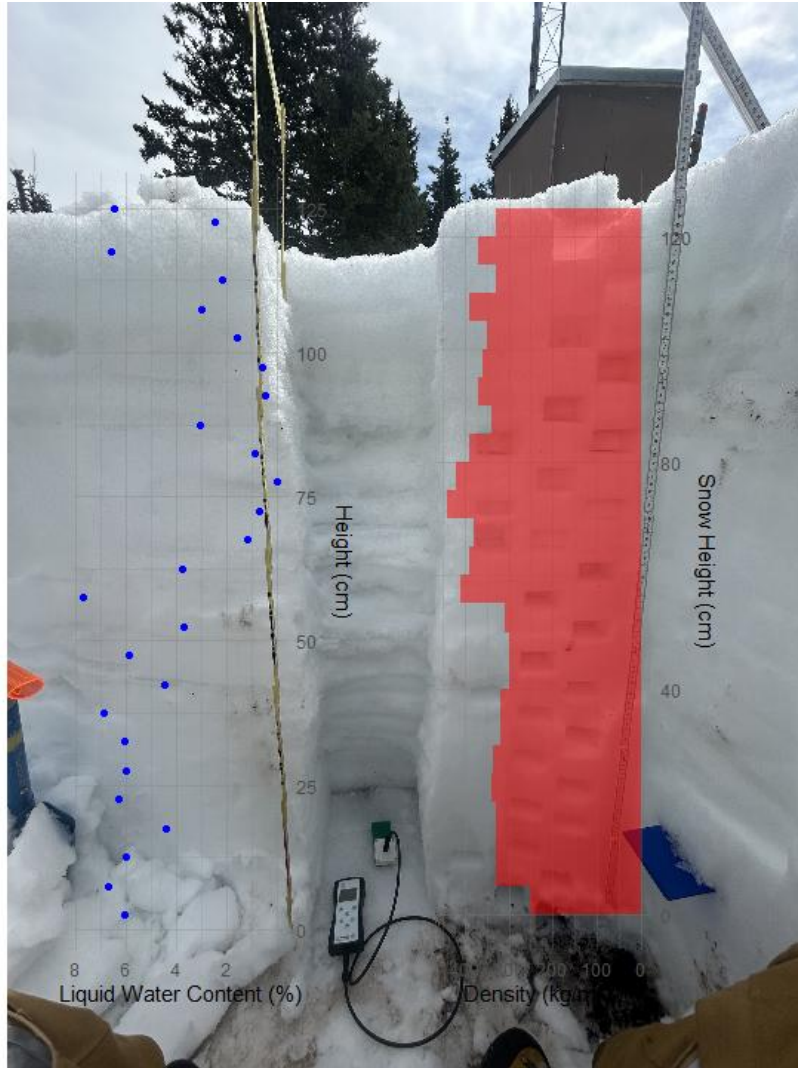


Figure 21: Liquid water content (dots) and density (red bars) profiles at the Brackett Creek SNOTEL site. Density is in kg/m^3 , and liquid water content is in relative percent.

Figure 21 above graphs the results of the liquid water content and density profiles. We can see that the density (red) is consistent throughout the snowpack, with the bottom half slightly lower and more consistent than the top half. The liquid water content in the bottom half of the snowpack was approximately 6% for the entire snowpack. The water in the top 20 cm was also around 6%, while the snow between these two areas had a liquid water content of around 0%. There is some error in the exact percentage of lwc in the snow from the sensor used, since it is

meant to be used with a dry snow density as an input and we used a wet snow density. The sensor also needs to be on top of the snow, potentially exposing it to meteorological factors it wouldn't otherwise encounter, although care was taken to ensure the pit wall remained in the shade. However, the overall shape of the liquid water content curve is correct based on observations made in the snow pit using the hand squeeze test (Association of Cryospheric Sciences, 2009. Techel & Pielmeier, 2011).

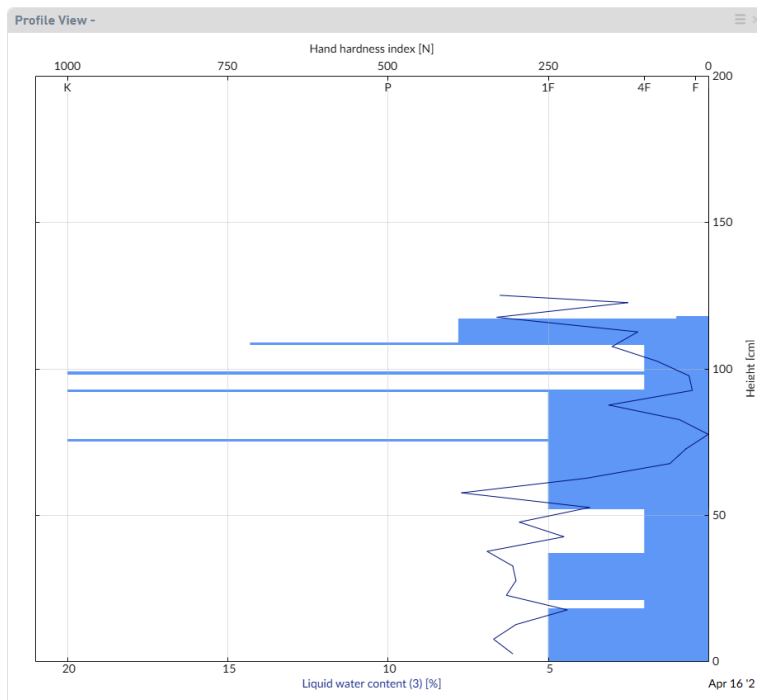


Figure 22: NIVIZ visualized profile of measured liquid water content (line) and hand hardness (blocks) at Brackett Creek

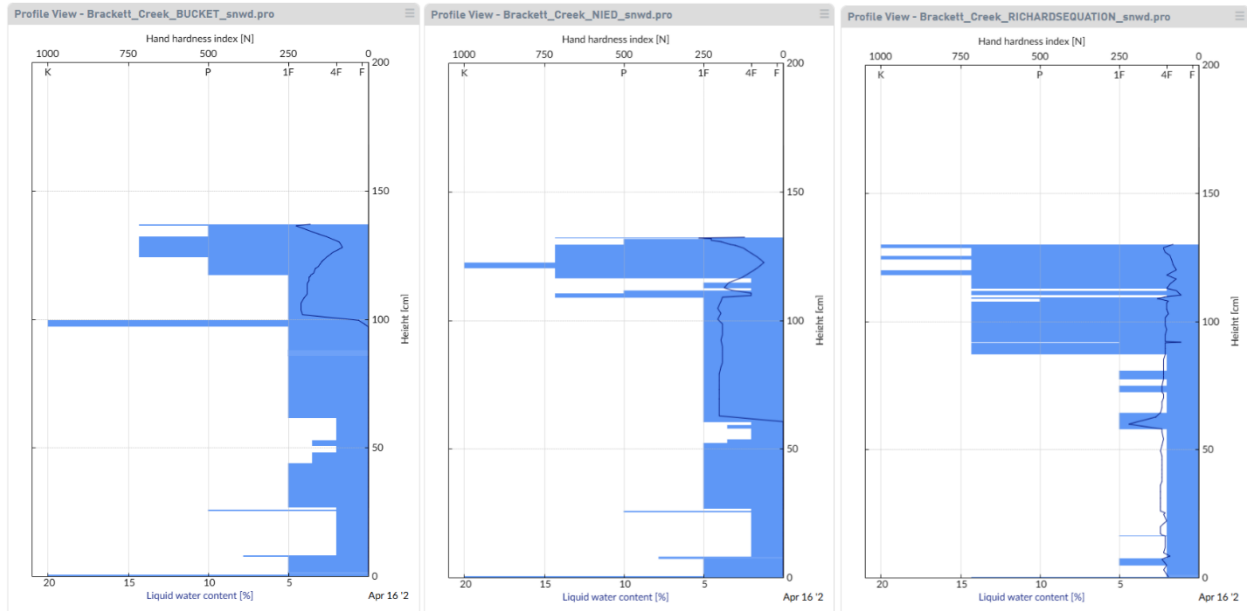


Figure 23: NIVIZ outputs showing liquid water content and hardness profiles for snow depth model runs using each water transport equation: Bucket (left), NIED (middle), and Richards (right)

The depths of the pits do not line up exactly. This is because even though the pit was dug near the snow pillow where the snow depth readings are taken above, the depths were not the same. We can see, by comparing the measured liquid water content with the modelled liquid water content, that the bucket and NIED methods capture the wetting front, although it has moved further down the snowpack than was measured. Neither of these two models held water in the snow from the day before. Richards has a mostly constant liquid water content profile, holding water in the snow better but not catching the new wetting front. Richards did account for some pooling found above a layer near 55 cm from the bottom of the snowpack. Since this was just one data point, we cannot draw any conclusions from the field work. This work aided my understanding of what the water-transport equations aim to model.

Water Transport Methods

Melt season length

Here, we will switch from analyzing general model performance to examining differences in water transport methods, both on a daily and a sub-daily timescale. First, we look at the daily timescale. Below are four figures showing the melt season lengths for the three water transport equations and the observed data (all model runs are forced with snow depth here). The figures also have the average error in melt season length and are broken up by continental, intermountain (Figure 26), and maritime (Figure 27) snow regimes. The continental snowpack sites are broken further into higher (Figure 24) and lower (Figure 25) elevation sites, separated by sites below or above 10,500 ft.

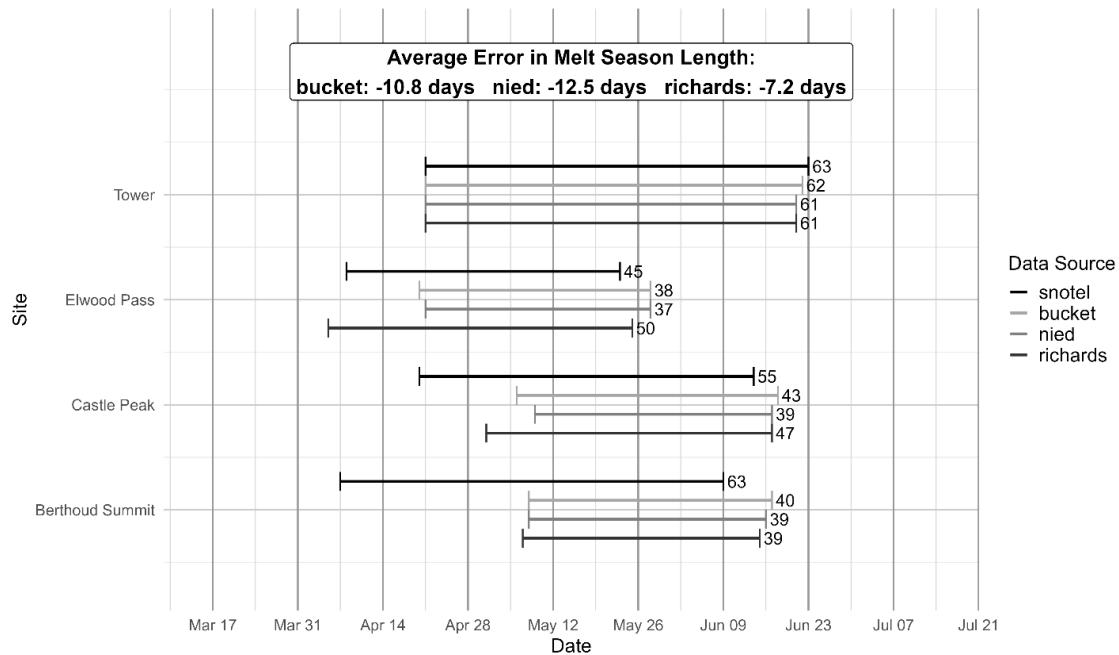


Figure 24: Melt season lengths for observed SNOTELs (Tower, Elwood Pass, Castle Peak, Berthoud Summit) and three water transport equations at high elevation sites (above 10,500 ft) with a continental snowpack, numbers at the end of lines represent the total days of melt season,

and for each site the observed length is followed by model results with Bucket, NIED, then Richards method

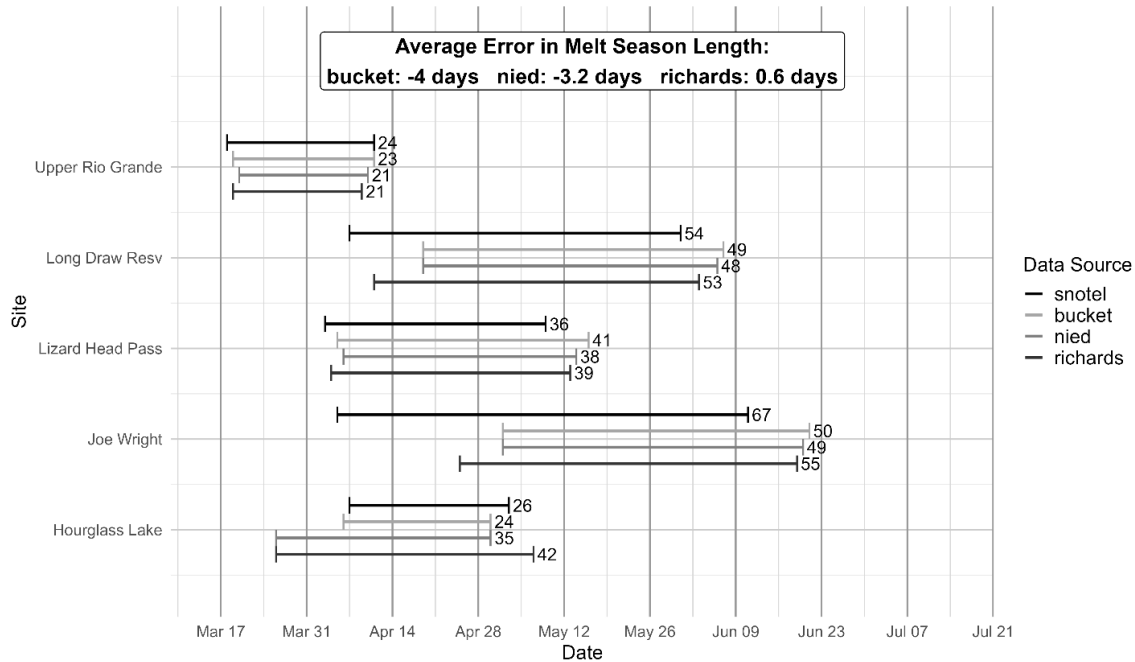


Figure 25: Melt season lengths for observed sites (Upper Rio Grande, Long Draw Resv, Lizard Head Pass, Joe Wright, and Hourglass Lake) and three water transport equations at low elevation sites (below 10,500 ft) with a continental snowpack

At continental sites above 10,500 feet (Figure 24), melt season length was on average 10.8 days shorter for the bucket method, 12.5 days shorter for the NIED method, and 7.2 days shorter for the Richards method compared to the observed melt season length. At the lower elevation sites with a continental snowpack (Figure 25), the melt season length was 4 days shorter for Bucket, 3.2 days shorter for NIED, and 0.6 days longer for Richards. At the intercontinental snow regime sites (Figure 26). The bucket method yielded a melt season length 3.2 days longer, NIED 2.8 days longer, and the Richards equation 1 day shorter. Finally, the two maritime sites (Figure 27) had melt seasons that were 11 days longer with the bucket method, 9.5 days longer with the NIED method, and 13 days longer than observed with the Richards method.

At all sites with a continental snowpack, except at Hourglass Lake and when using the Richards Equation at Elwood pass, the modeled melt season started on or later than the observed oncoming of the melt season. The snow season also ended later than observed at most sites. All intermountain sites also had the onset of the melt season start on or after the observed date across all three water transport equations. These results suggest that the onset of melt in the SNOWPACK model is delayed compared to observed values. When looking at the daily melt rates in the figures in the next section on sub-daily timescale melt, we can see that at the Brackett Creek site, water is observed leaving the snowpack before this is captured in the model. Also, for about the first month of melt, the observed daily decrease in SWE is greater than the modeled decrease in SWE (Figure 28), suggesting that the model indeed retains water in the snow longer than is real, as Wever et al. found in their 2014 study.

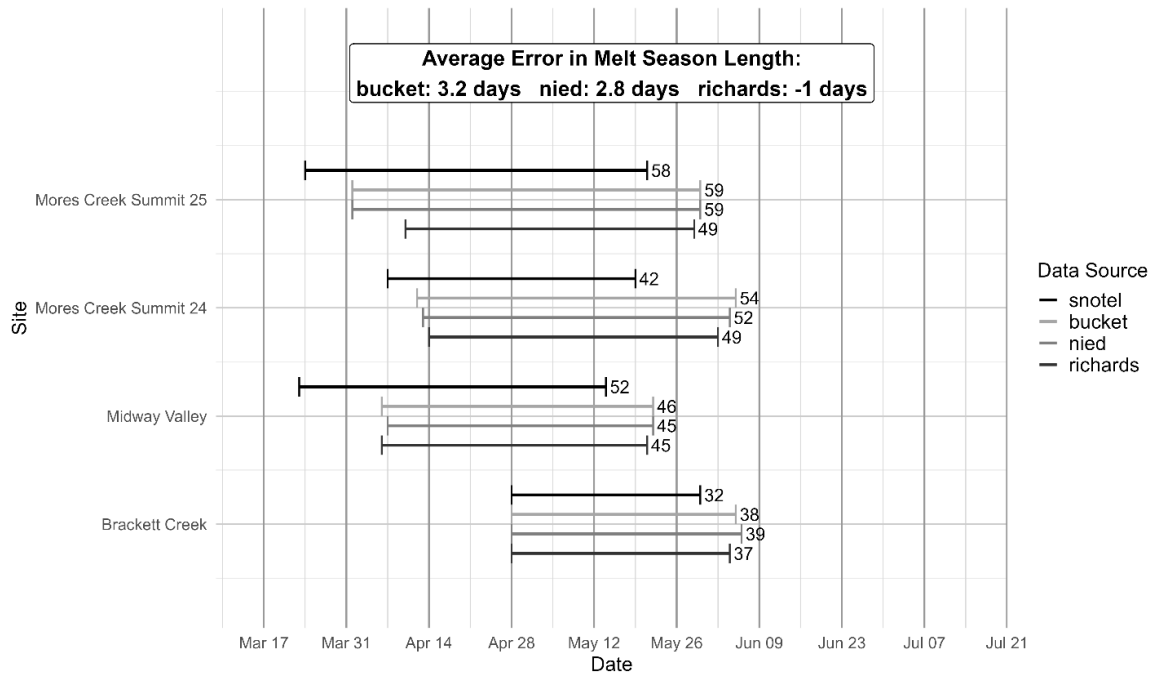


Figure 26: Melt season lengths for observed sites (Mores Creek Summit, Midway Valley, and Brackett Creek) and three water transport equations at sites with an intermountain snowpack

The difference between sites modelled in the continental snowpack regime and the intermountain regime is that while both have the onset of melt starting later than is observed, the continental sites mostly underpredict melt season overall length, while the intermountain sites slightly overpredict melt season length when Bucket and NIED transport methods are used. Meaning that at continental sites, water is drained from the snowpack too quickly, while at intermountain sites the rate of water leaving the snowpack is modelled relatively well. Note that what we are calling intermountain sites generally exhibit an intermountain snowpack and are in the intermountain “zone”. However, year to year and month to month, the site may have a more continental or a more maritime snowpack.

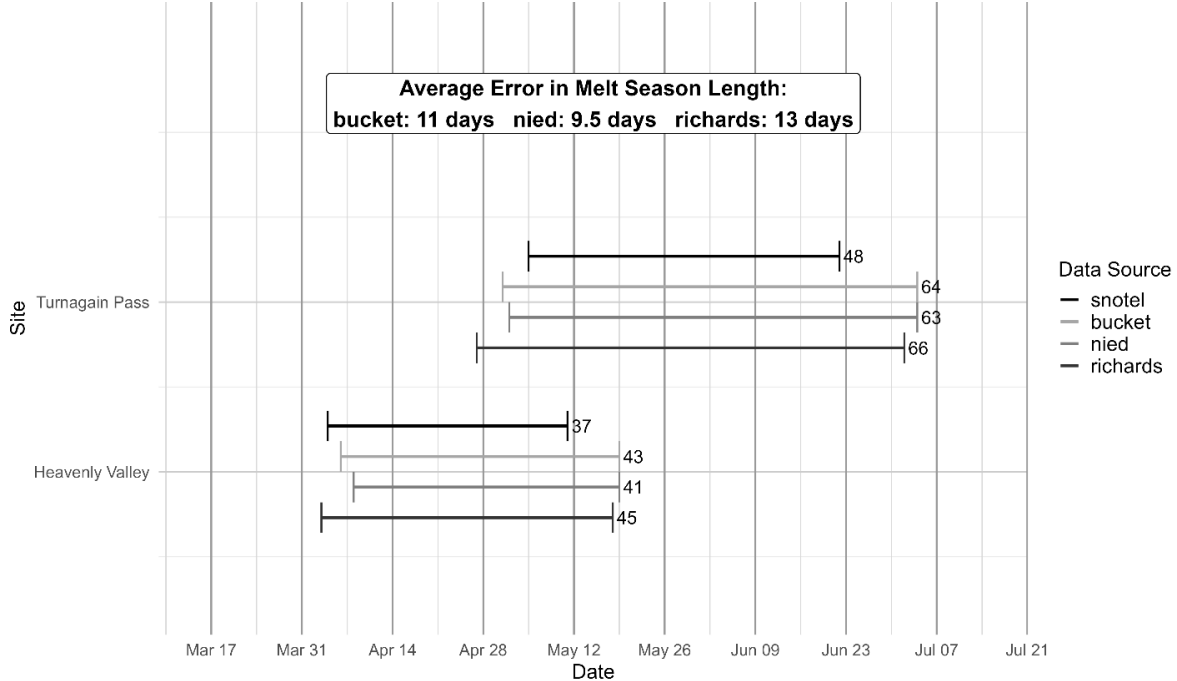


Figure 27: Melt season lengths for observed sites (Turnagain Pass and Heavenly Valley) and three water transport equations at sites with a maritime snowpack

The maritime results differ from those of the other regimes, though we have only two sites with this snow regime to compare with. At Heavenly Valley, the onset of melt is slightly later for the Bucket and NIED methods, while being slightly earlier for the Richards method. For all transport methods, the melt season is longer than observed. At Turnagain Pass, the onset of water leaving the snowpack occurred earlier than observed with all methods, and the melt season was about 10 days longer with all transport methods. This difference may be due to a deeper overall snowpack, denser snow, or a combination of the two (when compared to the other snow regimes in this study and to the snow regimes in Switzerland where the empirical formulas for the model were created). The difference in error at the Maritime sites will be discussed further in the empirical formula section.

At most sites outside a maritime snow regime, the figures show a delay in the start of the melt season. Previous studies found that Bucket and NIED retain meltwater in the snow for too long, delaying its arrival at the base of the snowpack in the early stages of the melt season. The lag of meltwater arriving at the base of the snowpack on this seasonal scale was found to be more noticeable at sites with higher average snowpack than other sites observed in the studies (Wever et al., 2014, Wever et al., 2015).

Liquid water content

At the daily timescale, we observe greater differences between modelled and observed melt season lengths than between melt season lengths obtained with different transport methods. Meaning each transport method produces similar error on a daily timescale when investigating the SWE melt rate. In this section, we analyze model outputs at a sub-daily timescale. We see many differences between the three transport methods on this scale. The differences highlight that the transport methods model internal snow properties differently. We will compare daily melt rates observed to assess overall accuracy, then examine differences in liquid water content between the transport equations. We do not have liquid water content observations to compare, but we will relate our results to other studies and to the meteorological variables of the day.

The next five figures (Figure 28, Figure 29, Figure 30, Figure 31, and Figure 32) highlight different periods during the melt season at the Bracket Creek SNOTEL site. The results at this site have similar trends on the sub-daily timescale as those at other sites. We opted to analyze only the daily SWE melt rate for the observations due to sensor fluctuations during the day. Since the site is flat, diurnal increases in liquid water content (lwc) shouldn't exceed 1.7% and for most days bulk volumetric lwc should not exceed 4-5% (Heilig et al., 2015).

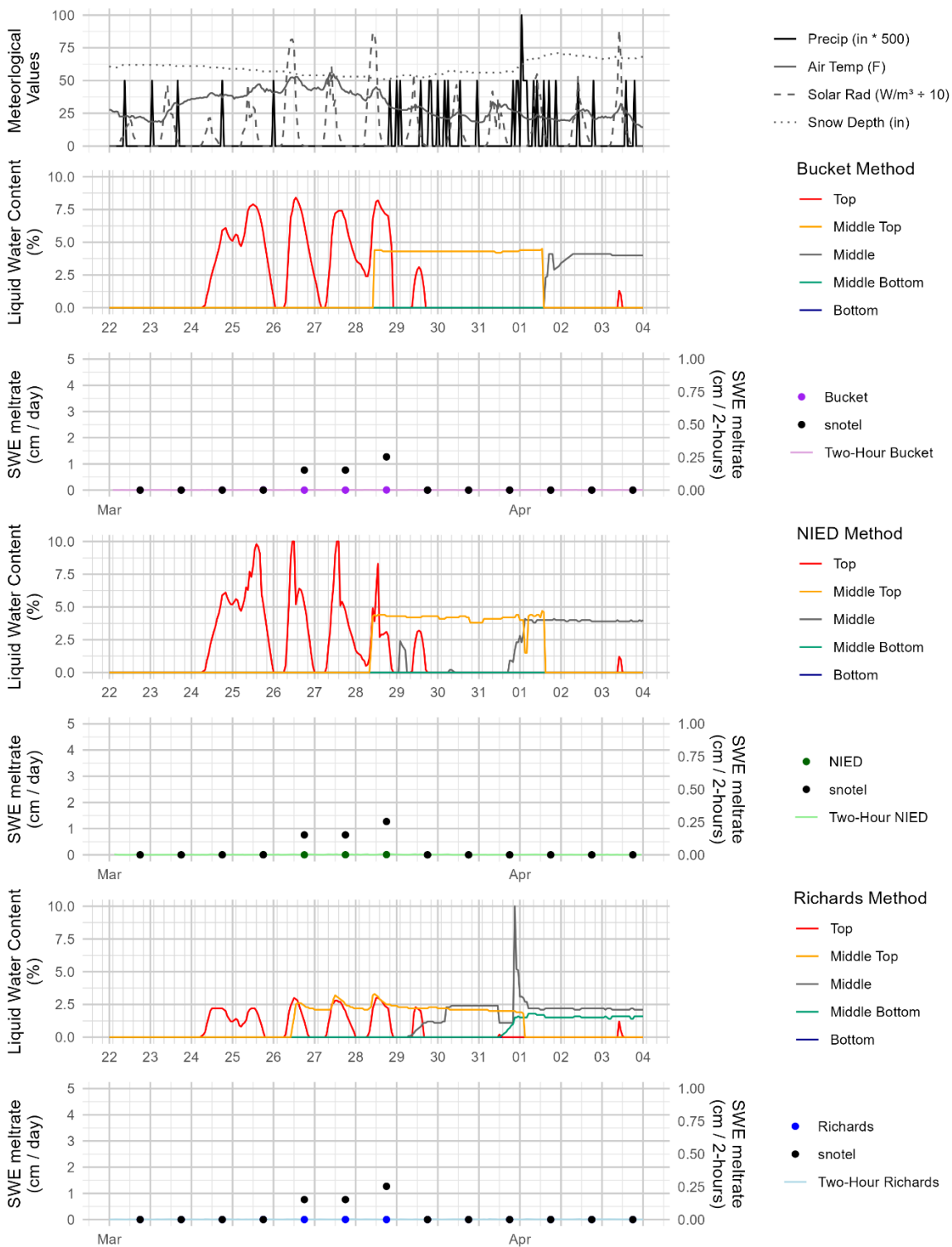


Figure 28: Liquid water content outputs at Brackett Creek SNOTEL site for three different water transport equations at the start of the melt season. The top chart shows observed precipitation, air

temperature, solar radiation, and snow depth as recorded from the SNOTEL site to help identify what may be affecting water transport at any given time (along with the type of melt occurring). Next, each transport equation has two charts. The first shows liquid water content outputs at the top of the snow, at the middle between the top and middle of the snowpack, the middle of the snowpack, at the middle between the middle and the bottom of the snowpack, and at the bottom layer. The second plot shows observed and modeled daily SWE loss in centimeters per day. The plot also has two-hour SWE loss from the model to show the timing of melt for each transport method. The data are shown in two-hour increments because decreases in SWE occur only at two-hour intervals in our model outputs.

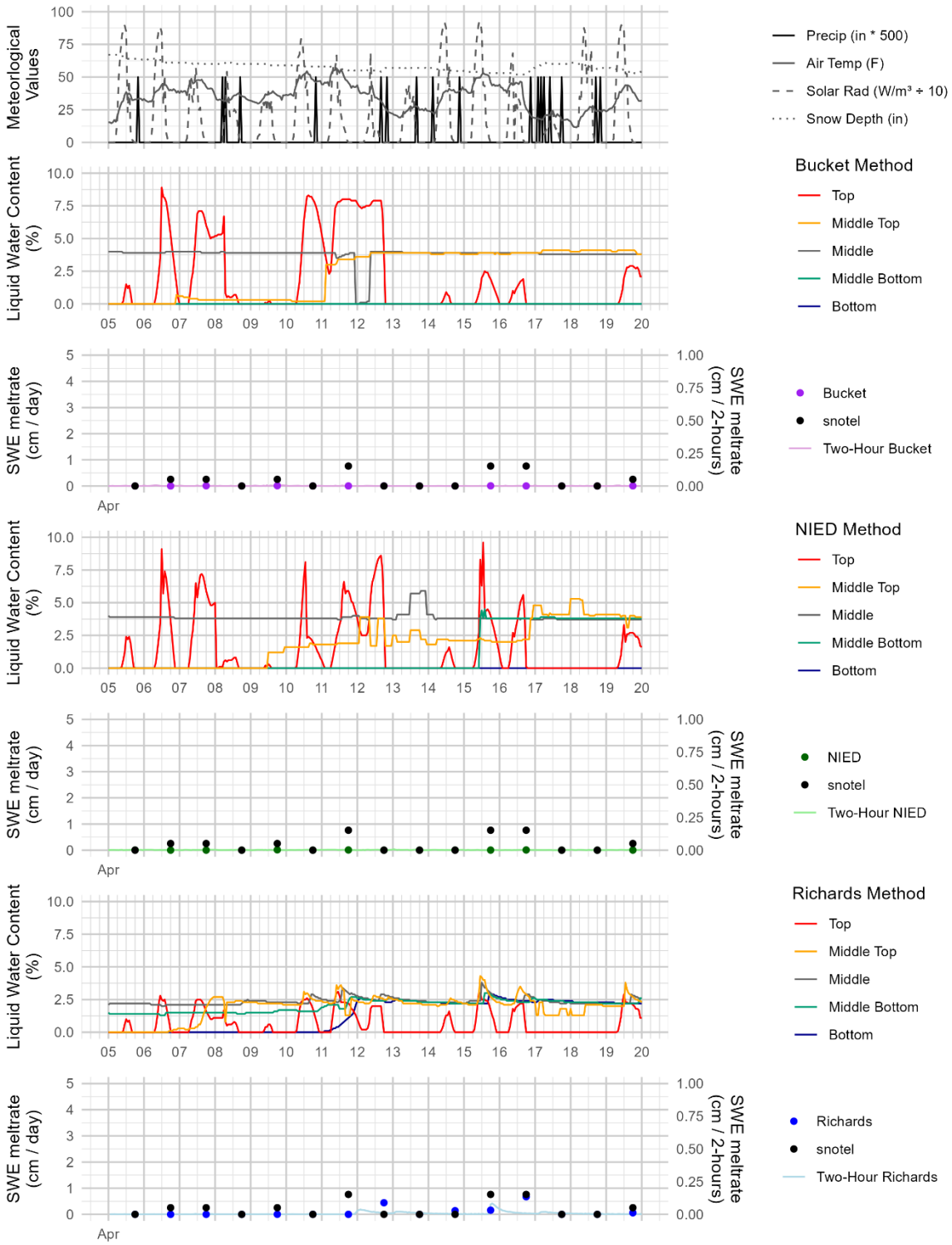


Figure 29: Liquid water content outputs at Brackett Creek SNOTEL site for three different water transport equations from April 5th to April 20th

Figure 28 and Figure 29 show the beginning of the melt season at the site. We can see that across all days and transport methods (except the Richards method on the 13th and 16th of April), the observed daily SWE loss is higher than the modeled loss, and in most cases, there is no SWE loss. This adds to the previously discussed lag in the model's start of the melt season compared to what was observed. We observe a diurnal melt-freeze in the top layer of the snowpack with all transport methods, though the liquid water content is much higher with NIED and bucket than with the Richards method.

We can also observe the start of lwc “thresholds” in all three methods. Besides the very top layer, we see that with the Bucket method the liquid water content is either 0% or 4%. This is because 4% is set as the constant for lwc. In the NIED method, the same 4% is observed inside most of the snowpack. Here, empirical formulations and constants are used to calculate the residual water content. This is why a 4% threshold occurs in NIED as well, though it is not always followed. The Richards method has a threshold around 2.5%, though, unlike the other methods, this value is primarily observed in the bottom half of the snowpack and not as often. We can also see diurnal effects propagating throughout the entire snowpack in Richards, whereas in the other two methods they are confined to the surface. This lwc threshold will be discussed further in the formulas and error section.

We also observe that the first instance of liquid water remaining internally in the snowpack occurs before peak SWE (as indicated by the meteorological variables). The first days of modelled lwc in the snowpack happen during a stretch of above-freezing temperatures and higher solar radiation than previous days. Indicating in this case the melt is from solar input rather than rain on snow.

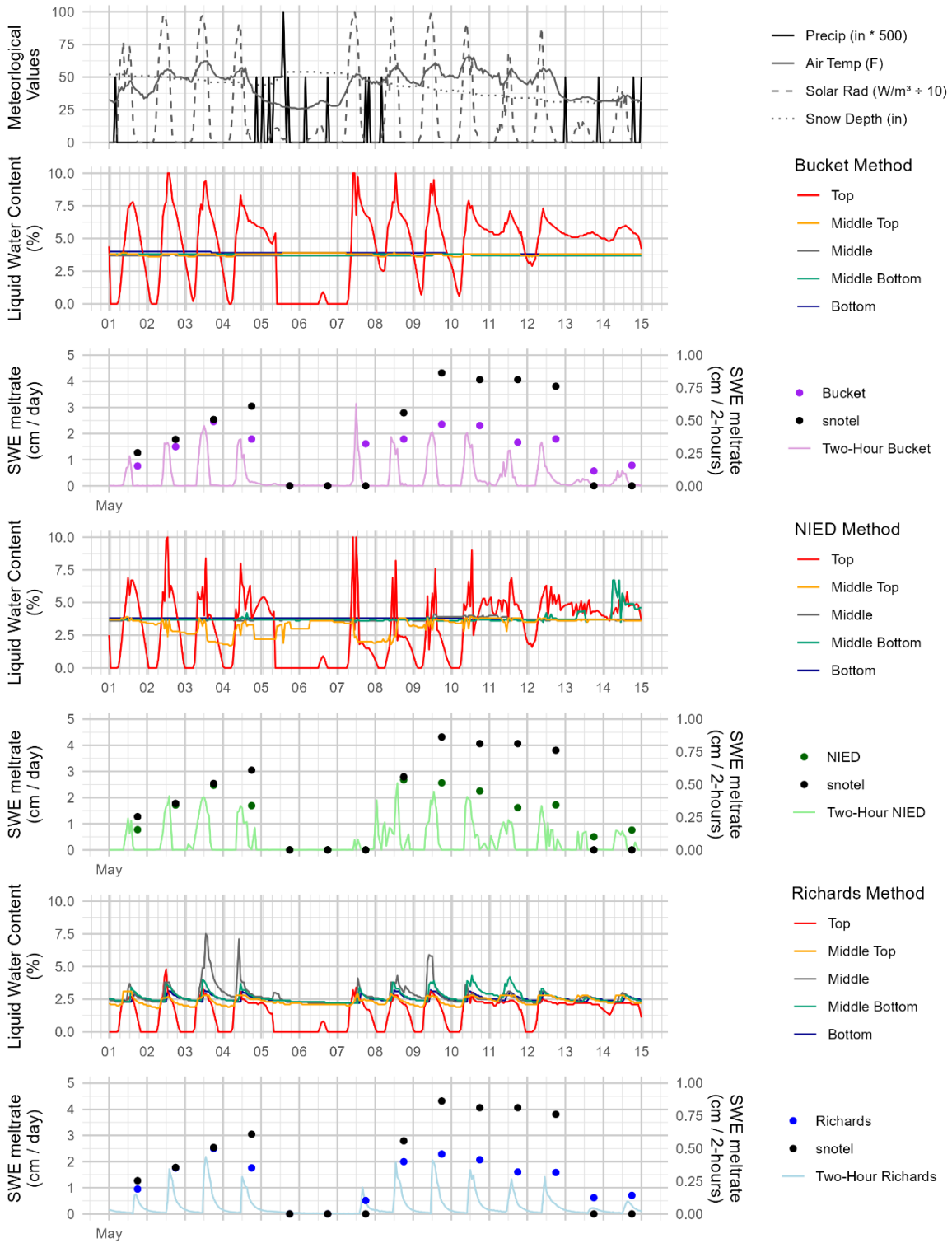


Figure 30: Liquid water content outputs at Brackett Creek SNOTEL site for three different water transport equations from May 1st to May 15th

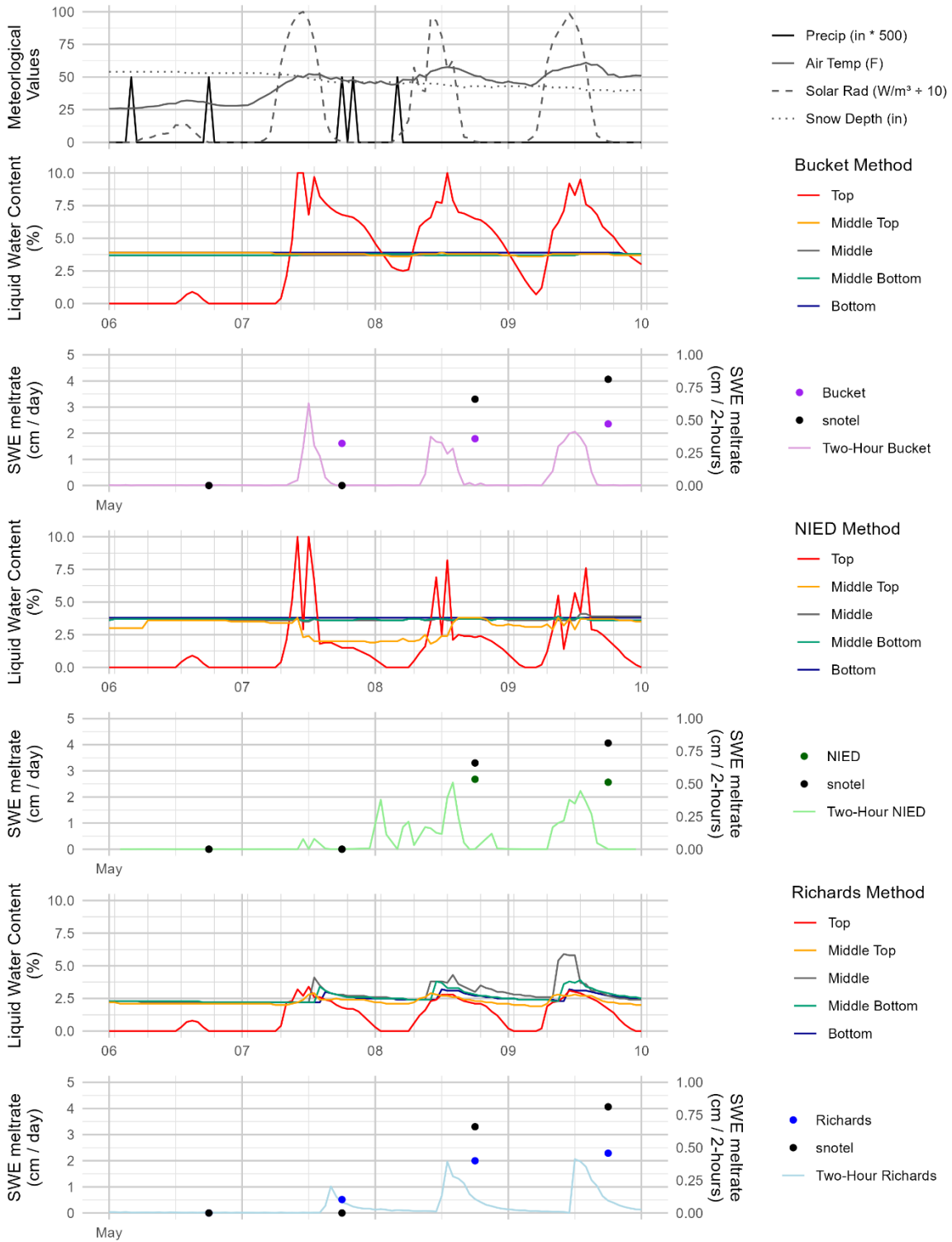


Figure 31: Liquid water content outputs at Brackett Creek SNOTEL site for three different water transport equations from May 6th to May 10th

Figure 30 shows model outputs from May 1st until May 15th and Figure 31 zooms into a melt period immediately following a cool-down period, where the SWE melt rate was zero for three observed days. We see again that across all three transport equations, the observed daily SWE melt rate is greater than the modeled. At the end of the freeze period (on the 8th) there is no observed loss of SWE, the NIED model has no loss of SWE, but both the Richards and Bucket methods model a loss in SWE. The modelled melt rate is higher than the observed during another cooldown on the 14th and 15th. Here, no melt is observed, but all three models output between 0.5 and 1 cm of SWE loss.

The peak observed melt on May 10th was 4.1 cm of SWE. Bucket modeled 2.4 cm, NIED modeled 2.2 cm, and Richards modeled 2.1 cm of SWE loss. The observations of smaller daily SWE melt rates in the models compared to the observed is the reason for the larger error in snow water equivalent we found during the melt season in the models compared to during the accumulation period.

In all three models, we see the diurnal melt-freeze halt and liquid water content at the top of the snowpack go to zero. This is because the top of the snowpack changed to a different calculation layer during the refreeze due to the snowfall event. The melt observed afterward is caused by higher air temperatures and solar radiation. In these charts (Figure 30, Figure 31, and Figure 32), we can observe hourly melt rates from the models. The shapes of this plot are similar for bucket and NIED. The Richard's method melt during the day is initially high then exponentially lowers to zero after midnight. All modelled peak hourly melt rates are around 0.4 cm of SWE loss.

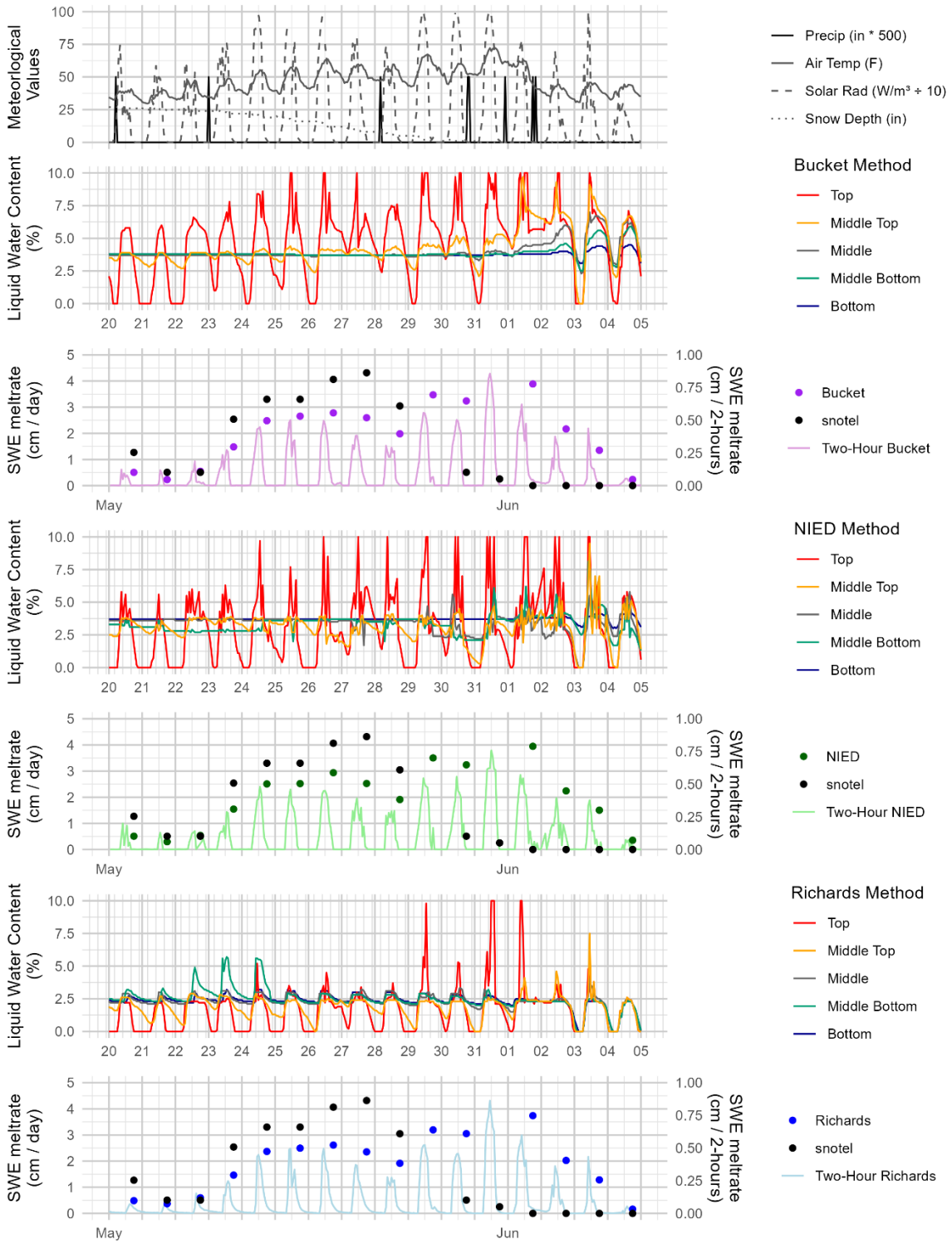


Figure 32: Liquid water content outputs at Brackett Creek SNOTEL site for three different water transport equations at the end of the snow year

Figure 32 is the outputs for the end of the snow year. We can see, like in the previous plots, that the observed SWE melt rate is greater than the modeled in all cases. The switch to models with a higher melt rate is because the observed SWE is approaching or reaching zero. Our findings here agree with previous studies (Wever et al., 2014, Wever et al., 2015, Heilig et al., 2015) that the SNOWPACK model (regardless of water transport method) underestimates melt amounts.

We see a uniform diurnal effect on the lwc through all snow layers in Figure 32 for the Richards equation. We again see this effect only in the top layer of the snow for the other two methods. NIED and Bucket methods start showing diurnal effects across the entire snowpack near meltout, though (especially for NIED) this is chaotic. We see the same hourly melt patterns across the three transport methods as previously discussed.

The next set of figures are outputs from NIVIZ.org using .pro files to visualize outputs from the Brackett Creek model runs. These figures provide a clear visual representation of the liquid water content throughout the entire snow profile. Note that values are capped at 4% so that it is easier to discern lwc differences between different layers. The plots also give snow grain type. In both figures the grain types are similar between the three models, although the transition to only having melt forms happens fastest in the Richards equation and the slowest using the bucket method (Figure 33). In the bucket method rounded grains (pink), faceted crystals (light blue), and depth hoar (dark blue) persist in the bottom of the snowpack for an additional two weeks compared to the Richards method. The Richards equation is also the only method that consistently produces a melt-freeze crust (red with black hash marks). In Figure 34 the three

methods are almost identical in terms of modeled grain types, though with Richards again having a melt-freeze crust appear.

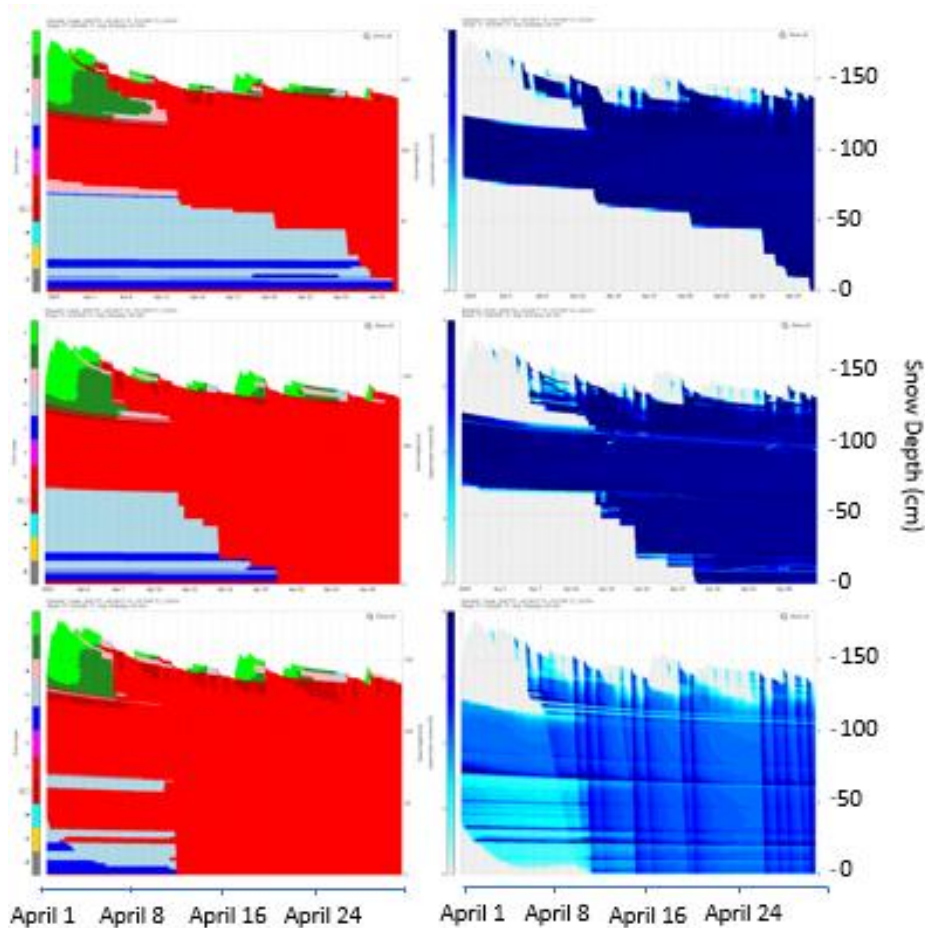


Figure 33: NIVIZ outputs for three water transport equations (Bucket – top, NIED – middle, Richards – bottom) with snow grain type (left) and liquid water content (right) from April 1st 2025 to April 30th 2025 at the Brackett Creek SNOTEL site. Red on the snow grain chart represents melt forms and darker blue on the liquid water content charts represent higher liquid water content (ranging from 0 to 4 %).

In Figure 33 we see that in the models when the snow grain transitions to melt forms, threshold liquid water content values are reached. This is when there is residual water in the snow. In the Richards method outputs, we can clearly see horizontal lines of darker blue indicating higher water content. These lines form at capillary barriers, and Richard's method is

the only one of the three that can model this ponding effect. Being able to discern water content in the snow above or below elements such as ice crusts is important for wet snow avalanche prediction (E. H. Peitzsch, 2009).

With the Richards method we also observe a clear diurnal pattern in the snowpack. In Figure 34, we see three days of melt, followed by water leaving the snowpack. Each day with the Richards method, we also observe the lag in a higher lwc at the top of the snowpack before it gets to the bottom, which is indicated by the slight diagonal tilt that is darker blue in color. This is not seen in either the bucket or the NIED method outputs. Although we do see a small refreeze at the surface with these two methods. The melt in Figure 34 is from solar radiation on new snow. In the Richards lwc plot we see light grey indicating no water transition to a light blue then an hour later dark blue. The snow height then decreases, and we see ponding the next day at the new-snow-old-snow interface. After this, the ponding on the top breaks down and we see a deeper freeze occurring the next night. Wever et al. (2015) found that the Richards method more accurately models water flow through snow and subsequent changes in snow microstructure. Accurately modelling internal processes creates a positive feedback loop, as density, grain size, saturated water content, residual water content, and ice fraction from previous timesteps are used in the Richards method to calculate the current timestep.

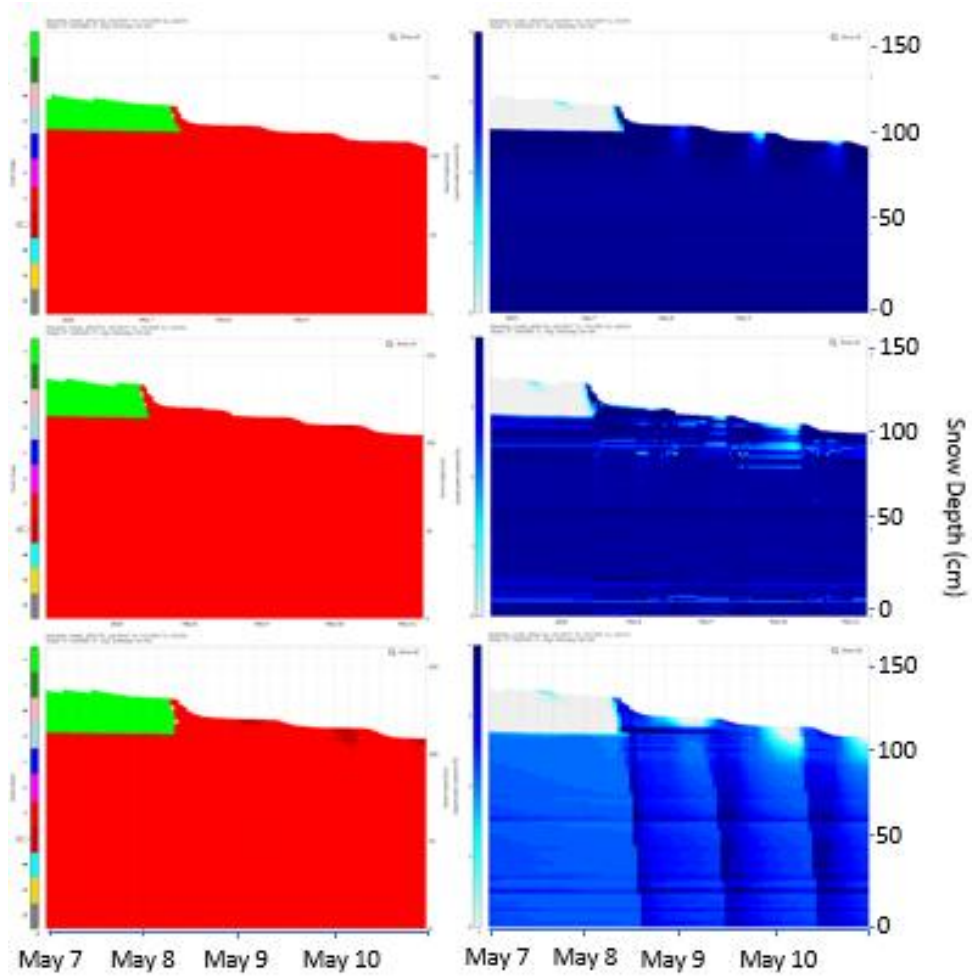


Figure 34: NIVIZ outputs for three water transport equations (Bucket – top, NIED – middle, Richards – bottom) with snow grain type (left) and liquid water content (right) from May 6th 2025 to May 10th 2025 at the Brackett Creek SNOTEL site.

Parameter, Empirical Formula, and Uncertainty DiscussionWind sensitivity study

A brief look at the effect of using wind inputs from SNOTEL sites on SNOWPACK results was conducted to determine the role of wind in our study. The results are shown in Table 7 and Table 8 below. Table 7 gives results during the accumulation period and Table 8 is for the melt period. Both tables have three sites, one for each snow regime, with 18 model runs per site to correspond with transport equations, forcing data, and three wind trials. The sensitivity analysis was done using three wind scenarios: 1) the observed wind speed compared to model runs, 2) wind speed set to zero, and 3) doubling the observed speed. The wind speed is doubled in our analysis to test the model's sensitivity to wind. Also, the wind sensors at SNOTEL sites have a threshold wind speed, and a doubling of the wind may account for missed values. The last block in each chart shows the absolute average error in SWE for the specific model run across the three sites. Finally, both tables present an overall absolute average for each wind speed scenario (a combination of the six model runs at the three sites for each scenario).

Table 7: Results from a wind sensitivity study during the accumulation period, results show error in SWE from model to observed (cm), the first three model results were forced with snow depth and the second three were forced with precipitation

<i>Site</i>	<i>Wind Test</i>	<i>Bucket</i>	<i>NIED</i>	<i>Richards</i>	<i>Bucket</i>	<i>NIED</i>	<i>Richards</i>
<i>Bracket</i>	Observed	0.185	0.266	-0.221	3.588	3.406	3.569
<i>Creek</i>	None	0.121	0.126	-0.332	3.570	3.374	3.436
	Wind x2	0.772	0.840	0.444	2.602	2.587	3.221
<i>Heavenly</i>	Observed	-2.447	-2.502	-2.899	6.024	6.031	7.030
<i>Valley</i>	None	-2.623	-2.646	-2.961	5.816	5.816	6.704
	Wind x2	-0.660	-0.632	-0.694	5.937	5.974	6.818
<i>Tower</i>	Observed	-1.821	-1.832	-1.874	-0.289	-0.403	-1.076
	None	-3.890	-3.781	-4.164	-0.197	-0.323	-1.075
	Wind x2	2.448	2.611	2.802	-2.727	-2.837	-4.075
<i>Absolute</i>	Observed	1.484	1.533	1.665	3.300	3.280	3.892
<i>Average</i>	None	2.211	2.184	2.486	3.194	3.171	3.738
	Wind x2	1.293	1.361	1.313	3.755	3.799	4.705
<i>Totals</i>	Observed:	2.526	None:	2.831	Windx2:	2.705	

Heavenly Valley is one of two sites in this study with a maritime snowpack. Since this snow is dense, wind is likely to have a smaller effect on model outputs than at intercontinental and continental sites. The results from the wind study support this hypothesis, with the most significant difference in the sensitivity analysis being at Tower (continental), Brackett Creek is in between (intercontinental), and Heavenly Valley was the least affected. We did not find a strong enough difference between using wind data and not, so we decided to run SNOWPACK with sites that have wind data. This is why only “enhanced” SNOTEL sites are used, to avoid introducing additional variables that could introduce error into our study. Overall, using the observed wind data performed slightly better than not using wind data.

Table 8: Results from a wind sensitivity study during the melt period

<i>Site</i>	<i>Wind Test</i>	<i>Bucket</i>	<i>NIED</i>	<i>Richards</i>	<i>Bucket</i>	<i>NIED</i>	<i>Richards</i>
<i>Bracket</i>	Observed	3.192	3.468	5.312	9.935	9.163	16.707
<i>Creek</i>	None	3.166	2.938	4.749	9.469	8.782	15.505
	Wind x2	3.081	3.119	4.776	7.908	8.240	13.656
<i>Heavenly</i>	Observed	4.676	4.098	8.872	15.345	13.919	22.744
<i>Valley</i>	None	3.941	4.027	8.991	13.964	12.438	20.569
	Wind x2	4.089	3.702	7.633	9.810	9.265	16.136
<i>Tower</i>	Observed	5.598	5.112	6.250	12.602	11.546	14.166
	None	7.011	6.778	8.946	18.376	16.040	17.129
	Wind x2	0.627	0.658	0.957	1.059	1.627	1.583
<i>Absolute</i>	Observed	4.489	4.226	6.811	12.627	11.543	17.872
<i>Average</i>	None	4.706	4.581	7.562	13.936	12.420	17.734
	Wind x2	2.599	2.493	4.455	6.259	6.377	10.458
<i>Totals</i>	Observed:	9.595	None:	10.157	Windx2:	5.440	

What is most intriguing about this sensitivity analysis is the large improvement in model performance observed during the melt season when the wind data were doubled. This leads us to believe that the wind data may be under-represented, especially at windier sites. The largest difference was observed at Tower, which is the windiest of the three sites examined. This issue most likely stems from our use of average wind speed rather than the maximum wind speed for the hour. This should be investigated further if deciding to use SNOTEL data for operational use of SNOWPACK. We used average wind from SNOTEL sites because this is what Katz et al. (2023) used; however, their wind data were from sensors on ridge lines, whereas ours is at the SNOTEL site. Having a more accurate wind speed improves latent and sensible heat and energy balance equations at the top of the snowpack.

New snow density

The SNOWPACK model contains many empirically derived formulas and constants that have been laboratory- and field-tested. Some of these may be the reason for the error when running the model, since the formulas were developed in specific regions and snow climates. These formulas can be adjusted for different regions if desired. In our study, we did not adjust any empirical formulas. One example of a field-tested empirical formula is the new snow density formulation. The density of snow is an important input to many of the model's equations. The density of the snowpack is determined by stress, time, temperature, and grain metamorphism. The new snow density is determined based on an empirical formula created with a statistical relationship derived from measurements in Davos, Switzerland (Lehning et al., 2022). The relationship is shown below in equation 4 and is valid for 30-60 minute intervals, not for 24 hour snow totals.

$$\text{Eq 4: } \rho_{new} = 70 + 6.5T_a + 7.5T_{ss} + 0.26Rh + 13VW - 4.5T_aT_{ss} - 0.65 T_aVW - 0.17RhVW + 0.06 T_aT_{ss}Rh$$

In equation 4, T_a is air temperature in Celsius, T_{ss} is surface temperature in Celsius, Rh is the relative humidity (%), and VW is wind speed in m/s. The statistical model for new snow density and albedo was developed with measurements from sites in the Swiss Alps, and may not always be applicable to other areas around the globe (Lehning et al., 2002). For example, a study in Canada changed the original parameterization of new snow density to keep densities lower for snow falling during periods less than 10 degrees Celsius (Bellaire et al., 2011).

Wind is an important factor in new snow density, as shown in Eq. 4, and is another reason for choosing sites with wind. As discussed before, the wind was potentially underrepresented at

some sites in this study and is an important factor to consider when running SNOWPACK with weather stations.

Liquid water content thresholds

As discussed previously, when observing the liquid water content outputs from the three transport methods, a threshold emerges. For both NIED and Bucket methods this threshold is around 4%, and for Richards method it is around 2.5%. These thresholds are based on the volumetric liquid water content and have to do with how the residual water content is calculated. Water will only flow through a porous medium when the pressure head is great enough, and the capillary retention is the liquid water that is left in the medium due to surface tension (unable to flow and in the medium when saturated). This is the residual water content. For the Bucket method the residual water content represents the volumetric water content most of the time and was initially set to a constant of 0.08 (Bartelt & Lehning, 2002), with the goal of the constant eventually being a function of snow microstructure. The constant 0.08 allowed for correct modelling of intense melt in the spring. The constant is now set to 4% (Hirashima et al., 2010). This change is interesting since we now see that water is retained in the snow too long with the 0.04 constant for residual water.

When water flow is modeled with the Bucket method, if the water content exceeds the residual, water moves to the next layer (with a relationship between residual water content and volumetric ice content). As such, the water content remains constant at 4% when the snowpack is saturated using the Bucket method. In reality, the liquid water content in the snow is rarely uniform in a heterogeneous snowpack (Techel & Pielmeier, 2011).

In the Bucket method transport only occurs in a saturated snowpack, though in a real snowpack flow can occur in unsaturated conditions. Water-saturated layers in a real snowpack also occur along capillary barriers, boundaries in the snowpack along layers with different grain sizes or grain types (Hirashima et al., 2010). The NIED and then the Richards method were introduced to the model to attempt to model these elements.

With the NIED method, the suction pressure head and hydraulic conductivity are calculated using empirical formulas. There are equations for both saturated and unsaturated hydraulic conductivity. Grain size and density are used for input. A potential issue with the NIED method is that the experiments done to create a water retention curve for use with the van Genuchten equation were done for high-density snow (550 kg/m^3) (Yamaguchi et al., 2012).

The residual water content is set to 0.024 in the model (this number is found in WaterTransport.cc in the source code but I have not been able to find it anywhere else). The saturated water content is calculated using an empirical formula that uses grain size as the upper bound for the calculation layer and volumetric ice content. However, the NIED method appears to have a similar “threshold” or floor as the Bucket method. In searching through published papers and the source code I could not determine why the NIED method appears to be similar to the Bucket method in outputs, when the calculation process followed is more similar to the Richards method. Many of the same empirical formulas found through experiments for the water retention curve created for the NIED method are also used in the Richards method (Yamaguchi et al., 2012, Wever et al., 2014).

The NIED and Richards methods both use the van Genuchten equation for water transport equation inputs. They both find hydraulic pressure head and saturated/unsaturated

hydraulic conductivity using calculated saturated water content, residual water content, effective saturation, current water content, snow density, and layer thickness. Note that the water content is the previous timestep's water content after applying a melt/refreeze and an energy balance equation. The NIED method solves the formulas (using other empirical formulas when necessary) and inputs the results into Darcy's Law to calculate flow. The Richards method iteratively solves partial differential equations with the van Genuchten model and the Richards equation to calculate flow. The Richards method uses physical modelling to calculate the total water content.

(5.1-3) The residual water content, saturated water content, and volumetric water contents are calculated with the equations below (snowpack 3.7.0 ReSolver.cc):

$$(5.1) \theta_t^r = \min [0.02, \max (\theta_{t-1}^r, f * \theta_w)]$$

$$(5.2) \theta_s = (1 - \theta_i) \frac{\rho_i}{\rho_w}$$

$$(5.3) \theta = \theta_r + (\theta_s - \theta_r) \frac{(1+(\alpha|h|)^n)^{-m}}{Sc}$$

Here θ_t^r is the residual water content for the current timestep, 0.02 is the upper limit for θ_t^r , θ_{t-1}^r is the residual water content from the previous timestep, f is an empirical tuning factor between 0.1 and 0.3 (Wever et al., 2014), and θ_w is the current total liquid water content. When $\theta_w > \theta_r$ and the capillary forces or input of meltwater is greater than the drainage capacity water transport occurs. The total liquid water content in Richards when the snow is saturated is generally around 0.025, giving the 2.5% lwc “threshold”. Although in the source code there is a

line, $\theta_r = 0.024$ (watertransport.cc). This would also correlate to the threshold we see for residual water content, but this is not mentioned in the papers explaining the model. The source code suggests that different θ_r values are used under different snow conditions. To wrap the “threshold” question up, it appears that in all three equations the threshold occurs when the water content for that layer in the model is equal to the residual water content.

Increases in error with deeper snowpacks

Here, we discuss the observed increase in error when sites have higher peak snow water equivalent and whether this error stems from the snow regime, model performance with deeper snowpacks, or another factor. We create a linear model of peak SWE at each site compared to the site's error in SWE during both the accumulation and melt periods, combining all three water transport equations errors when is snow depth forcing the model. The precipitation forced models were ignored for this relationship, given the higher model error we observed compared to when snow depth forces SNOWPACK. From our linear model, we have 95% confidence that for each 1-centimeter increase in peak SWE at a SNOTEL site, the true mean error in SWE increase from model to observed during the melt period is between 0.0327 and 0.1794 centimeters. We found very strong evidence that there is a linear relationship between peak SWE and the average mean hourly error in modelled SWE in water year 2025 when combing all sites (t-test, $t_{13} = 3.125$, p-value = 0.008). However, we find that only approximately 42.89% of the increase in error can be explained by peak SWE at the site ($r^2 = 0.4289$). The relationship did not yield a significant result during the accumulation period, as the confidence interval for the slope crossed zero, and the p-value was 0.109. Below are plots of the average SWE error vs. snow depth during the accumulation period (Figure 35) and during the melt period (Figure 36).

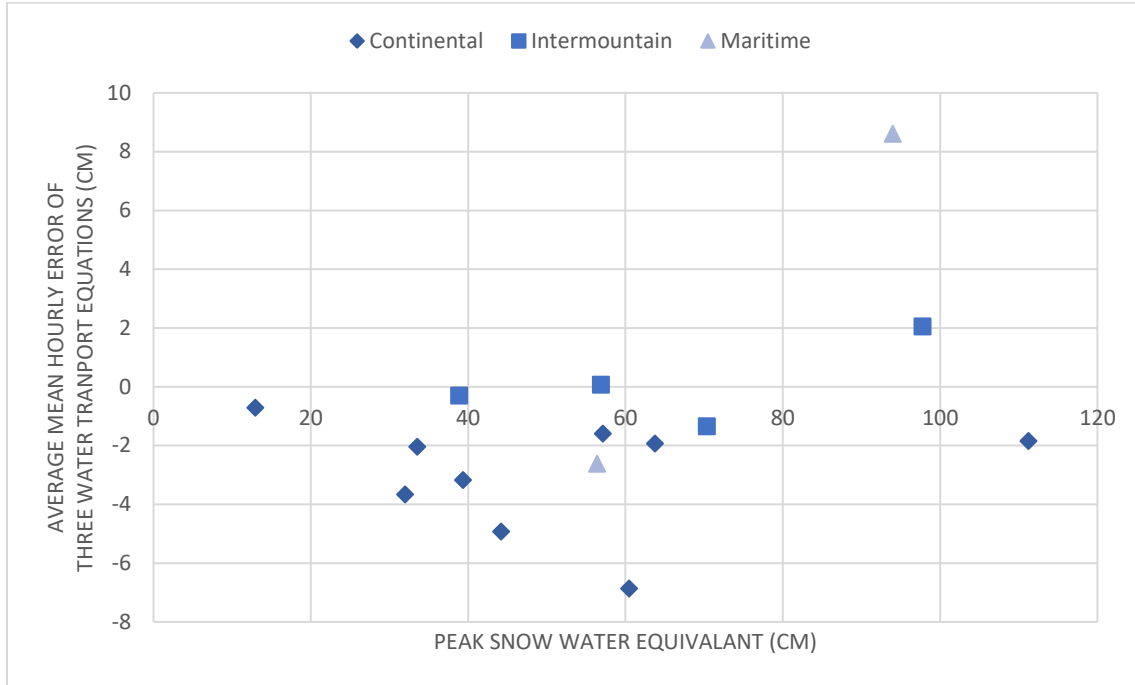


Figure 35: Scatterplot of the average mean error in SWE for three water transport equation model outputs at each SNOTEL site versus the peak SWE at that site for the accumulation period. The points are also broken up into Continental (diamonds), Intermountain (squares), and Maritime (triangles)

In Figure 35, we see that the error increases both negatively and positively with peak SWE at some sites. On average, at continental sites, the model increasingly underestimates SWE during the accumulation period, with a corresponding increase in peak SWE. At intermountain sites, there is a slight increase in overestimation of SWE, although we only have four data points. At maritime sites, we see a range from slight underestimation to high overestimation, again with only two data points.

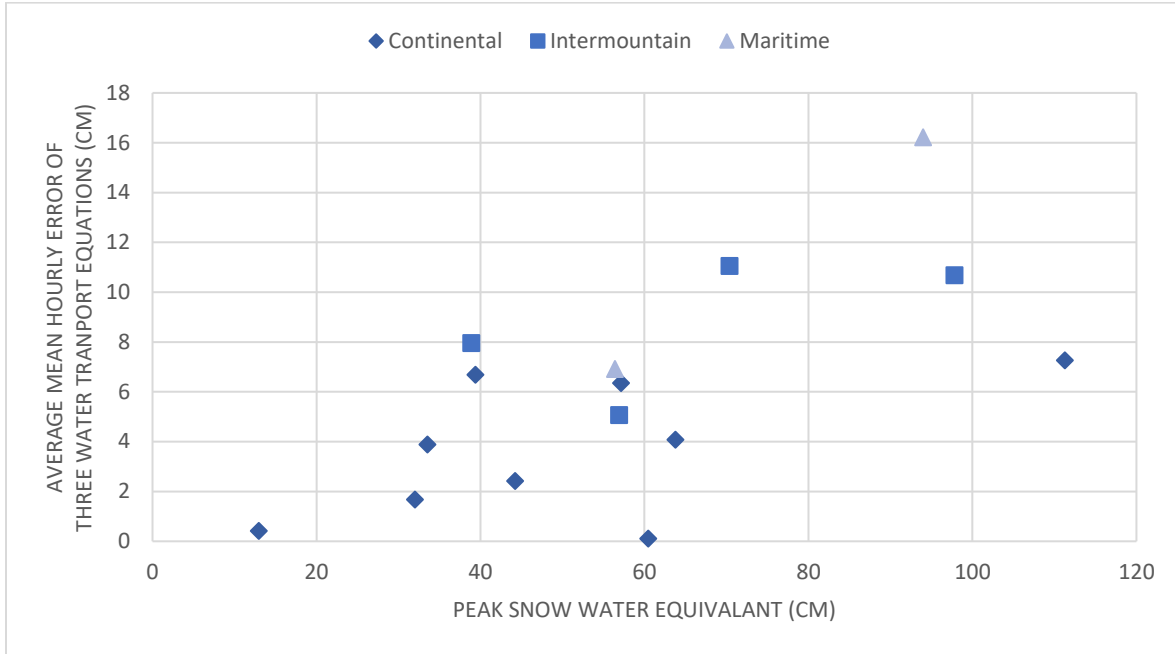


Figure 36: Scatterplot of the average mean error in SWE for three water transport equation model outputs at each SNOTEL site versus the peak SWE at that site for the melt period. The points are also broken up into Continental (diamonds), Intermountain (squares), and Maritime (triangles)

From Figure 36, see that the error increases with peak SWE. We also see that, on average, the continental sites have less snow and less error, the intermountain sites are next, and the maritime sites have the most snow and error. Tower is the site that bucks this trend the most, having the highest peak SWE but an average amount of error. While we conclude that sites with higher peak SWE have more error, we would need more data to make a case for why. For instance, in higher snow years would the continental sites see more error or not? We would also ask the same question for other snow regimes. Answering this question would give clues as to whether the error was purely due to deeper snow and more calculation layers, or whether it also has to do with snowpack properties. On the surface, it seems that maritime sites would have the

least error since the snowpacks are less complex and therefore easier to model, but this is not what we observe.

At the Mores Creek Summit site, we modeled two winters. Here, the peak SWE was 70.4 cm in water year 2024, with an average SWE error of 11.06 cm during the melt period. During water year 2025, the site had a peak SWE of 97.8 cm and an SWE error of 10.68 cm. This was the only site with more than one winter of data and shows the need for more winters of data to definitively determine when the SNOWPACK model has greater error. In a higher snow year, the model had less error at Mores Creek Summit. This is the opposite of the overall trend we found.

The last step for determining why error in our model outputs increases with a sites peak SWE is to add a quality control tracker to our quality control script. Currently, the step will not work if there is too much data that needs correction, and the user must go through the raw data to determine the extent of the error. While we found the number of data points that needed correction to be similar across sites that successfully ran the SNOWPACK model, having an error tracker would allow the user to quantitatively assess whether errors in model output correlate with errors in input data. For example, there is the potential for compounding variables if sites with deeper snowpacks also have more sensor errors than sites with shallower snowpacks.

Sources of uncertainty with my workflow and model setup

Some sources of uncertainty could be improved when running SNOWPACK with this workflow using SNOTEL data. First, the wind data used could be improved. As discussed in the wind sensitivity analysis, we used the average hourly wind speed as our model input. We did not add the double wind analysis to the sensitivity study until after model runs were completed.

However, it gave some evidence that higher wind speeds may have improved model

performance. If you use maximum hourly wind speeds rather than average wind speeds from SNOTEL sites, you may achieve better model agreement.

Another source of uncertainty in our workflow was using a single representative soil profile for the model when running Richard's equation in soil (which needs to be used when running the Richard's equation in snow, the other transport methods for snow use a Bucket approach for soil). If detailed soil profiles are obtained or performed for the specific SNOTEL site being used, model performance may be enhanced. This is because modelling water flow from the snowpack into the ground would be improved.

Also, the same model parameterization was used for all sites. We only changed the water-transport method and the precipitation or snow-depth forcing used to force the model. The error when running SNOWPACK with precipitation would likely decrease if the model were tuned for a specific region. Tuning can be done for parameters such as the rain/snow temperature cut-off and the mixed precipitation range. The model can also be run with both snow depth and precipitation. We wanted to see the difference between the two, but combining them could improve model performance. Even with the standard parameters, we still had good model agreement across most sites and model run types.

The error in the precipitation model runs did not solely come from model parameters. The raw precipitation data also has more inherent errors than the raw snow depth data; this could lead to greater errors in model outputs. At SNOTEL sites, there can be a lag in when snow falls and when the amount is measured in the precipitation can. This happens when snow gets caught in the can or on top and takes time to reach the fluid in the can where the pressure is measured from. Also, the pressure sensor for precipitation has bounce during the day because of

fluctuations in temperature. This bounce is typically between 0.1 and 0.5 inches and was not corrected in this study. The snow depth measurements do not have these issues. Lastly, the model can correct modeled snow depth when it is used as an input, but not when precipitation is used (Wever et al., 2015).

CHAPTER FIVE

SUMMARY AND CONCLUSIONS

In this study, we developed a novel workflow to run the SNOWPACK model with freely available SNOTEL data and to convert its outputs to a usable format. Our analysis answers the following questions: (1) Can the SNOWPACK model be run effectively in the United States using free, publicly available data from SNOTEL sites? And (2) what are the differences between the three water transport schemes available in SNOWPACK, how does each transport scheme affect model results, and when should each be used? In answering these questions, we also determined which SNOTEL sites currently have the data needed to run the model. For sites that don't currently have the data to run SNOWPACK, we present the data that would be needed for future use. We examined different model parameters to aid others in model setup. Lastly, we found higher error in model results at sites with deeper snowpacks.

Running of SNOWPACK with SNOTEL Data

Determining whether the SNOWPACK model could be effectively run with SNOTEL data involved identifying SNOTEL sites with the data needed to run the model, determining which sensors would be required, and creating a workflow in R. The R workflow facilitated downloading data, performing quality control, creating input and parameter files for the model, running the model, cleaning outputs, and creating visuals for the outputs. Each of these files in the workflow was run from a single primary file, where the user can make the necessary alterations for different model run types and SNOTEL sites.

We found that the model outputs fit the observed SWE well, as indicated by NSE values exceeding 0.8 for the full season and during the accumulation period. We found that during the accumulation period, models forced with snow depth had a mean absolute average hourly error in SWE of 2.79 cm, and an error in SWE of 4.35 cm when forced with precipitation. During the melt period, we found the mean absolute average hourly error in SWE to be 6.08 cm for models forced with snow depth, and 15.78 cm for models forced with precipitation. From these results, we determined that the model is more accurate during accumulation than during the melt period. These results suggest that the SNOWPACK model run with SNOTEL data may be useful as an aid to avalanche forecasting, as forecasting is more difficult during the accumulation period, when complex snowpacks and weather affect the forecast. However, for water supply and hydrologic purposes, our results indicate that the model is less effective during spring melt out when these forecasts are most useful.

Our analysis improves the current understanding of the SNOWPACK model by leveraging the large spatial extent of our study, which spans three snow regimes, and by using SWE as a validation metric. Wever et al. (2015) found that SWE is a better indicator of snow accumulation and snowmelt than snow height, which many previous studies use for hourly validation. This is an advantage of validating the model at SNOTEL sites as all sites have SWE data.

The spatial extent of our study enabled us to find that an increase in SWE error occurred at sites with higher peak SWE compared to sites with lower peak SWE, and that this error could be caused by different snow regimes. We found with 95% confidence that for each 1-centimeter increase in peak SWE at a SNOTEL site, the true mean error in SWE increase from model to

observed during the melt period is between 0.0327 and 0.1794 centimeters. We also found that the model fit, determined by the NSE, during the accumulation phase and when using the Richards method and snow depth was 0.834 at continental sites, 0.979 at intermountain sites, and 0.901 at maritime sites. During the melt period, we found that the NSE (for the same model type as above) was 0.787 at continental sites, 0.671 at intermountain sites, and 0.627 at maritime sites.

Based on our results, SNOWPACK can effectively be run using SNOTEL data inputs. As additional seasons of usable data are collected for testing model outputs, avalanche centers across the United States (such as the Gallatin National Forest Avalanche Center, the Utah Avalanche Center, the Colorado Avalanche and Information Center, and avalanche centers in Alaska) considering the use of SNOWPACK as an aid in forecasting, will be able to trust the model outputs more. The workflow and analysis of different parameters created in this study can be integrated into the systems currently under development at some avalanche centers across the United States.

To run SNOWPACK at SNOTEL sites, the following inputs with the associated sensor are needed: air temperature (ST300), wind (RM Young 5108 or 5103), snow depth (Sommer USH-9), short and longwave solar radiation (SN-500), relative humidity (HMP-155, or older sensor), and potentially precipitation (Rocket Gauge and Druck Pressure Sensor). In addition to these sensors, the snow pillow for SWE and the beaded stream for snow temperature profiles provide good metrics for validating the model at each hour the model is run. Pit validation is also important when using the model operationally, though these will have lower temporal resolution than the model outputs.

When running SNOWPACK with SNOTEL data, we recommend forcing the model with snow depth rather than precipitation. This is because precipitation data at SNOTEL sites can have more data errors and requires more model tuning to achieve accurate results, whereas using snow depth data with standard parameters yields good model performance. We did not run the model with both precipitation and snow depth, which is an option that could be explored.

Water Transport Equations

To determine the differences among the Bucket, NIED, and Richard's water transport methods and when each should be used, we analyzed the three methods by comparing their model performance. We determined that, on seasonal and daily timescales, the three methods perform similarly. Each method had a similar amount of error in SWE compared to the observed SWE error. Also, it was found the three methods drain a similar amount of water from the snowpack each day. All three methods, but especially the Bucket and NIED methods, drain water from the snow faster than the true daily value. On a seasonal scale, all methods retain water in the snowpack for too long due to a delay in onset of melt. As such, even at sites where the total length of melt season is similar to the observed, generally, the start of water draining from the snowpack in the model is later than observed. Our findings corroborate those of Wever et al. (2014), who found that the Bucket and NIED methods seem to retain meltwater in the snowpack for too long, underestimating its arrival at the base of the snowpack in the early stages of the melt season. In our findings, we observe the same trend for Richard's method.

On an hourly timescale, we found many differences between the three methods. The Richard's method models internal snow processes the best, as evident by more reasonable daily

melt patterns and diurnal freeze-thaw events. Due to the improved microstructural and liquid water content outputs with the Richard's method, we recommend running the Richard's method when possible for avalanche prediction purposes. Otherwise, the Bucket or NIED methods work well. The Richard's method is not always recommended because of the need for a soil profile and longer computation time compared to the other two methods. Further, the similarity we found between the three methods on daily-to-seasonal timescales indicates that either the Bucket or NIED method would work well for hydrologic purposes.

Considerations for the Future

During this study, we identified aspects of running SNOWPACK with SNOTEL data that should be considered when using this workflow, as well as work that should be continued. First, we did not edit empirical formulas or tune the model much from the standard parameters. Empirical formulas, such as the new snow density formula, can be adjusted to better match a particular region if desired, though this would require considerable testing. The model can also be tuned for specific areas. Constants such as the rain-to-snow temperature line can be changed to best match the elevation and climate of a particular site. There are also many options for soil boundary conditions, using preferential flow or not, wind scaling factors, and acceptable ranges for a given input that can all be tuned to a specific region and the use of the model within the parameter file.

Another important factor in the model parameter file is the height of meteorological sensors. We used a standard height of 4.5 meters for all sites. Inputting the exact height of a sensor may improve model results. You can only input the height for wind sensors; then, the rest

of the sensors are combined in the parameter file. It seems this is not an issue however because the wind value is the only one that would change considerably in a vertical cross-section. As discussed in our wind sensitivity study, more work on the best wind output from a SNOTEL site to be used as an input should be done as well.

We found in our study that the SWE error from the SNOWPACK model increases with peak SWE at a site. With only one winter of data and limited sites outside of a continental snow regime, it is difficult to say exactly what is causing the increase in error. It may be due to deeper snowpacks having more calculation layers. We also found that there was an increase in error from continental to maritime snow regime sites, and that, when analyzing sites in each snow regime separately, this increase persisted with increasing peak SWE. This observation will need to be studied further as more winters of data become available and more SNOTEL sites can run the model. However, it is something to consider when running the model.

Lastly, we only used SWE to validate our model runs. In the future, it would be advantageous to validate with a snow temperature profile as well. The temperature profile will be better for validating internal snow processes and properties. This is because correctly modelling a temperature profile is important for the energy balance, vapor transport, and snow metamorphism. Both the temperature gradient and snow hardness are important factors in avalanche risk. We did not verify with the observed temperature profile because the beaded stream sensor is still being tested at SNOTEL sites.

Our workflow for running the SNOWPACK model with SNOTEL data was a success and provides a framework for avalanche professionals and snow hydrologists to use the model for both disaster prediction and research. Research with our workflow could include topics such as:

the arrival of meltwater at the snow-soil interface during different melt event types; identifying and analyzing cold-snow vs warm-snow rain-on-snow events; and correlating streamflow peaks and amounts with snowpack melt timing and snow properties.

Finally, I want to thank you for reading my work and I hope you found it useful and interesting. Feel free to reach out to me with any questions or to request access to my code or more examples of my work. Hopefully, our paths cross around one of the many ways we can enjoy water.

REFERENCES CITED

- American Avalanche Association. (2022). *Snow, Weather, and Avalanche Guidelines (SWAG)*. <https://www.americanavalancheassociation.org/swag>
- Association of Cryospheric Sciences, I. (2009). *The International Classification for Seasonal Snow on the Ground Prepared by the ICSI-UCCS-IACS Working Group on Snow Classification*. <http://www.unesco.org/water/ihp>
- Bartelt, P., & Lehning, M. (2002). A physical SNOWPACK model for the swiss avalanche warning Part I Numerical Model. *Cold Regions Science and Technology*.
- Bellaire, S., Jamieson, J. B., & Fierz, C. (2011). Forcing the snow-cover model SNOWPACK with forecasted weather data. *Cryosphere*, 5(4), 1115–1125. <https://doi.org/10.5194/tc-5-1115-2011>
- Donahue, C., & Hammonds, K. (2022). Laboratory Observations of Preferential Flow Paths in Snow Using Upward-Looking Polarimetric Radar and Hyperspectral Imaging. *Remote Sensing*, 14. <https://doi.org/10.3390/rs14102297>
- Fleming, S. W., & Goodbody, A. G. (2019). A Machine Learning Metasystem for Robust Probabilistic Nonlinear Regression-Based Forecasting of Seasonal Water Availability in the US West. *IEEE Access*, 7, 119943–119964. <https://doi.org/10.1109/ACCESS.2019.2936989>
- Fleming, S. W., Zukiewicz, L., Strobel, M. L., Hofman, H., & Goodbody, A. G. (2023). SNOTEL, the Soil Climate Analysis Network, and water supply forecasting at the Natural Resources Conservation Service: Past, present, and future. In *Journal of the American Water Resources Association* (Vol. 59, Issue 4, pp. 585–599). John Wiley and Sons Inc. <https://doi.org/10.1111/1752-1688.13104>
- fpga company SLF. (2024). *SLF SNOWPRO-USER MANUAL SNOWPRO-17 SENSOR SNOWPRO-4040 SENSOR SNOWPRO-2525 SENSOR*.
- Gagliano, E., Shean, D., Henderson, S., & Vanderwilt, S. (2023). Capturing the Onset of Mountain Snowmelt Runoff Using Satellite Synthetic Aperture Radar. *Geophysical Research Letters*, 50(21). <https://doi.org/10.1029/2023GL105303>
- HEC-HMS Technical Reference Manual. (n.d.). *Snow Properties*.
- Heilig, A., Mitterer, C., Schmid, L., Wever, N., Schweizer, J., Marshall, H. P., & Eisen, O. (2015). Seasonal and diurnal cycles of liquid water in snow - Measurements and modeling. *Journal of Geophysical Research: Earth Surface*, 120(10), 2139–2154. <https://doi.org/10.1002/2015JF003593>

- Hirashima, H., Yamaguchi, S., Sato, A., & Lehning, M. (2010). Numerical modeling of liquid water movement through layered snow based on new measurements of the water retention curve. *Cold Regions Science and Technology*, 64(2), 94–103.
<https://doi.org/10.1016/j.coldregions.2010.09.003>
- Horton, S. (2025). *AvaCollabra*. <https://avacollabra.org>
- Horton, S., Nowak, S., Schroers, B., McWhae, R., Dunning, C., & Helgeson, G. (2025). *Avalanche Canada Models User Guide*.
- Khider Mawlood, D., & Neyaz Adnan, K. (2020). Comparison of the water movement by ZANCO. <https://doi.org/10.21271/zjpas>
- Legates, D. R., & McCabe, G. J. (1999). Evaluating the use of “goodness-of-fit” measures in hydrologic and hydroclimatic model validation. *Water Resources Research*, 35(1), 233–241. <https://doi.org/10.1029/1998WR900018>
- Lehning, M., Bartelt, P., Brown, B., & Fierz, C. (2002). A physical SNOWPACK model for the swiss avalanche warning Part III Meteorological forcing, thin layer formation and evaluation. *Cold Regions Science and Technology*.
- Lehning, M., Bartelt, P., Brown, B., Fierz, C., & Satyawali, P. (2002). A physical SNOWPACK model for the swiss avalanche warning Part II Snow Microstructure. *Cold Regions Science and Technology*.
- Lehning, M., Bartelt, P., Brown, B., Russi, T., Stöckli, U., & Zimmerli, M. (1999). *A NETWORK OF AUTOMATIC WEATHER AND SNOW STATIONS AND SUPPLEMENTARY MODEL CALCULATIONS PROVIDING SNOWPACK INFORMATION FOR AVALANCHE WARNING*.
- Li, D., Wrzesien, M. L., Durand, M., Adam, J., & Lettenmaier, D. P. (2017). How much runoff originates as snow in the western United States, and how will that change in the future? *Geophysical Research Letters*, 44(12), 6163–6172.
<https://doi.org/10.1002/2017GL073551>
- Lundy, C. C., Brown, B., Adams, E., Birkeland, K., & Lehning, M. (2001). A statistical validation of the snowpack model in a montana climate. *Cold Regions Science and Technology*.
- Mock, C. J., & Birkeland, K. (2000). *Snow Avalanche Climatology of the Western United States Mountain Ranges*.

- Morin, S., Horton, S., Techel, F., Bavay, M., Coléou, C., Fierz, C., Gobiet, A., Hagenmuller, P., Lafaysse, M., Ližar, M., Mitterer, C., Monti, F., Müller, K., Olefs, M., Snook, J. S., van Herwijnen, A., & Vionnet, V. (2020). Application of physical snowpack models in support of operational avalanche hazard forecasting: A status report on current implementations and prospects for the future. In *Cold Regions Science and Technology* (Vol. 170). Elsevier B.V. <https://doi.org/10.1016/j.coldregions.2019.102910>
- Nash, J. E., & Sutcliffe, J. V. (1970). RIVER FLOW FORECASTING THROUGH CONCEPTUAL MODELS PART I-A DISCUSSION OF PRINCIPLES*. In *Journal of Hydrology* (Vol. 10). © North-Holland Publishing Co.
- Peitzsch, E. H. (2009). *WATER MOVEMENT IN A STRATIFIED AND INCLINED SNOWPACK: IMPLICATIONS FOR WET SLAB AVALANCHES*.
- Peitzsch, E., Hendrikx, J., Fagre, D., & Reardon, B. (2010). *Characterizing Wet Slab and Glide Slab Avalanche Occurrence Along the Going-To-The-Sun Road, Glacier National Park, Montana, USA. ISSW*.
- Richards, L. A. (1931). Capillary conduction of liquids through porous mediums. *Journal of Applied Physics*, 1(5), 318–333. <https://doi.org/10.1063/1.1745010>
- Schneebeli, M. (1995). *Development and stability of preferential flow paths in a layered snowpack* (Issue 228). <https://www.researchgate.net/publication/237798449>
- Schweizer, J., Knappe, L., Reuter, B., & Mayer, S. (2024). *ON SNOW AND AVALANCHE CLIMATES IN THE SWISS ALPS*.
- Techel, F., & Pielmeier, C. (2011). Point observations of liquid water content in wet snow – Investigating methodical, spatial and temporal aspects. *Cryosphere*, 5(2), 405–418. <https://doi.org/10.5194/tc-5-405-2011>
- Trujillo, E., & Molotch, N. P. (2014). Snowpack regimes of the Western United States. *Water Resources Research*, 50(7), 5611–5623. <https://doi.org/10.1002/2013WR014753>
- Webb, R. W., Williams, M. W., & Erickson, T. A. (2018). The Spatial and Temporal Variability of Meltwater Flow Paths: Insights From a Grid of Over 100 Snow Lysimeters. *Water Resources Research*, 54(2), 1146–1160. <https://doi.org/10.1002/2017WR020866>
- Wever, N., Fierz, C., Mitterer, C., Hirashima, H., & Lehning, M. (2014). Solving Richards Equation for snow improves snowpack meltwater runoff estimations in detailed multi-layer snowpack model. *Cryosphere*, 8(1), 257–274. <https://doi.org/10.5194/tc-8-257-2014>

- Wever, N., Schmid, L., Heilig, A., Eisen, O., Fierz, C., & Lehning, M. (2015). Verification of the multi-layer SNOWPACK model with different water transport schemes. *Cryosphere*, 9(6), 2271–2293. <https://doi.org/10.5194/tc-9-2271-2015>
- Yamaguchi, S., Watanabe, K., Katsushima, T., Sato, A., & Kumakura, T. (2012). Dependence of the water retention curve of snow on snow characteristics. *Annals of Glaciology*, 53(61), 6–12. <https://doi.org/10.3189/2012AoG61A001>
- Young, R. M. (2014). *R.M. Young Wind Monitors*.
- Zukiewicz, L. (2024). *USDA-NRCS Snow Survey and Water Supply Forecasting Program SSWSFP Program and GOES Telemetry Upgrade Overview National Water and Climate Center*.

APPENDICES

APPENDIX A

SITE SPECIFIC MODEL OUTPUTS

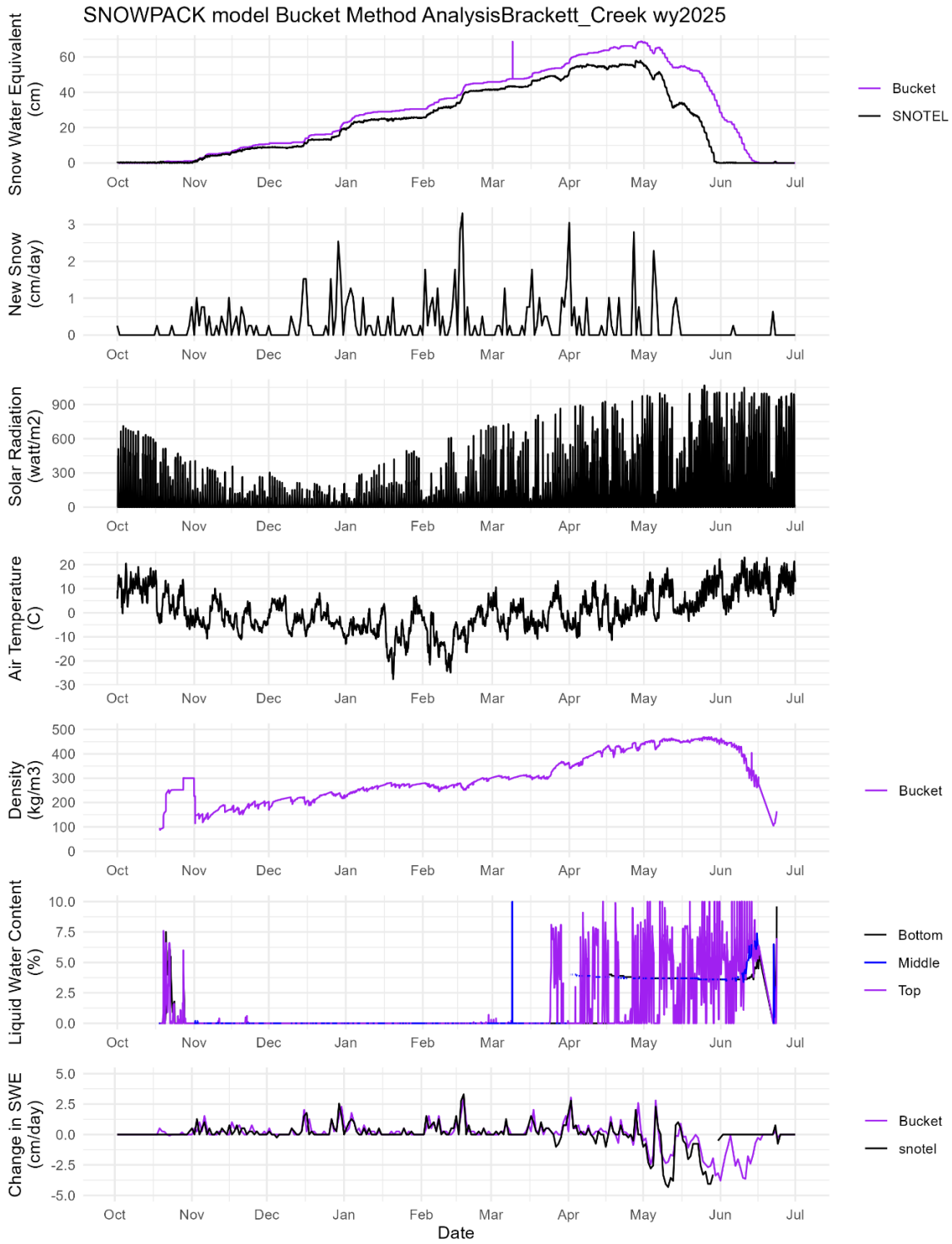


Figure 37: SNOWPACK results at Brackett Creek for a model forced with precipitation data and run with the Bucket water transport method

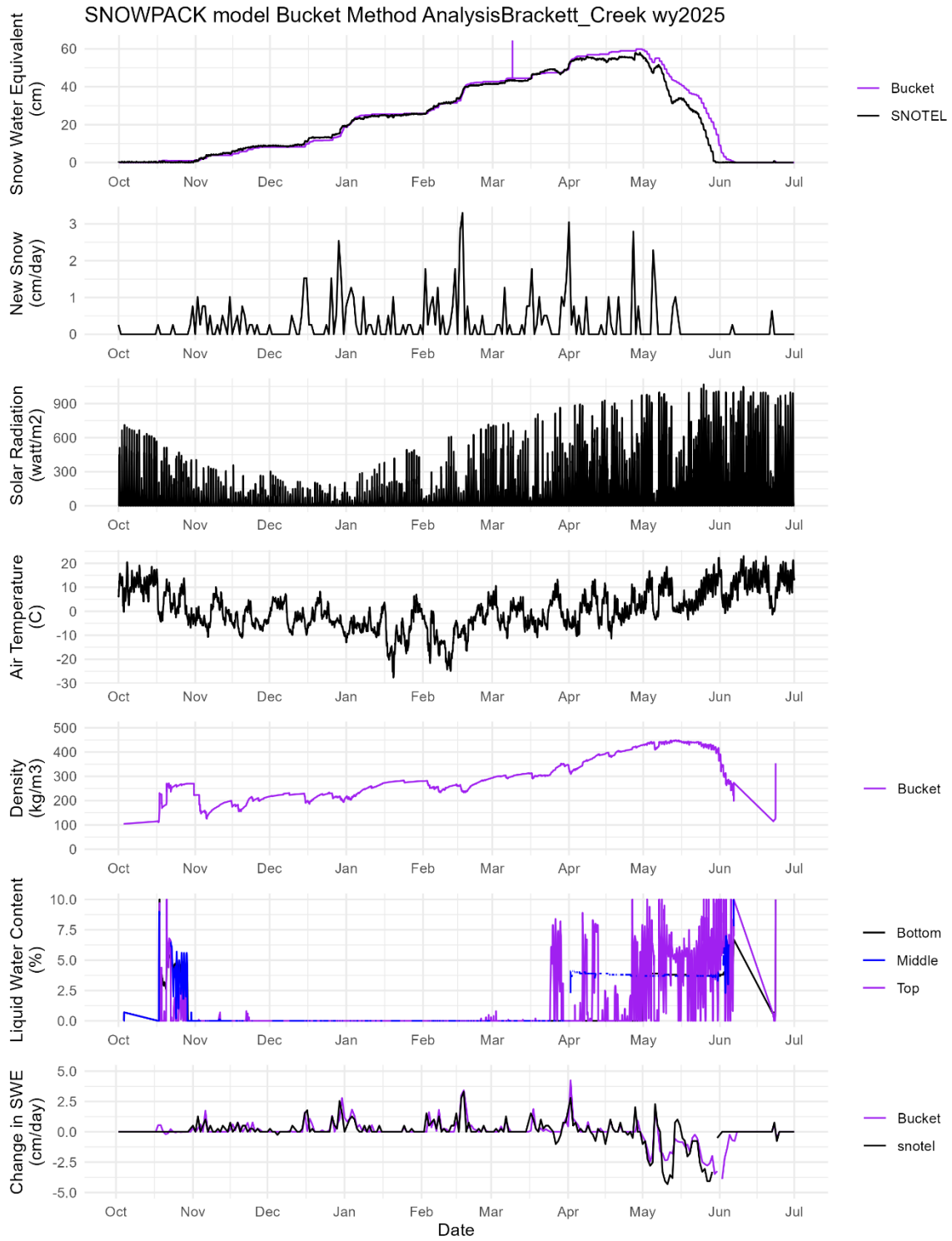


Figure 38: SNOWPACK results at Brackett Creek for a model forced with snow depth data and run with the Bucket water transport method

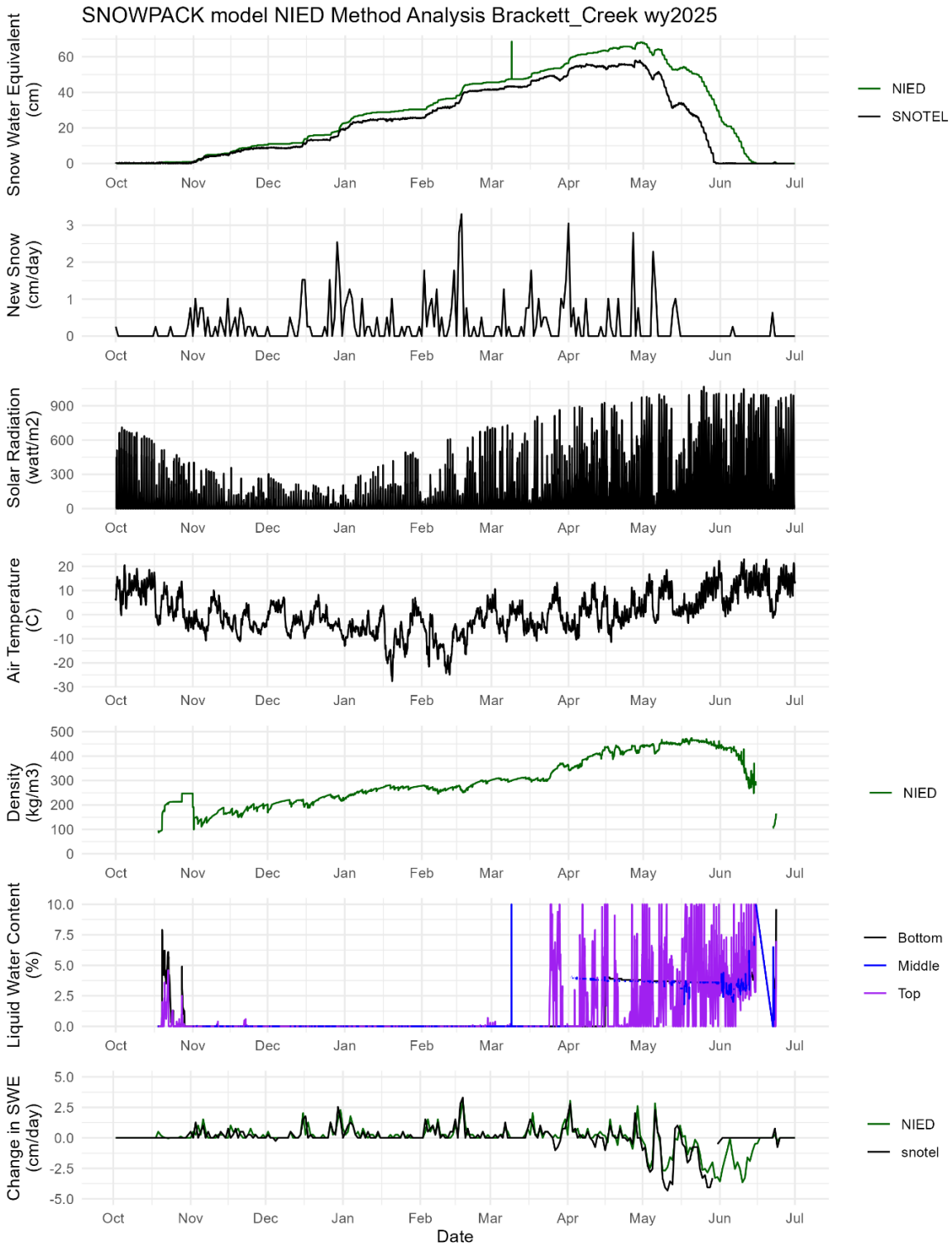


Figure 39: SNOWPACK results at Brackett Creek for a model forced with precipitation data and run with the NIED water transport method

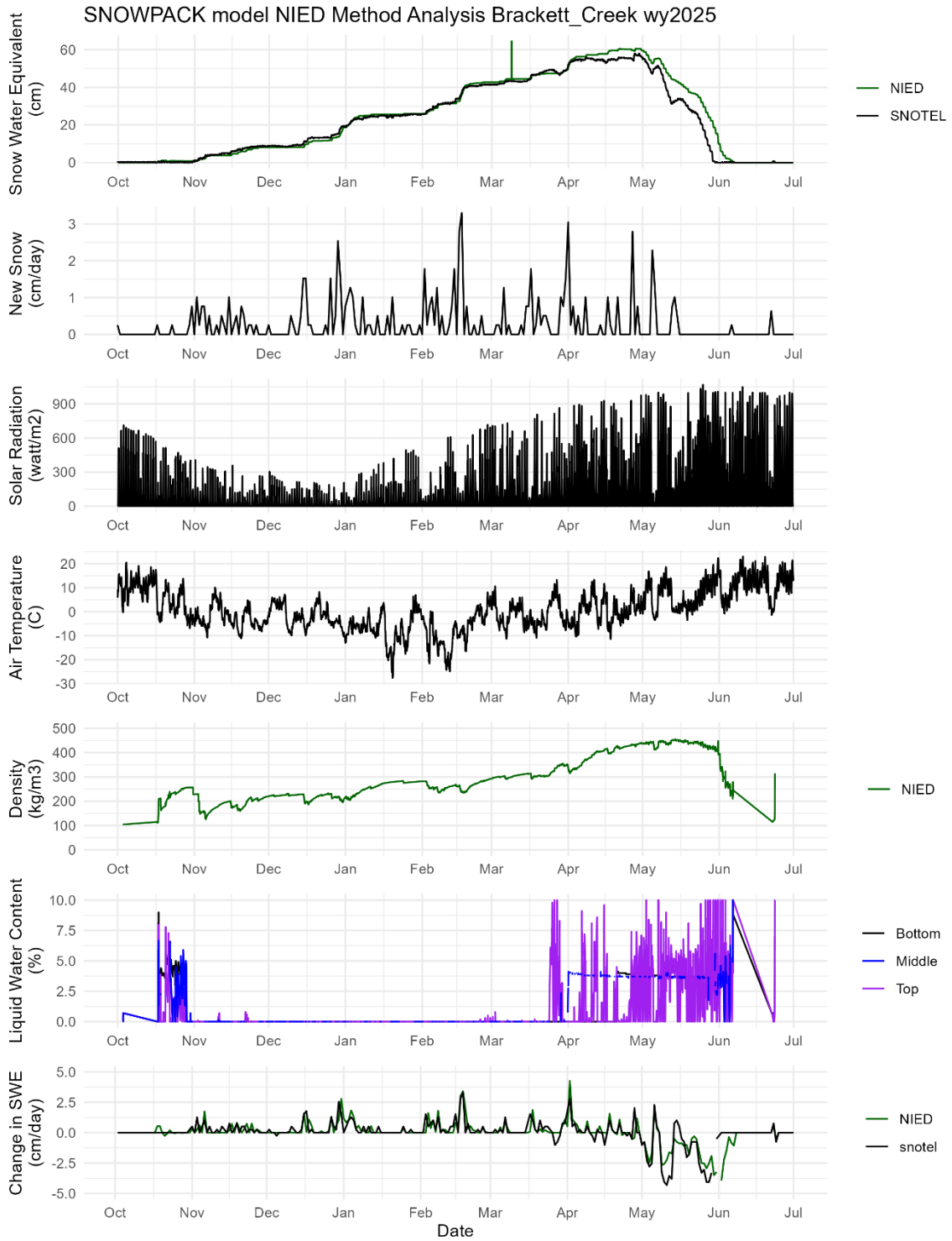


Figure 40: SNOWPACK results at Brackett Creek for a model forced with snow depth data and run with the NIED water transport method

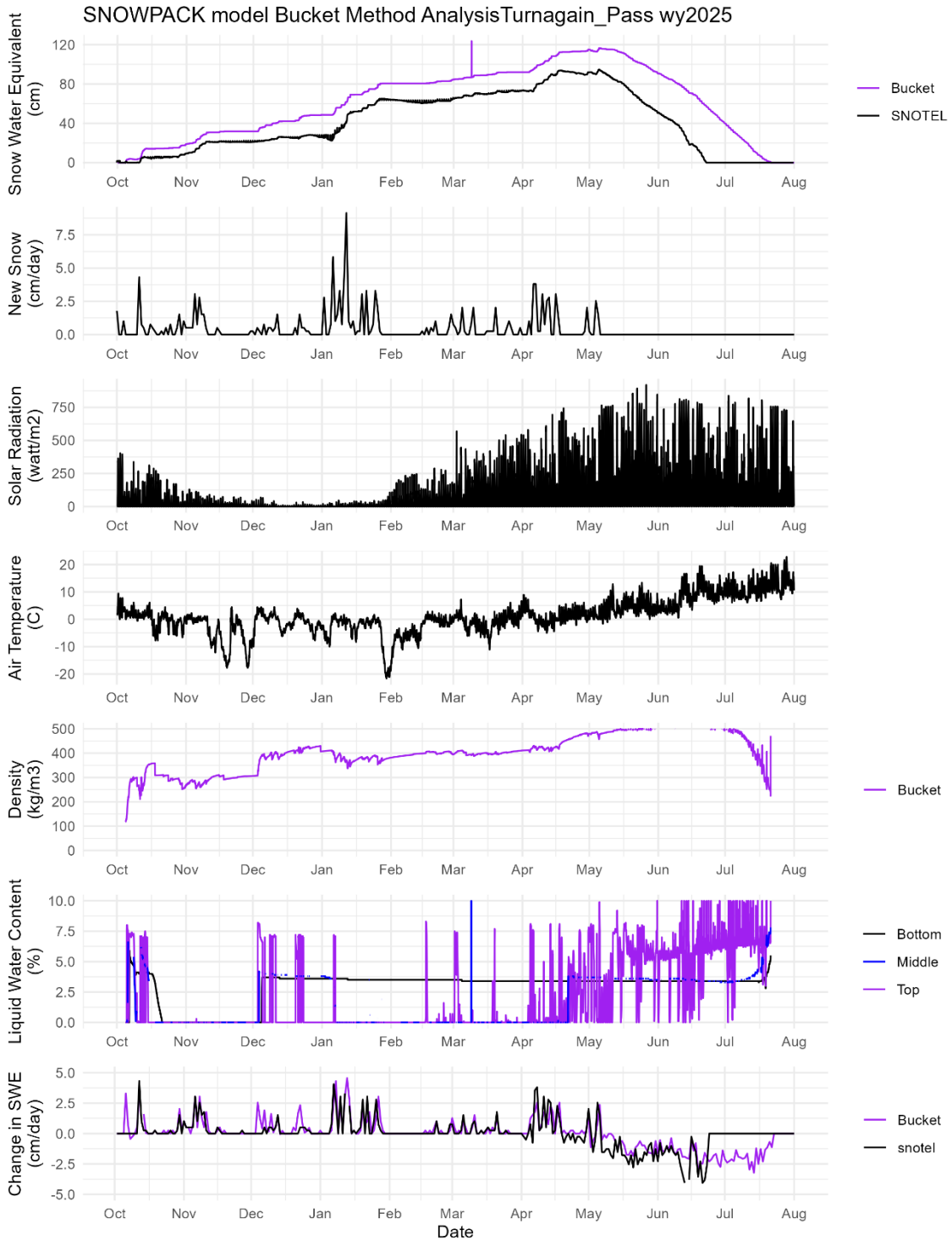


Figure 41: SNOWPACK results at Turnagain Pass for a model forced with precipitation data and run with the Bucket water transport method

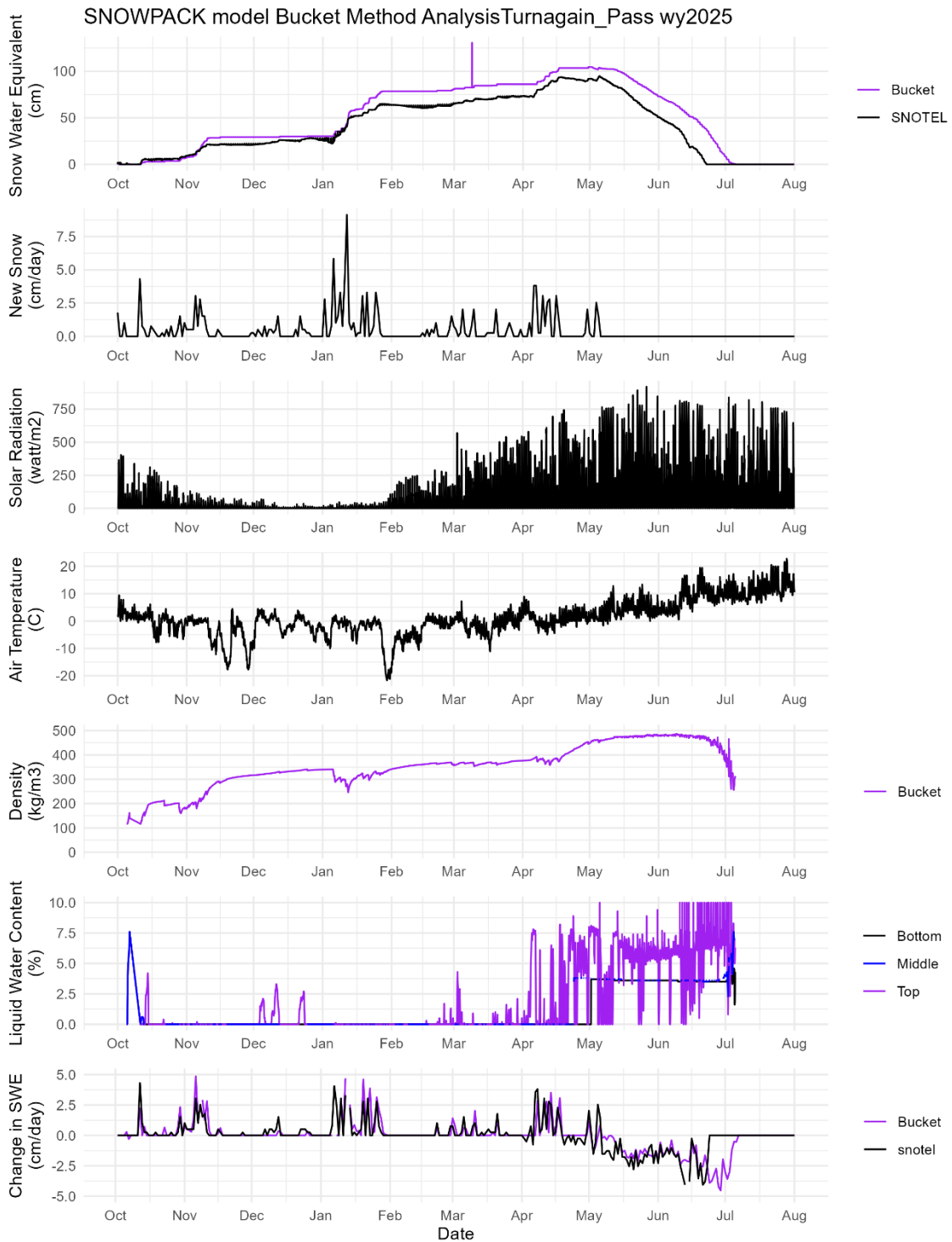


Figure 42: SNOWPACK results at Turnagain Pass for a model forced with snow depth data and run with the Bucket water transport method

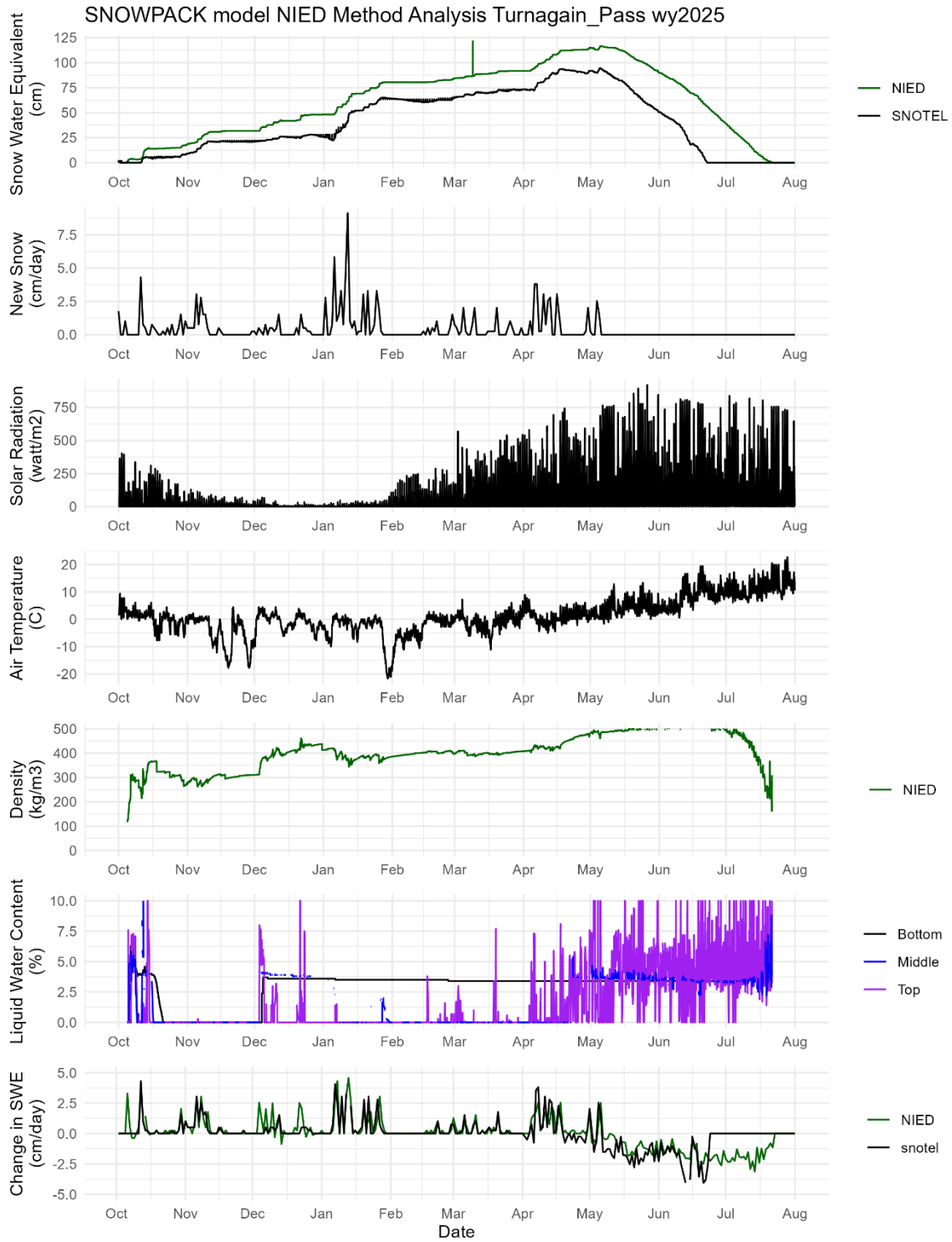


Figure 43: SNOWPACK results at Turnagain Pass for a model forced with precipitation data and run with the NIED water transport method

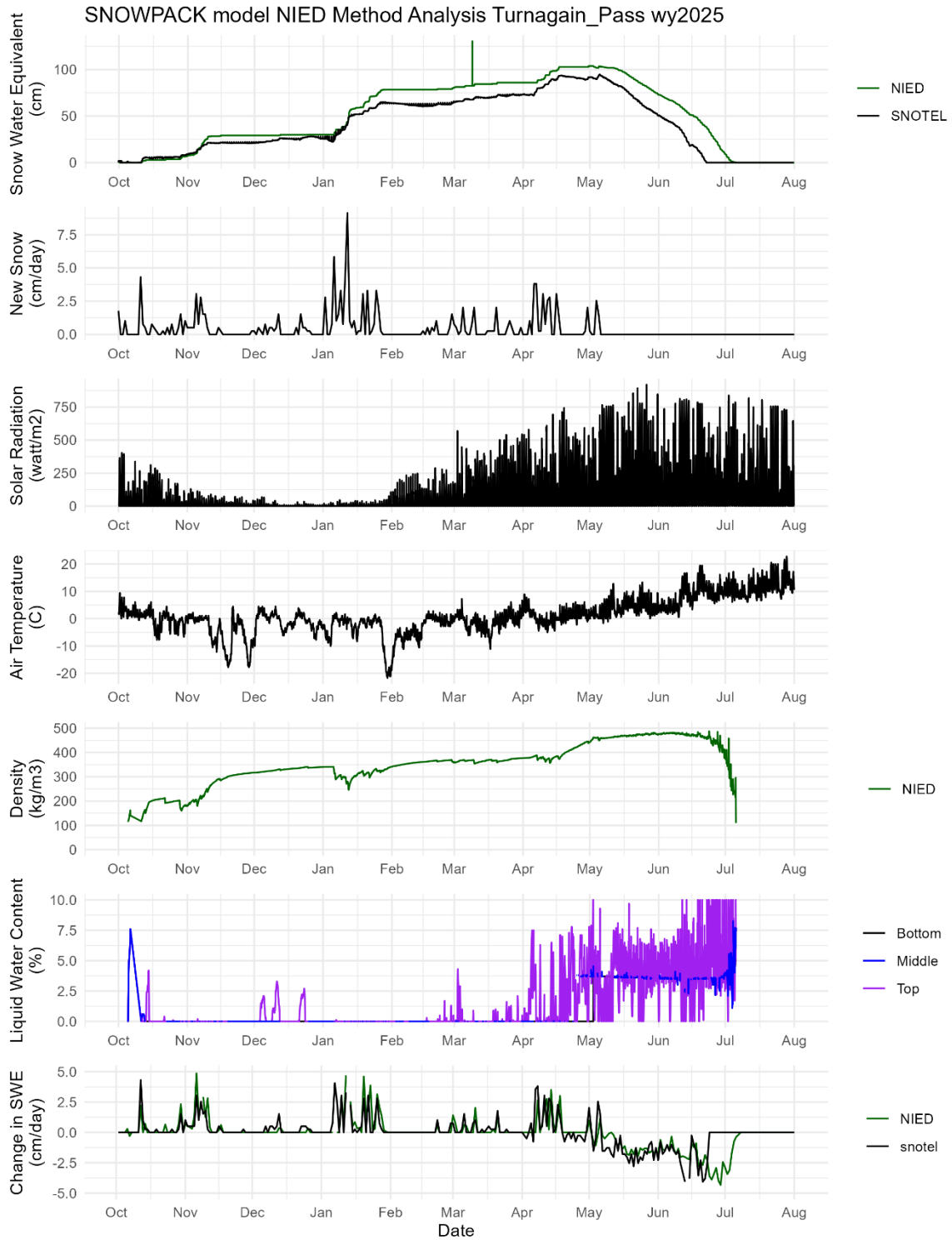


Figure 44: SNOWPACK results at Turnagain Pass for a model forced with snow depth data and run with the NIED water transport method

APPENDIX B

NASH-SUTCLIFFE EFFICIENCY RESULTS

Table 9: Full season Nash-Sutcliffe Efficiency table

	Site	Bucket SNWD	NIED SNWD	Richards SNWD	Bucket PREC	NIED PREC	Richards PREC
1	Berthoud_Summit	0.886	0.942	0.890	-0.254	-0.245	-0.044
2	Brackett_Creek	0.968	0.962	0.968	0.757	0.789	0.744
3	Castle_Peak	0.968	0.970	0.967	0.770	0.813	0.823
4	Elwood_Pass	0.719	0.745	0.769	0.296	0.401	0.462
5	Heavenly_Valley	0.867	0.887	0.888	0.233	0.337	0.373
6	Hourglass_Lake	0.884	0.879	0.752	0.807	0.857	0.899
7	Joe_Wright	0.883	0.886	0.828	0.047	0.158	0.327
8	Lizard_Head_Pass	0.838	0.896	0.819	0.380	0.665	0.838
9	Long_Draw_Resv	0.824	0.858	0.809	0.131	0.214	0.525
10	Midway_Valley	0.740	0.756	0.728	0.904	0.882	0.952
11	Mores_Creek_Summit_24	0.857	0.890	0.859	0.541	0.643	0.708
12	Mores_Creek_Summit_25	0.886	0.906	0.886	0.820	0.846	0.854
13	Tower	0.977	0.981	0.982	0.921	0.934	0.942
14	Turnagain_Pass	0.813	0.812	0.766	0.424	0.439	0.478
15	Upper_Rio_Grande	0.918	0.931	0.614	-1.606	-1.460	-2.340
16	Absolute Average	0.868	0.887	0.835	0.345	0.418	0.436

Table 10: Accumulation period Nash-Sutcliffe Efficiency table

	Site	Bucket SNWD	NIED SNWD	Richards SNWD	Bucket PREC	NIED PREC	Richards PREC
1	Berthoud_Summit	0.989	0.989	0.984	0.888	0.887	0.875
2	Brackett_Creek	0.995	0.993	0.996	0.945	0.950	0.946
3	Castle_Peak	0.987	0.987	0.983	0.907	0.907	0.888
4	Elwood_Pass	0.875	0.879	0.849	0.688	0.688	0.307
5	Heavenly_Valley	0.970	0.969	0.962	0.851	0.851	0.814
6	Hourglass_Lake	0.824	0.835	0.731	0.984	0.985	0.989
7	Joe_Wright	0.838	0.832	0.754	0.783	0.770	0.784
8	Lizard_Head_Pass	0.928	0.930	0.911	0.816	0.926	0.956
9	Long_Draw_Resv	0.853	0.854	0.779	0.951	0.942	0.949
10	Midway_Valley	0.964	0.964	0.958	0.985	0.985	0.985
11	Mores_Creek_Summit_24	0.994	0.994	0.989	0.988	0.990	0.996
12	Mores_Creek_Summit_25	0.984	0.985	0.977	0.993	0.993	0.994
13	Tower	0.996	0.996	0.995	0.996	0.996	0.994
14	Turnagain_Pass	0.872	0.873	0.839	0.663	0.668	0.745
15	Upper_Rio_Grande	0.852	0.852	0.519	-3.373	-3.250	-4.624
16	Absolute Average	0.928	0.929	0.882	0.604	0.619	0.507

Table 11: Melt period Nash-Sutcliffe Efficiency table

Melt Nash-Sutcliffe Efficiency SWE(cm) Summary Table							
	Site	Bucket SNWD	NIED SNWD	Richards SNWD	Bucket PREC	NIED PREC	Richards PREC
1	Berthoud_Summit	0.722	0.866	0.680	-2.078	-2.055	-1.185
2	Brackett_Creek	0.890	0.873	0.869	0.217	0.328	0.211
3	Castle_Peak	0.935	0.940	0.927	0.532	0.650	0.701
4	Elwood_Pass	0.446	0.507	0.582	-0.392	-0.121	0.479
5	Heavenly_Valley	0.669	0.730	0.681	-0.951	-0.648	-0.484
6	Hourglass_Lake	0.861	0.792	0.808	-0.203	0.121	0.537
7	Joe_Wright	0.922	0.934	0.898	-0.596	-0.325	-0.209
8	Lizard_Head_Pass	0.633	0.801	0.642	-0.544	0.129	0.639
9	Long_Draw_Resv	0.780	0.864	0.858	-1.092	-0.873	-0.063
10	Midway_Valley	0.627	0.651	0.387	0.862	0.829	0.910
11	Mores_Creek_Summit_24	0.577	0.677	0.676	-0.376	-0.066	0.115
12	Mores_Creek_Summit_25	0.788	0.828	0.770	0.646	0.698	0.708
13	Tower	0.925	0.938	0.935	0.709	0.761	0.812
14	Turnagain_Pass	0.675	0.671	0.573	-0.101	-0.066	-0.093
15	Upper_Rio_Grande	0.931	0.967	0.757	-1.538	-1.263	-0.417
16	Absolute Average	0.759	0.803	0.735	-0.327	-0.127	0.177

APPENDIX C

SAMPLE MODEL PARAMETER AND INPUT FILES

Below is the parameter file used for the Bracket Creek snow depth run using the bucket method for water transport. The same parameters were used for every model run besides changing water snow and soils water transport method is used.

```
[FILTERS]
ENABLE_METEO_FILTERS = TRUE
ENABLE_TIME_FILTERS = TRUE
HS::ARG1::MIN = 0.0
HS::ARG1::SOFT = true
HS::ARG2::MAX = 5.55e-5
HS::FILTER1 = MIN
HS::FILTER2 = RATE
ILWR::ARG1::MAX = 600
ILWR::ARG1::MIN = 188
ILWR::ARG2::MAX = 400
ILWR::ARG2::MAX_RESET = -11.000000
ILWR::ARG2::MIN = 200
ILWR::ARG2::SOFT = true
ILWR::FILTER1 = MIN_MAX
ILWR::FILTER2 = MIN_MAX
ISWR::ARG1::MAX = 1500
ISWR::ARG1::MIN = -10
ISWR::ARG2::MAX = 1500
ISWR::ARG2::MIN = 0
ISWR::ARG2::SOFT = true
ISWR::FILTER1 = MIN_MAX
ISWR::FILTER2 = MIN_MAX
PSUM::ARG1::MIN = 0.0
PSUM::ARG1::SOFT = true
PSUM::FILTER1 = MIN
RH::ARG1::MAX = 1.2
RH::ARG1::MIN = 0.01
```

RH::ARG2::MAX = 1.0
RH::ARG2::MIN = 0.05
RH::ARG2::SOFT = true
RH::FILTER1 = MIN_MAX
RH::FILTER2 = MIN_MAX
RSWR::ARG1::MAX = 1500
RSWR::ARG1::MIN = -10
RSWR::ARG2::MAX = 1500
RSWR::ARG2::MIN = 0
RSWR::ARG2::SOFT = true
RSWR::FILTER1 = MIN_MAX
RSWR::FILTER2 = MIN_MAX
TA::ARG1::MAX = 320
TA::ARG1::MIN = 240
TA::FILTER1 = MIN_MAX
TSG::ARG1::MAX = 320
TSG::ARG1::MIN = 200
TSG::FILTER1 = MIN_MAX
TSS::ARG1::MAX = 320
TSS::ARG1::MIN = 200
TSS::FILTER1 = MIN_MAX
VW::ARG1::MAX = 70
VW::ARG1::MIN = -2
VW::ARG2::MAX = 50.0
VW::ARG2::MIN = 0.0
VW::ARG2::SOFT = true
VW::FILTER1 = MIN_MAX
VW::FILTER2 = MIN_MAX
[GENERAL]
BUFFER_SIZE = 370
BUFF_BEFORE = 1.5
BUFF_GRIDS = 10

[INPUT]

COORDPARAM = 12T

COORDSYS = UTM

METEO = SMET

METEOPATH = C:/Users/hcl-o/OneDrive - Montana State University/Desktop/RA Work/SNOWPACK
inputs/Brackett_Creek

NUMBER_OF_SOLUTES = 0

PSUM_PH::CREATE = PRECSPLITTING

PSUM_PH::PRECSPLITTING::SNOW = 274.35

PSUM_PH::PRECSPLITTING::TYPE = THRESH

SNOW = SMET

SNOWFILE1 = Brackett_Creek_profile.sno

SNOWPATH = C:/Users/hcl-o/OneDrive - Montana State University/Desktop/RA Work/SNOWPACK
inputs/Brackett_Creek

SOLUTE_NAMES = NITRATE

STATION1 = Brackett_Creek.SMET

TIME_ZONE = -6.00

[INPUTEDITING]

ENABLE_TIMESERIES_EDITING = TRUE

[INTERPOLATIONS1D]

DW::NEAREST::EXTRAPOLATE = true

DW::RESAMPLE = NEAREST

ENABLE_RESAMPLING = TRUE

HS::LINEAR::WINDOW_SIZE = 43200

HS::RESAMPLE = LINEAR

PSUM::ACCUMULATE::PERIOD = 900

PSUM::RESAMPLE = ACCUMULATE

VW::NEAREST::EXTRAPOLATE = true

VW::RESAMPLE = NEAREST

WINDOW_SIZE = 86400

[OUTPUT]

ACDD_WRITE = false

AGGREGATE_PRF = false
AGGREGATE_PRO = FALSE
AVGSUM_TIME_SERIES = true
CLASSIFY_PROFILE = TRUE
COORDPARAM = 12T
COORDSYS = UTM
CUMSUM_MASS = false
EXPERIMENT = BUCKET_snowd
FIRST_BACKUP = 400.
HARDNESS_IN_NEWTON = FALSE
HAZARD_STEPS_BETWEEN = 1
HAZ_WRITE = true
METEO = SMET
METEOPATH = C:/Users/hcl-o/OneDrive - Montana State University/Desktop/RA Work/SNOWPACK
inputs/Brackett_Creek
OUT_CANOPY = false
OUT_HAZ = true
OUT_HEAT = true
OUT_LOAD = false
OUT_LW = true
OUT_MASS = true
OUT_METEO = true
OUT_SOILEB = false
OUT_STAB = true
OUT_SW = true
OUT_T = true
PRECIP_RATES = true
PROF_AGE_OR_DATE = AGE
PROF_DAYS_BETWEEN = 0.041666
PROF_FORMAT = PRO
PROF_ID_OR_MK = ID
PROF_START = 0.0

PROF_WRITE = TRUE
SNOW = SMET
SNOW_DAYS_BETWEEN = 365.
SNOW_WRITE = FALSE
TIME_ZONE = -6.00
TS_DAYS_BETWEEN = 1
TS_FORMAT = MET
TS_START = 0
TS_WRITE = FALSE
WRITE_PROCESSED_METEO = FALSE
[SNOWPACK]
ATMOSPHERIC_STABILITY = MO_MICHLMAYR
CALCULATION_STEP_LENGTH = 60.000
CANOPY = FALSE
CHANGE_BC = FALSE
ENFORCE_MEASURED_SNOW_HEIGHTS = TRUE
HEIGHT_OF_METEO_VALUES = 4.5
HEIGHT_OF_WIND_VALUE = 4.5
MEAS_TSS = FALSE
ROUGHNESS_LENGTH = 0.002
SNP_SOIL = FALSE
SW_MODE = INCOMING
[SNOWPACKADVANCED]
ADJUST_HEIGHT_OF_METEO_VALUES = TRUE
ADJUST_HEIGHT_OF_WIND_VALUE = TRUE
ADVECTIVE_HEAT = FALSE
ALBEDO_AGING = TRUE
ALBEDO_AVERAGE_SCHMUCKI = ALL_DATA
ALBEDO_FIXEDVALUE = -999.
ALBEDO_PARAMETERIZATION = LEHNING_2
ALLOW_ADAPTIVE_TIMESTEPPING = TRUE
ALPINE3D = false

ALPINE3D_PTS = false
AVG_METHOD_HYDRAULIC_CONDUCTIVITY = ARITHMETICMEAN
AVG_METHOD_HYDRAULIC_CONDUCTIVITY_PREF_FLOW = ARITHMETICMEAN
CANOPY_HEAT_MASS = TRUE
CANOPY_TRANSMISSION = TRUE
COMBINE_ELEMENTS = TRUE
COUPLEDPHASECHANGES = false
DETECT_GRASS = FALSE
ENABLE_VAPOUR_TRANSPORT = false
FIXED_POSITIONS = 0.25 0.5 1.0 -0.25 -0.10
FORCE_RH_WATER = TRUE
FORCE_SW_MODE = FALSE
FORESTFLOOR_ALB = TRUE
HARDNESS_PARAMETERIZATION = MONTI
HEAT_BEGIN = 0.0
HEAT_END = 0.0
HEIGHT_NEW_ELEM = 0.02
HN_DENSITY = PARAMETERIZED
HN_DENSITY_FIXEDVALUE = 100.
HN_DENSITY_PARAMETERIZATION = LEHNING_NEW
HOAR_DENSITY_BURIED = 125.
HOAR_DENSITY_SURF = 100.
HOAR_MIN_SIZE_BURIED = 2.
HOAR_MIN_SIZE_SURF = 0.5
HOAR_THRESH_RH = 0.97
HOAR_THRESH_TA = 1.2
HOAR_THRESH_VW = 3.5
HYDRAULIC_CONDUCTIVITY_FROZEN_SOIL = IGNORE
ICE_RESERVOIR = false
JAM = FALSE
LB_COND_WATERFLUX = FREEDRAINAGE
MASS_BALANCE = false

MAX_NUMBER_MEAS_TEMPERATURES = 5
MEAS_INCOMING_LONGWAVE = false
METAMORPHISM_MODEL = DEFAULT
MINIMUM_L_ELEMENT = 0.0025
MIN_DEPTH_SUBSURF = 0.07
MULTI_LAYER_SK38 = TRUE
NEWSNOW_LWC = false
NEW_SNOW_GRAIN_SIZE = 0.3
NUMBER_FIXED_RATES = 0
NUMBER_SLOPES = 1
PERP_TO_SLOPE = FALSE
PLASTIC = FALSE
PREF_FLOW = false
PREF_FLOW_PARAM_HETEROGENEITY_FACTOR = 1.0
PREF_FLOW_PARAM_N = 0.0
PREF_FLOW_PARAM_TH = 0.1
PREF_FLOW_RAIN_INPUT_DOMAIN = MATRIX
PREVAILING_WIND_DIR = 0.
READ_DSM = false
REDUCE_N_ELEMENTS = false
REQ_INITIALIZE_SOIL = false
RESEARCH = TRUE
RIME_INDEX = false
SALTATION_MODEL = SORENSEN
SNOW_ALBEDO = PARAMETERIZED
SNOW_EROSION = TRUE
SNOW_REDISTRIBUTION = false
SOIL_EVAP_MODEL = EVAP_RESISTANCE
SOIL_FLUX = false
SOIL_THERMAL_CONDUCTIVITY = FITTED
SSI_IS_RTA = TRUE
STRENGTH_MODEL = DEFAULT

SW_ABSORPTION_SCHEME = MULTI_BAND
TEMP_INDEX_DEGREE_DAY = 0.
TEMP_INDEX_SWR_FACTOR = 0.
THRESH_DTEMP_AIR_SNOW = 3.0
THRESH_RAIN = 1.2
THRESH_RH = 0.5
TWO_LAYER_CANOPY = TRUE
T_CRAZY_MAX = 340.
T_CRAZY_MIN = 210.
VARIANT = DEFAULT
VISCOSITY_MODEL = DEFAULT
WATERTRANSPORTMODEL_SNOW = BUCKET
WATERTRANSPORTMODEL_SOIL = BUCKET
WATER_LAYER = FALSE
WIND_SCALING_FACTOR = 1.0
[SNOWPACKSEAICE]
CHECK_INITIAL_CONDITIONS = FALSE
[TECHSNOW]
GROOMING_DEPTH_IMPACT = 0.4
GROOMING_DEPTH_START = 0.4
GROOMING_HOUR = 21
GROOMING_WEEK_END = 17
GROOMING_WEEK_START = 40
SNOW_GROOMING = FALSE

The next blocks are the headers with example data for the meteorological inputs (.smet file) and then the initial snow profile (.sno file). These are for the Brackett Creek precipitation model runs.

SMET 1.1 ASCII

[HEADER]

station_id = Brackett_Creek

station_name = Brackett_Creek_SNOTEL

altitude = 2247

latitude = 45.89107

longitude = -110.939

epsg = 32613

nodata = -999

tz = -6

source = Mountain Hydrology Research Group MSU

fields = timestamp TA RH ISWR ILWR PSUM TSG VW

[DATA]

2024-10-01T00:00	279.15	0.19	0	254	0	272.95	1.519936
------------------	--------	------	---	-----	---	--------	----------

2024-10-01T01:00	279.65	0.17	0	255	0	272.95	0.938784
------------------	--------	------	---	-----	---	--------	----------

APPENDIX D

CODE SCRIPT SAMPLES

The following is the master script for the R workflow we created. For the rest of the code to run SNOWPACK with SNOTEL data, feel free to reach out to me (hcl-osprey@comcast.net) with any questions.

```
#This file runs all scripts needed to download snotel data, run SNOWPACK, and perform analysis.
```

```
#To run correctly only make edits in the next section, you will also need to input correct soil information and add a file for the stations name in the directory. Make sure to have correct altitude, lat, long, and epsg for site location
```

```
#Created by Hayden Libby
```

```
# _____ #
```

```
#Only make edits in this section, make sure to change for correct station variables#
```

```
# _____ #
```

```
#Step 1: site variables for SNOWPACK input files
```

```
site = "Tower_doublewind"
```

```
snoteldata = "Tower_(825)"
```

```
start_date = "2024-10-01T00:00:00"
```

```
end_date = "2025-08-01T00:00:00"
```

```
alt = "3236"
```

```
lat = "40.5374"
```

```
long = "-106.677"
```

```
epsg = "3422" #"2256"

start_date_precip = "2024-10-01T01:00:00"

wateryear = "wy2025"

start_melt = "2025-05-22"

end_melt = "2025-05-25"

#Site variables for SNOTEL data download

#Variables: WTEQ = snow water equivalent, SNWD = snow depth, PREC = accumulated
precipitation, TOBS = observed temperature,

#RHUM = relative humidity, WSPDV = wind speed, SWINV = short wave incoming radiation,
LWINV = long wave incoming radiation

elements <- c('WTEQ', 'SNWD', 'PREC', 'TOBS', 'RHUM', 'WSPDV', 'SWINV', 'LWINV')

start_dateapi = "2024-10-01"

end_dateapi = "2025-08-01"

station_triplet = "825:CO:SNTL"

#running code with precip or snow height as variable in SNOWPACK?

snow_height = FALSE

#which water transport model do you want to run (BUCKET,NIED,RICHARDSEQUATION)

transport = "RICHARDSEQUATION"

#soil water transport (bucket for bucket and nied snow models and richards for richards snow)

soiltrans = "RICHARDSEQUATION"

#setting up directory's

computer = ""
```

```
base_dir = paste0("C:/Users/", computer, "/OneDrive - Montana State University/Desktop/RA
Work/SNOWPACK inputs/master programs/")
```

```
#working directory
```

```
wd = paste0("C:/Users/", computer, "/OneDrive - Montana State University/Desktop/RA
Work/SNOWPACK inputs/trial runs/wind_study/", site)
```

```
setwd(wd)
```

```
#code sources:
```

```
datadownload_path = paste0(base_dir, "snotel_api.R")
```

```
quality_control_path = paste0(base_dir, "quality_control.R")
```

```
inputfile_sd_path = paste0(base_dir, "inputfiles.R")
```

```
inputfile_precip_path = paste0(base_dir, "inputfiles_precip.R")
```

```
increation_path = paste0(base_dir, "ini_creation.R")
```

```
run_snowpack_path = paste0(base_dir, "run_snowpack.R")
```

```
cleaning_path = paste0(base_dir, "clean_profiles.R")
```

```
graph_path = paste0(base_dir, "graph.R")
```

```
#Remember to set up new folder in SNOWPACK inputs folder if running a new site!
```

```
#-----#
```

```
#Step 2: Download data from report generator with variables:
```

```
cat("Downloading SNOTEL data")
```

```
source(datadownload_path)
```

```
#Step 2.b: Run Quality Control on SNOTEL data:
```

```
cat("Running Quality Control on Raw SNOTEL Data")
```

```
source(quality_control_path)
```

```
#Step 3: choose precip or snow height, take raw data, perform QC, and create SNOWPACK
```

```
input files:
```

```
if (snow_height == TRUE) {
```

```
  cat("Creating SNOWPACK input file with Snow Height as variable")
```

```
  source(inputfile_sd_path)
```

```
} else {
```

```
  cat("Creating SNOWPACK input file with Precipitation as variable")
```

```
  source(inputfile_precip_path)
```

```
}
```

```
#Step 5: create .ini file for site for SNOWPACK use
```

```
cat("creating .ini file for site")
```

```
source(inicreation_path)
```

```
#Step 6: Run SNOWPACK
```

```
cat("Running SNOWPACK")
```

```
source(run_snowpack_path)
```

```
#step 7: run clean profiles to get outputs in a usable format
```

```
cat("cleaning SNOWPACK outputs")
```

```
source(cleaning_path)
```

```
#step 8: run "graph" script to create outputs for report
```

```
cat("Analysing SNOWPACK outputs")

source(graph_path)

#step 9: create avalanche forecast risk map and printed pdf of results

#cat("creating avalanche forecast")

#py_run_file("C:/Users/hcl-o/OneDrive - Montana State University/Desktop/RA
Work/SNOWPACK inputs/master programs/avalanche_forecast.py")
```